

2007

Characterizing sedimentary bedforms as habitat for fishes and invertebrates in the San Juan Archipelago, Washington, USA, and the Georgia Basin, British Columbia

Holly Linda Lopez
California State University, Monterey Bay

Follow this and additional works at: https://digitalcommons.csumb.edu/caps_thes

Recommended Citation

Lopez, Holly Linda, "Characterizing sedimentary bedforms as habitat for fishes and invertebrates in the San Juan Archipelago, Washington, USA, and the Georgia Basin, British Columbia" (2007). *Capstone Projects and Master's Theses*. 78.

https://digitalcommons.csumb.edu/caps_thes/78

This Master's Thesis is brought to you for free and open access by Digital Commons @ CSUMB. It has been accepted for inclusion in Capstone Projects and Master's Theses by an authorized administrator of Digital Commons @ CSUMB. Unless otherwise indicated, this project was conducted as practicum not subject to IRB review but conducted in keeping with applicable regulatory guidance for training purposes. For more information, please contact digitalcommons@csumb.edu.

CHARACTERIZING SEDIMENTARY BEDFORMS AS HABITAT FOR FISHES
AND INVERTEBRATES IN THE SAN JUAN ARCHIPELAGO, WASHINGTON,
USA, AND THE GEORGIA BASIN, BRITISH COLUMBIA

A Thesis
Presented to
The Faculty of California State University, Monterey Bay
through
Moss Landing Marine Laboratories

In Partial Fulfillment
of the Requirements for the Degree
Master of Science in Marine Science

by
Holly Linda Lopez
December 2007

©2007

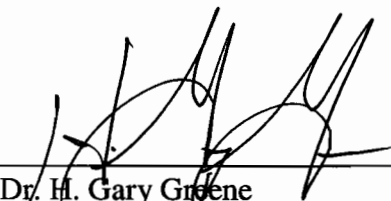
Holly Linda Lopez

ALL RIGHTS RESERVED

CERTIFICATION OF APPROVAL

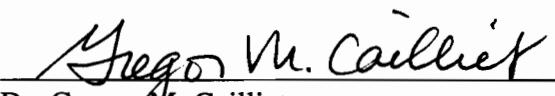
CHARACTERIZING SEDIMENTARY BEDFORMS AS HABITAT FOR FISHES AND
INVERTEBRATES IN THE SAN JUAN ARCHIPELAGO, WASHINGTON, USA, AND THE
GEORGIA BASIN, BRITISH COLUMBIA

by
Holly Linda Lopez



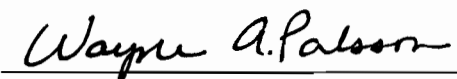
Dr. H. Gary Greene
Moss Landing Marine Laboratories

7 January 2008
Date



Dr. Gregor M. Cailliet
Moss Landing Marine Laboratories

14 January, 2008
Date



Mr. Wayne Palsson
Washington Department of Fish and Wildlife

10 January 2008
Date

ABSTRACT

Based on multibeam bathymetry, multibeam backscatter datasets, Remotely Operated Vehicle (ROV) observations and sediment grab data collected in the San Juan Archipelago and Georgia Basin region, sedimentary bedforms including sediment waves, ripples and ripples overlying waves were identified and characterized as habitat for fishes and invertebrates according to the deep-water classification scheme for marine benthic habitats by Greene et al. (1999). Analysis of long term bathymetric survey data in a GIS suggests that sediment waves were dynamic and influenced by modern physical oceanographic processes. Direct observational data collected in the sediment wave fields revealed that sediment waves were poorly sorted and composed of both fine-grained sediment (sand) and coarse-grained sediment (cobbles, pebbles and coquina). Density, percent composition and distribution of fishes and invertebrates, specifically in San Juan Channel, were calculated. Pacific sand lance (*Ammodytes hexapterus*) had high percent composition values among the observed fishes in both the mixed and sand substrates. Spot prawns (*Pandalus platyceros*) dominated the gravel, mixed sediment and sand substrates. There were significant density differences for individuals in the families Hexagrammidae and Scorpaenidae, but there were no significant density differences for the remaining fish or invertebrates observed in both the sand wave and non-sand wave areas. Percent composition varied between gravel, mixed sediment, rock and sand substrates; however, based on Chi-squared analyses, there were significant differences detected among varying substrate types in both sand wave and non-sand wave transects which suggest that species occurrences are not independent of habitat types.

ACKNOWLEDGMENTS

Private funding from the Dickinson Foundation has provided means for the collection of data in the San Juan Archipelago and the Georgia Basin. Additionally, funding received allowed for collaborative contracts between MLML, the SeaDoc Society (formerly known as Marine Ecosystem Health Program) at University of California, Davis (Award # K004431-16), and the National Oceanic and Atmospheric Administration Coastal Services Center (NOAA, CSC of Charleston, North Carolina) (Award #NA170C2646). As the sole collector of geophysical and remote sensing data, the Center for Habitat Studies at MLML has worked with a variety of institutions under cooperative contracts. California State University Monterey Bay's Seafloor Mapping Lab (CSUMB SFML) collected small desperate datasets of multibeam bathymetry and backscatter data in southern San Juan Channel, southeastern Haro Strait, and northeastern Strait of Juan de Fuca in the San Juan Islands. The GSC and the CHS have collected multibeam bathymetry, backscatter, sediment grabs, cores, video imagery and sub-bottom profile data for much of the area within the San Juan Islands. The WDFW collected ROV video and sediment samples. Marine benthic habitats were studied in San Juan Channel in 2004 and 2005 and funded under the Washington Sea Grant project #R/ES-59.

I would like to thank my thesis committee, Gary Greene and Greg Cailliet of Moss Landing Marine Laboratories and Wayne Palsson of the Washington Department of Fish and Wildlife (WDFW) for their support on this project. Thanks to the faculty, staff and students of MLML for their professionalism. Special thanks to Joe Bizzarro for his fisheries and statistical expertise. Thank you to Adrian Rocha for his expertise and

support. Thank you to the students at the Center for Habitat Studies, especially Janet Tilden, Steve Watt, Mercedes Erdey, Lee Murai, Charlie Endris, Bryan Dieter and Eric Niven. Thanks to Robert Pacunski at the WDFW for his support with the video analysis. Thank you to Patrick Mitts for his assistance with the sediment grain size analysis. Thanks to the crew of the *R/B Young*, *R/V Vector* and *R/V Molluscan*. Thank you to Fugro Pelagos, Inc., for their encouragement and support.

Special thanks to my family and a genuine *tack så mycket* to my Mother, Linda, who provided endless positivity and confidence throughout my MLML career. Thank you also to my Aunt and Uncle/Godparents, Betty and Will Meintzer, who sent me to sea to see the world. A sincere *dziekuje* to my soul matey, John Woytak, who was a strong support system and bestowed upon me much appreciated wit, gusto and mathematical skills while I worked on this project. This thesis is dedicated to my Grandparents, Henning and Florence Edlund, who inspired me and granted me with the perpetual blessings in my life.

TABLE OF CONTENTS

LIST OF FIGURES.....	ix
LIST OF TABLES.....	xi
1 INTRODUCTION.....	1
2 BACKGROUND INFORMATION.....	4
2.1 SEDIMENTARY BEDFORMS.....	4
2.1.1 SEDIMENTARY BEDFORMS AND CONSTRUCTION.....	4
2.1.2 BEDFORM CLASSIFICATION.....	7
2.1.3 GRAIN SIZE.....	8
2.1.4 SEDIMENT GRAIN MOVEMENT AND MIGRATION.....	9
2.1.5 BEDFORM SIZES.....	12
2.2 FISH AND INVERTEBRATE HABITAT.....	14
2.2.1 PREVIOUS STUDIES.....	17
2.3 PHYSICAL OCEANOGRAPHY.....	20
3 METHODS.....	25
3.1 DATA COLLECTION.....	25
3.1.1 MULTIBEAM BATHYMETRY AND BACKSCATTER.....	25
3.1.2 ROV SURVEYS.....	26
3.1.3 SEDIMENT SAMPLING.....	31
3.2 DATA ANALYSIS.....	32
3.2.1 MULTIBEAM BATHYMETRY AND BACKSCATTER.....	32
3.2.2 ROV SURVEYS.....	41
3.2.3 SEDIMENT SAMPLING.....	48
4 RESULTS.....	49
4.1 MULTIBEAM BATHYMETRY AND BACKSCATTER.....	49
4.1.1 MARINE BENTHIC HABITAT MAPS.....	49
4.1.2 SEDIMENTARY BEDFORMS.....	64

4.2	ROV SURVEY.....	70
4.2.1	HABITAT	70
4.2.2	FISH AND INVERTEBRATES.....	73
4.2.3	BPI AND SLOPES.....	92
4.3	SEDIMENT SAMPLING.....	95
5	DISCUSSION.....	97
6	CONCLUSION.....	107
7	LITERATURE CITED.....	109
 APPENDIX A: MULTIBEAM BACKSCATTER PROCESSING.....		122
 APPENDIX B: CREATION OF MARINE BENTHIC HABITAT MAPS.....		127
 APPENDIX C: HABITAT CLASSIFICATION DESCRIPTION AND SCHEME...		132

LIST OF FIGURES

Figure 1-1	Index map of study area.....	2
Figure 2-1	Sun-illuminated multibeam imagery of dune field.....	6
Figure 2-2	Hjulström curve.....	10
Figure 2-3	Plot of shear velocity and grain size.....	11
Figure 2-4	Modes of transport.....	12
Figure 2-5	Illustration of internal structure of longitudinal ripples.....	13
Figure 2-6	Ebbing and flooding directions in San Juan Channel.....	22
Figure 3-1	Tracklines from ROV surveys in San Juan Channel.....	27
Figure 3-2	Photo of Deep Ocean Engineering's® Phantom HD2 ROV.....	28
Figure 3-3	Location map of sediment grab samples in Boundary Pass region.....	32
Figure 3-4	Image of multibeam bathymetry outlining bedform field in San Juan Channel.....	37
Figure 3-5	Image of multibeam bathymetry outlining bedform field in Boundary Pass region.....	38
Figure 3-6	Example of bedforms measured in ArcGIS® in San Juan Channel.....	39
Figure 3-7	Current crescent's pattern of flow.....	41
Figure 3-8	Illustration of Bathymetric Position Index (BPI).....	46
Figure 3-9	Example of 5 m DEM with BPI analysis.....	47
Figure 4-1	Overview of multibeam bathymetry.....	50
Figure 4-2	Examples of multibeam bathymetry and backscatter data in Haro Strait.....	51
Figure 4-3	Examples of multibeam bathymetry and backscatter data in the Strait of Juan de Fuca.....	52

Figure 4-4	Marine benthic habitat maps.....	55
Figure 4-5	Marine benthic habitat map of San Juan Channel.....	56
Figure 4-6	Legend of marine benthic habitat map of San Juan Channel.....	57
Figure 4-7	Marine benthic habitat map of the Strait of Juan de Fuca.....	58
Figure 4-8	Legend of marine benthic habitat map of the Strait of Juan de Fuca.....	59
Figure 4-9	Marine benthic habitat map of Haro Strait.....	60
Figure 4-10	Legend of marine benthic habitat map of Haro Strait.....	61
Figure 4-11	Marine benthic habitat map of the Boundary Pass region.....	62
Figure 4-12	Legend of marine benthic habitat map of the Boundary Pass region.....	63
Figure 4-13	Distribution of bedforms of varying sizes.....	65
Figure 4-14	Multibeam bathymetry raster difference map created from data collected in the Boundary Pass region.....	67
Figure 4-15	Multibeam bathymetry raster difference map created from data collected in San Juan Channel.....	68
Figure 4-16	Obstacle marks identified in multibeam bathymetric data.....	69
Figure 4-17	Images from ROV dive in San Juan Channel.....	70
Figure 4-18	Multibeam bathymetry and associated marine benthic habitat map of San Juan Channel.....	72
Figure 4-19	Percent composition of fish families in non-sand waves and sand waves and among sediment features (crest and trough) in individual bedforms.....	78
Figure 4-20	Percent composition of fish families among various substrates.....	80
Figure 4-21	Percent composition of fish families among geological features of varying slopes.....	81
Figure 4-22	ROV image of sand lance emerging from sediment waves.....	82

Figure 4-23	Mussel shells in sediment wave troughs in San Juan Channel.....	84
Figure 4-24	Percent composition of invertebrate families in non-sand waves and sand waves and among sediment features (crest and trough) in individual bedforms.....	89
Figure 4-25	Percent composition of invertebrate families among various substrates...	90
Figure 4-26	Percent composition of invertebrate families among geological features of varying slopes.....	91
Figure 4-27	Image of BPI DEM overlaying multibeam bathymetry.....	93
Figure 4-28	Image of slope map derived from multibeam bathymetry.....	94
Figure 4-29	Pie charts showing results of sediment grab samples.....	95
Figure 4-30	Example of sediment grab sample collected in Boundary Pass sediment wave field.....	96
Figure A-1	Image depicting acoustic beams transmitted by multibeam sonar.....	124
Figure A-2	Processing backscatter data without slant range.....	125

LIST OF TABLES

Table 3-1	Sedimentary bedform classification scheme.....	35
Table 3-2	Beach grain size categories.....	35
Table 4-1	List of fish families observed in San Juan Channel.....	74
Table 4-2	List of transect area and fish density calculations from ROV survey in the San Juan Channel.....	76
Table 4-3	G-Test results for fishes.....	77
Table 4-4	List of invertebrate families observed in the San Juan Channel.....	84
Table 4-5	List of transect area and invertebrate density calculations from ROV survey in San Juan Channel.....	86
Table 4-6	G-Test results for invertebrates.....	88

1 INTRODUCTION

Diverse marine benthic habitats occur throughout the Puget Sound/Georgia Basin region. These include rocky bedrock outcrops, soft-sediment systems and dynamic sedimentary bedforms. Rocky habitats have been extensively studied in the Puget Sound/Georgia Basin region (Matthews, 1990a,b; Pacunski and Palsson, 2001; Tilden, 2004; Murie et al., 1994; Richards, 1986, 1987; West et al., 1995; Buckley, 1997); however, soft-sediment habitats for fishes and invertebrates in the area have not been thoroughly researched.

The Puget Sound/Georgia Basin region includes the San Juan Archipelago and the Straits of Juan de Fuca and Georgia Basin which are termed the Northwest Straits of Washington. This area is comprised of relatively narrow fjords and channels (Mackas and Harrison, 1997) and is located within the San Juan Thrust System (Bergh, 2002). This area is located between Vancouver Island, the North Cascades and the Olympic Peninsula and is the product of both past and present tectonic processes. It was formed in the Late Cretaceous period as a result of a collision of the Insular Superterrane with the western margin of North America (Feehan and Brandon, 1999).

The region has a complex tectonic history and has experienced convergence, thrust faulting and uplift, subsidence, glaciation, tidal scour and sediment transport. These processes have changed and shaped both the terrestrial and the marine environment. Metamorphic, plutonic and sedimentary rocks have been affected by these tectonic processes and have produced diverse marine benthic habitats which vary from dynamic sedimentary bedforms, to glacially scoured bedrocks, moraines, to fractured and

faulted bedrock outcrops. Geologic classifications of previously interpreted multibeam data varied in age and ranged from Holocene to Pleistocene to Quaternary (Tilden, 2004). Additionally, anticlines, synclines, and thrust faults were identified. Study areas included in this study encompass both shallow and deep waters within the Boundary Pass, Haro Strait, San Juan Channel, and Strait of Juan de Fuca regions in the San Juan Archipelago, Washington, and Georgia Basin, British Columbia (Figure 1-1).

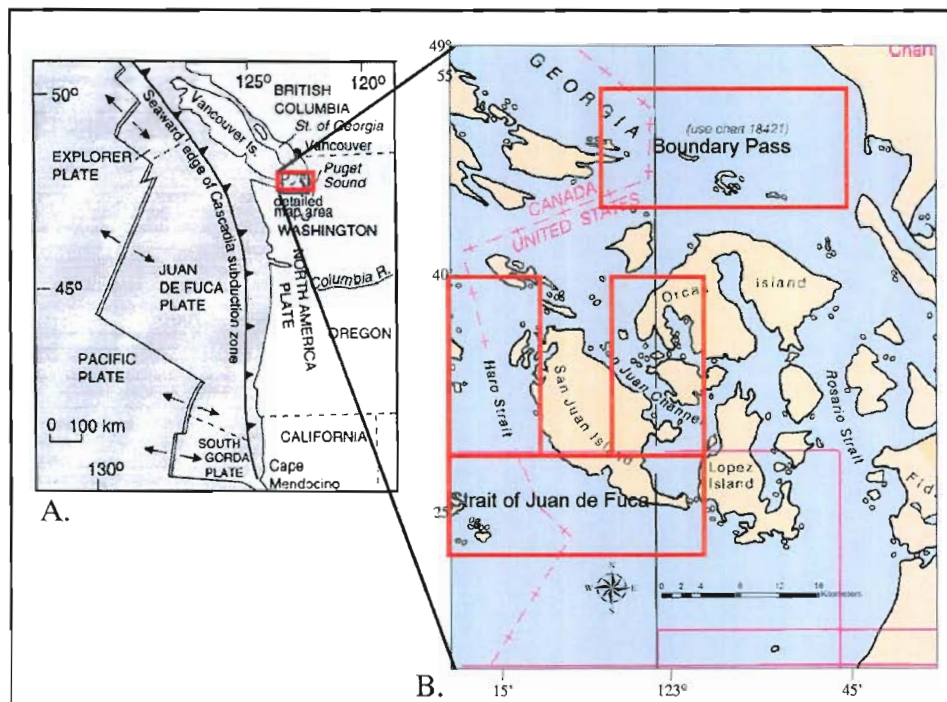


Figure 1-1 A. Index map of the Pacific Northwest depicting study area and tectonic elements where the Juan de Fuca Plate subducts beneath the North America Plate (after Williams and Hutchinson, 2000). B. Index map of the San Juan Islands, Washington, and Transboundary region, Canada. Study areas outlined in red include Boundary Pass, Haro Strait, Strait of Juan de Fuca and San Juan Channel.

There have been numerous studies regarding the relationship between marine fishes and highly rugose substrate; however, studies concerning the relationship between fishes and invertebrates and sedimentary bedforms as habitat, specifically, in the Puget Sound/Georgia Basin region, are few (Becker 1984). The broad goal of this study was to identify and characterize sedimentary bedforms occurring within this region and to map their distribution, placing emphasis on habitats for fishes and invertebrates associated with sedimentary bedforms. The specific goals were to identify and characterize bedforms using remote sensing data according to the deep-water classification scheme for marine benthic habitats created by Greene et al. (1999; 2005); to evaluate existing seafloor video imagery and sediment samples to determine relationships between sedimentary bedforms and fishes and invertebrates as a function of sediment grain size and composition; and, to gain a better understanding of the physical and biological characteristics of the Northwest Straits region, which may assist scientists with resource management objectives.

The hypothesis tested for this project was that there are substrate-specific relationships for fish and invertebrate families with a null hypothesis that species occurrences are independent of habitat types. The work presented here examined how fishes and invertebrates inhabiting varying substrate types elect habitat based on geological characteristics that influence their distribution and percent composition.

2 BACKGROUND INFORMATION

2.1 SEDIMENTARY BEDFORMS

2.1.1 SEDIMENTARY BEDFORMS AND CONSTRUCTION

Sedimentary bedforms are features of relief created on the bed of a fluid flow as a result of an unstable interaction involving the flow and the bed material (Allen, 1968). The bed may be composed of loose grains, cohesive mud or rock. Sedimentary bedforms occur in a variety of environments and water depths. They are compiled of assorted morphologies, dimensions and sediment types. Sedimentary bedforms can be classified and characterized based on their environment and processes of formation and grain size (Wynn and Stow, 2002).

Sedimentary bedforms can be observed in a variety of aquatic environments throughout the world. Examples include the Monterey Canyon and the San Francisco Bay, California; the Hudson Estuary, New York; the Danish Wadden Sea; the Cyclades Plateau in the northeast Mediterranean; the Gulf of Cadiz in the Atlantic Ocean; and, the Strait of Juan de Fuca and the Strait of Georgia, British Columbia (Verhagen, 1989; Hughes Clarke et al., 1996; Wynn et al., 2000; Mosher and Thomson, 2000, 2002; Normark et al., 2002; Todd, 2005; Barnard et al., 2006). Submarine sedimentary bedforms have been researched for the purpose of understanding sediment transport, deposition and dynamics associated with bottom currents, turbidity currents and gravity flows (Wynn et al., 2002b; Habgood et al., 2003; Cattaneo, et al., 2004; Hoekstra et al., 2004; Gutierrez et al., 2005), and for characterizing bedforms (Wynn and Stow, 2002; Goff et al., 2005). Studies have also been made describing associations where sediment

waves were considered habitat for fishes (Auster, 1985; Gerstner 1998; Gerstner and Webb, 1998; Norcross et al., 1999; Auster et al., 2003; Stoner and Titgen, 2003).

A field of well-formed submarine sand dunes was identified south of the junction of Haro Strait and the Strait of Juan de Fuca, British Columbia, and was surveyed with sub-bottom profile, sidescan sonar and multibeam bathymetric systems (Mosher and Thomson, 2000; 2002). The field included sand and fine gravel (> 0.5 mm). The largest of the sand dunes were 25 m in height, 300 m in wavelength, 1,200 m in width and occurred in 97 m water depth (Figure 2-1). Based on grain size analysis, the dunes are composed of coarse sand (Mosher and Thomson, 2000). It has not been determined whether these sand dunes are modern or relict, but it is thought that high currents in the Strait of Juan de Fuca contribute to their construction (Mosher and Thomson, 2000) and are evidence that sediments are being actively transported (Hewitt and Mosher, 2001).

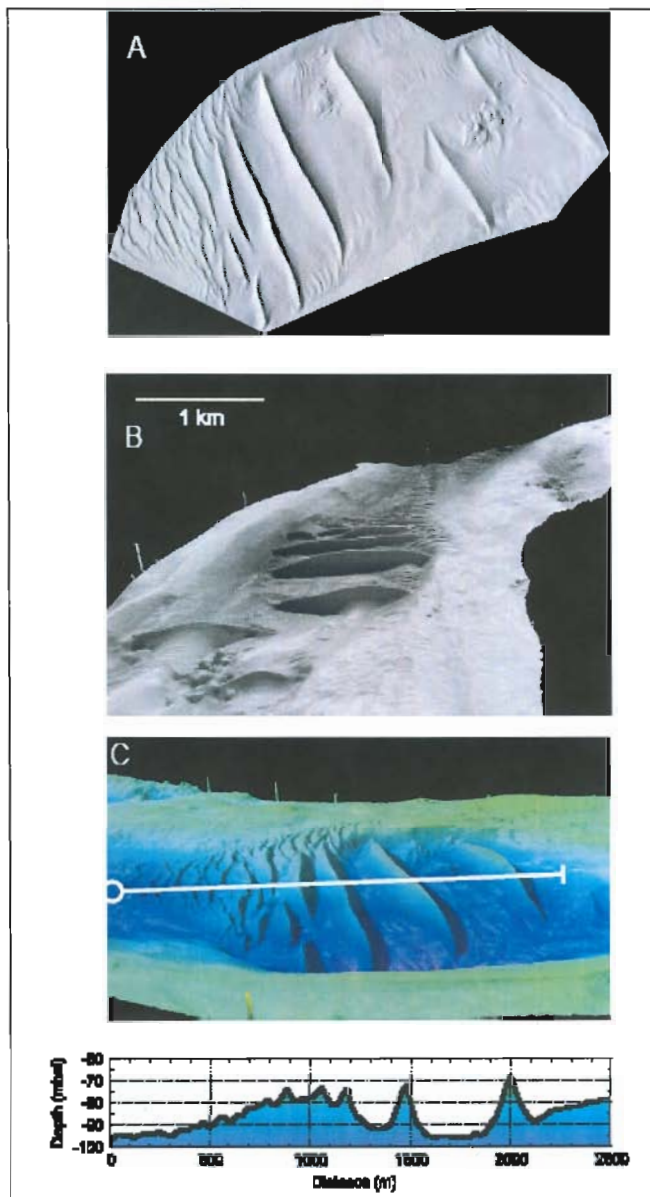


Figure 2-1 Sun-illuminated multibeam imagery of dune field in eastern Juan de Fuca Strait. Vertical exaggeration is 6x. A) plan view, B) view facing west, C) view facing north (after Mosher and Thomson, 2000).

In the marine environment, variables influencing the creation of bedforms include velocity, slope, water viscosity, sediment concentration, water depth and sediment grain size. Sediment wave generation requires rugosity on the initial seabed surface (Mosher and Thomson, 2000). Waves and currents shape the seafloor as depositional and erosional features (Seibold and Berger, 1996). These features range in size from small ripples to large submarine dunes fields. Height to wavelength relationships are not the only result of grain size. For instance, the wavelengths of coarse-grained sediment waves are directly proportional to flow velocity, or, bed shear stress (Wynn et al., 2002a,b).

2.1.2 BEDFORM CLASSIFICATION

Bedforms are classified using a variety of schemes and can be based on wave forming processes including bottom currents, turbidity currents or unknown processes (Wynn and Stow, 2002; Wynn et al., 2002b). When it is known that the sediment waves originated from a bottom current, the waves are classified as *bottom current sediment waves*. When turbidity currents are responsible for producing sediment waves, they are classified as *turbidity current sediment waves*. When the process or processes producing sediment waves are unknown, waves are classified as *fine-grained sediment waves* dominated by mud and silt or *coarse-grained sediment waves* composed mostly of sand and gravel (Wynn and Stow, 2002; Wynn et al., 2002b).

The scheme used in this study is a working classification system of all wave types created by Wynn and Stow (2002), who classify and characterize deep-water sediment waves, including bottom current sediment waves with bottom current origin. The bedforms studied for this project are bottom current sediment waves which can be

classified as fine- or coarse-grained. Fine-grained bottom current sediment waves are composed of mud and silt. Coarse-grained bottom current sediment waves consist of sand and gravel.

2.1.3 GRAIN SIZE

The grain size of clastic sediment is a measure of the energy of the depositing medium and the energy in the basin of deposition (Reineck and Singh, 1980). Grain size decreases in the direction of transport (Reineck and Singh, 1980). Pebbles move according to this process, whereas, sand-sized sediments do not show as dramatic a decrease in grain size downcurrent. A downcurrent decrease in grain size is attributed to abrasion and progressive sorting processes (Pettijohn, 1957) where abrasion is the key factor in the decrease in grain size. During progressive sorting processes, energy decreases and coarser sediments are deposited first and finer sediments are deposited farther downstream from the source than the coarser sediments (Reineck and Singh, 1980).

The size (wavelength and height) of sedimentary bedforms is a function of a variety of environmental factors, such as water depth, current speed, and grain size (Mosher and Thomson, 2000). Previous studies have shown that the size of sedimentary bedforms increases as water depth increases (Yalin, 1964, 1977, 1987; Allen, 1982; Ashley, 1990; Southard and Boguchwal, 1990; Dalrymple and Rhodes, 1995). It has been postulated that dune wavelength (L_D) is about six times the water depth (h) and dune height (H_D) is about 17% of the water depth (Yalin, 1964, 1977, 1987) where:

$$L_D = 6h \text{ and } H_D = 0.167h$$

Water depth cannot be considered as a primary control for determining bedform size as an increase in mean flow velocity is also a factor (Flemming, 2000). Additionally, water depth limits bedform growth once the flow acceleration above bedform crests arrives at a grain-size dependent critical suspension velocity (Flemming, 2000).

2.1.4 SEDIMENT GRAIN MOVEMENT AND MIGRATION

Sediment grains begin moving when the collective lift and drag forces produced by the fluid surpass the gravitational and cohesive forces of the sediment grain (Reineck and Singh, 1980). The entrainment of grain on a sediment bed is established by the water flow velocity and sediment grain size (Reineck and Singh, 1980). Other factors that may affect the entrainment velocity of sediment grains include the shape and position of the sediment grains, composition of sediment, flow turbulence and packing type of the sediments (Reineck and Singh, 1980).

Hjulström (1935, 1939) created a plot which illustrates the relationship between grain size and critical tractive velocity at which grain movement begins. This can be determined by analyzing the flow conditions that move the largest grain. The effects of specific gravity, suspension load concentration and deposition velocity were later added to Hjulström's diagram by Sundborg (1956, 1967) (Figure 2-2). Once the grains are in motion, they continue to move even if the flow velocity is below the critical value of erosion (Reineck and Singh, 1980). For coarse grains, Hjulström (1935, 1939) found that the size of sediment that is moved is proportional to the velocity. For finer grains (<0.1 mm), Hjulström (1935, 1939) found that to move grains with greater cohesive forces, more energy is needed for movement as the grain size decreases.

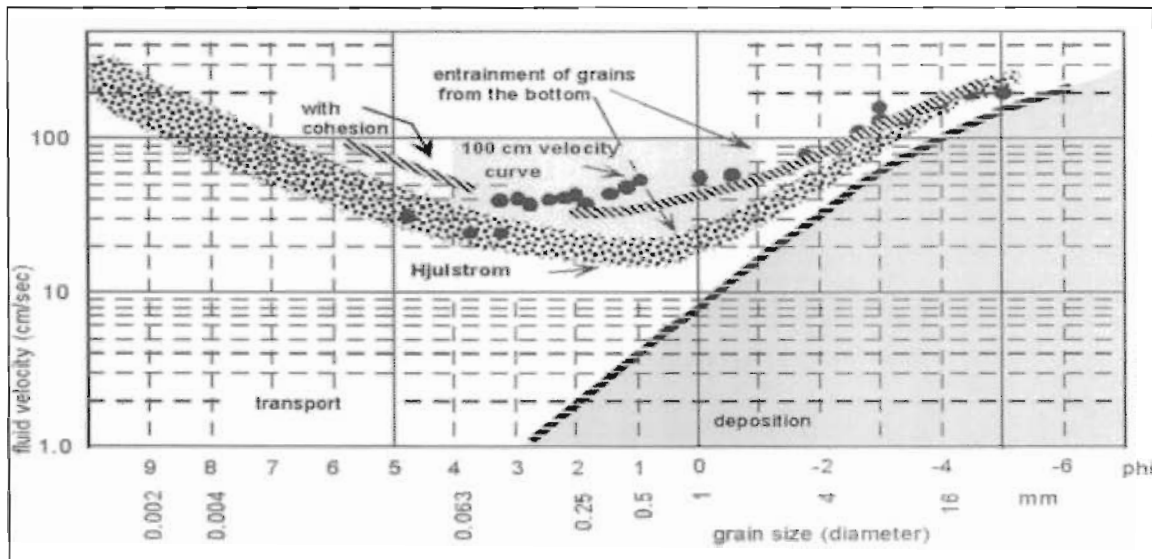


Figure 2-2 Hjulström curve showing the relationship between current velocity, shear stress and grain size. Entrainment, transport and deposition are depicted and compared with the flow velocity versus grain size. The boundary between the deposition area and the transport area (shown with arrows) represents the velocity needed to initiate transportation of the grain (after Brockport, 2005).

The relationship between shear velocity, grain size and suspension criteria is illustrated in a modified version of the Hjulström diagram (Figure 2-3) where there is a change from sand wave (straight-crested megaripples) to dune (three-dimensional megaripples) above the suspension criteria (Reineck and Singh, 1980). Suspension criteria refer to the suspension and traction of sediment in the water. Reineck and Singh (1980) found that the rate of migration of ripples is dependent on the current velocity and the grain size. As the current velocity increases, the average rate of ripple migration increases. Maintaining current velocities, the rate of ripple movement is higher for coarser sand than in finer sand (Reineck and Singh, 1980). Small ripples move at a rate faster than megaripples. On average, large sand waves migrate at rates of 30–100 m/24

hours (m/hr), or, 30–100 m/86,400 s (m/s) (Coleman, 1969) and waves up to 16 m have been known to move at a rate of 700 m/24 hr (m/hr), or 700 m/86,400 s (m/s) (Reineck and Singh, 1980).

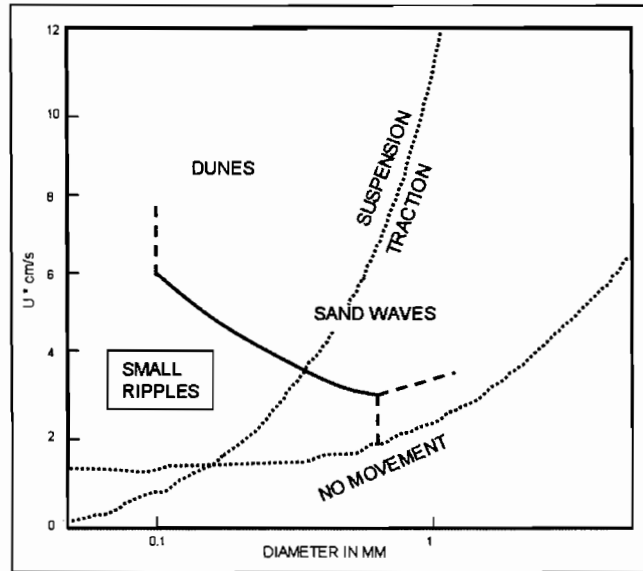


Figure 2-3 Plot of shear velocity and grain size depicting fields of no movement, traction movement, and suspension transport. The Y-axis units refer to calculations where the shear velocity (U) is multiplied by centimeters per second and x-axis refers to the diameter of the grains in millimeters. Modified after Reineck and Singh, (1980), which was modified from Hjulström (1935, 1939).

There are three modes of sediment transport which include rolling, saltation and suspension (Reineck and Singh, 1980). Sediments that undergo rolling transport are usually the most coarse-grained. Hydrodynamic factors such as current velocity, water depth and the nature of the bed influence the maximum size of sediment grains transported by saltation (Figure 2-4). The maximum size of a grain held in suspension depends on the turbulence energy of the transporting medium (Reineck and Singh, 1980) and is less than 0.1 mm (Lane 1938). As grains undergo saltation, they are suspended

periodically and bounce along the bed due to their heaviness. The suspended load involves particles in suspension which rarely make contact with the bed.

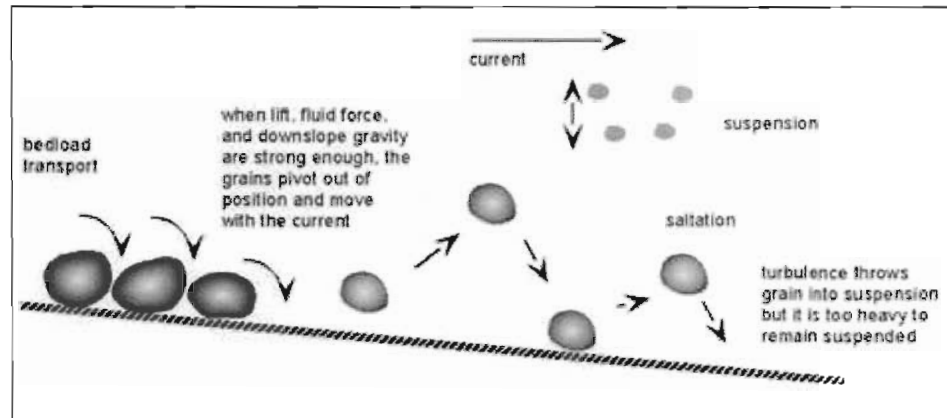


Figure 2-4 Modes of transport in an aqueous environment include sliding, rolling, saltation and suspension. As grains slide and roll, they remain in continuous contact with the bed (after Brown et al., 2000).

2.1.5 BEDFORM SIZES

Small ripples are small sedimentary bedforms with gentle upstream slopes and steep downstream slopes (Reineck and Singh, 1980). The ripples are generally less than 30 cm in distance from trough to trough and are not over 60 cm in wavelength (Reineck and Singh, 1980). At the time of formation, ripples are parallel, long-crested and have small amplitudes. As flow intensity increases, larger irregular ripples can be constructed. The length of the ripples does not depend on sediment grain size. For example, a velocity of 0.2 m/s is required to create ripples composed of fine sand.

Longitudinal wave ripples are characterized as straight-crested and are found in shallow-water muddy environments (Figure 2-5). Ripple lengths vary from 0.0025–0.05 m. They form from the combination of wave action and currents. Ripple crests are

oriented parallel to the current; and, wave propagation is situated at right angles to the current (Reineck and Singh, 1980). The currents cause erosion in the ripple troughs, but also maintain crest form.

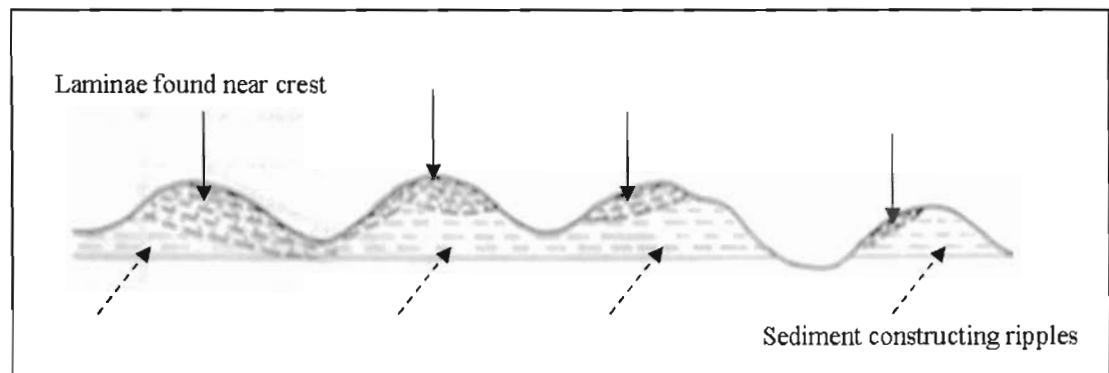


Figure 2-5 Illustration of internal structure of longitudinal ripples which are features that are erosive where laminae (solid arrows) are found near the crest. Dashed arrows indicate sediment constructing longitudinal ripples (after Reineck and Singh, 1980).

Southard (1975) characterizes megaripples as having heights of 1–5 m with high length/height (L/H) ratios. Megaripples also have sinuous to cusate shapes that form at flow velocities ranging from 0.7–1.5 m/s. Dune refers to three-dimensional forms (sinuous to lunate megaripples) with strongly sinuous crests, whereas sand wave signifies two-dimensional forms (straight-crested megaripples) (Middleton and Southard, 1978).

Megaripples are created when there is an increase in the rate of bed material transport, an increase in magnitude of velocity, and an increase in the degree of turbulence (Reineck and Singh, 1980). When shear stress values decrease, small ripples form on the backs of megaripples. As shear stress values increase, the ripples disappear. The lengths of megaripples vary from 0.6 m to several meters. The length and shape of

megaripples are the function of the grain size of the bed material (Reineck and Singh, 1980).

Sand waves are formed at lower current velocities than megaripples and are depicted by straight, continuous crests (Reineck and Singh, 1980). Sand waves have high length/height ratios. Sand waves commonly have lengths of 5–100 m and can be constructed under flow conditions with velocities of 0.3–0.8 m/s. (Reineck and Singh, 1980).

High-energy sand waves are the largest bedforms found. They are composed of coarser sediments and occur in water depths in excess of 4–5 m. They show superimposed megaripples on the stoss side. Sand waves are produced at higher energies than megaripples.

2.2 FISH AND INVERTEBRATE HABITAT

A marine benthic habitat is defined by its geology, depth, chemistry, sedimentology and associated biotic communities (Greene et al., 1999; 2005, 2007). Habitat structure includes the variety, abundance and spatial arrangement of physical and biological processes (Thrush et al., 2001). The term habitat is abstract and includes the combination of dynamic features and ecological processes that supply a functional space for a particular species (Stoner, 2003).

These definitions can also be applied to fishes and invertebrates. Stoner (2003) used the queen conch (*Strombus gigas*), a multi-habitat living organism (shallow, coral-rubble; bare sand; seagrass and turtlegrass beds; algae-covered hard bottom), as an example of whose distribution is dependent on settlement-stage larvae and water

circulation. Stoner (2003) emphasized that benthic marine species are not always associated with predictable habitat type including depth, temperature and bottom type. For example, ecological processes, physical and biological variables, including larval delivery systems, presence or absence of predators or prey, sediment size, bedform type, tube worm density, habitat complexity and depth were shown to have had an effect on flatfish distribution at varying spatial scales (Stoner et al., 2007).

Pacific sand lance are small forage fishes and are known for their utilization of sedimentary habitats. They play a role as the main linkage between zooplankton and upper level predators including marine mammals, seabirds and commercial fish (Robards et al., 1999a,b; Auster and Stewart, 1986; Field, 1988). Sand lance generally reach maturity at age two and spawn once a year (Robards and Piatt, 2000; Robards et al., 1999b). Sand lance spawn intertidally in late September/October on fine gravel/sandy beaches (Robards and Piatt, 2000); however, spawning season varies in time and length depending on the geographic location of a certain species of sand lance (Pinto, 1984).

Pacific sand lance are significant to this study because they are a common schooling forage fish and prey to upper level trophic species including commercial fishes such as Atlantic cod, haddock, silver hake, white hake, yellowtail flounder, longhorn sculpin (Auster and Stewart, 1986), lingcod and salmon (Geiger, 1987; Beaudreau and Essington, 2006). Other organisms which use sand lance as a crucial food source include common murres, rhinoceros auklets, harbor seals and minke whales (Geiger, 1987; Field 1988; Robards and Piatt, 2000).

Pacific sand lance are distributed along the coast from southern California to western Alaska (Robards et al., 1999a,b) and are commonly found in the San Juan Islands and the Georgia Basin (Garrison and Miller, 1982). Sand lance typically occur at depths less than 100 m and feed on zooplankton in the upper 20–25 m of the water column (Porter, 1997).

Sand lance are associated with mixed fine to coarse grain sand or gravel sediments in nearshore, estuarine, open coastal, and offshore habitats (Pinto et al., 1984; Wright et al., 2000; Reay, 1970; Auster and Stewart, 1986, Robards et al., 1999a,b). Sand lance have developed two practices of protecting themselves from predation. First, during the daytime, sand lance form schools while swimming in the water column; and, second, during the nighttime, sand lance bury themselves in the sand as they are unable to detect neither predators nor prey in limited to no light conditions (Garrison and Miller, 1982; Field 1988; Auster and Stewart, 1986; Hobson, 1986). Relatively high bottom current velocities must be present to provide aeration of the interstitial water (Auster and Stewart, 1986; Quinn, 1999). The interaction of substrate type with the oxygenated interstitial water is more critical in defining habitat for sand lance than is the variety of substrate particle sizes (Reay, 1970). Little is known as to why sand lance submerge themselves in the sand (Clayman, 2001), but it has been shown that such behaviors decrease the threat of predation and increase energy expenditure (Pinto et al., 1984; Wright et al., 2000; Hobson, 1986).

2.2.1 PREVIOUS STUDIES

Previous studies have demonstrated the relationship between fish distribution and physical, chemical, biological and geological oceanographic variables. Habitat selection by Pacific sand lance in Prince William Sound, Alaska, were modeled by investigating their distribution in relation to water depth, distance to shore, bottom slope, bottom type, distance from sand bottom and shoreline type (Ostrand et al., 2005). It was found that sand lance inhabited sand bottoms more than other bottom types.

Light intensity can play a part in the behavior, development and survival of fishes. Sand lance have been observed emerging from the sand and consuming larger quantities of prey (2-3 times greater) during higher light levels than levels of lower light (Clayman, 2001; Ireland, 2004; Porter, 1997). Sand lance were found to be more susceptible to predation during the transition period between day (when sand lance school and feed) and night (when sand lance seek refuge in sand) (Hobson, 1986).

Previous studies have also demonstrated the relationship between higher marine rockfish abundances and areas of hard substrate with high relief (Matthews, 1990a,b; O'Connell and Carlisle, 1994). There have also been studies in shallow-water rocky habitats in Puget Sound (Pacunski and Palsson, 2001) regarding fish-habitat relationships. However, these studies have not addressed sedimentary bedforms as marine benthic habitats using methods of Greene et al. (1999; 2005) for the Puget Sound/Georgia Basin region.

Certain demersal fishes in varying age groups are associated with benthic habitat features, such as biogenic structures and sand waves that provide complexity to a

homogeneous seafloor (Stoner and Titgen, 2003). A lab experiment designed by Stoner and Titgen (2003) investigated habitat suitability and the influence of seafloor structures on juvenile Pacific halibut and northern rock sole, two species found in the Gulf of Alaska and the Bering Sea in depths less than 50 m (Norcross et al., 1999). These flatfish were found to have significant utilizations for structured habitats, such as sponges and small sand waves rather than smooth sand substrate; and, increasing light levels played a role in distribution of the organisms. The utilization of habitats with structure offers shelter from predators and availability of foods (Stoner and Titgen, 2003, Becker 1984.)

Gerstner (1998) and Gerstner and Webb (1998) demonstrated that Atlantic cod (*Gadus morhua*) and American plaice (*Pleuronectes platessa*) utilized ripples as a refuge in which to save energy. The potential for ripples to slow current and to provide shelter from the flow was measured as a velocity ratio. The maximum velocity tested on any ripple was from 0 to 1.11 m/s. The ripples would therefore allow Atlantic cod and American plaice to maintain position in a current without actively swimming.

Ripples had an effect on plaices' station-holding performance by creating flow refuges in areas of delayed flow, by hindering behaviors that induce active swimming, and, by offering occasions for new plaice behaviors instead of active swimming. As the current speed increased, plaice situated their bodies parallel to the flow. With even more increasing current speed, plaice engaged in swim-deferring postures such as "body clamping" and "posterior fin beating." This position illustrated plaice pressing marginal fins to the substratum and raising the center of the body whereas posterior fin beating involved undulations passed posteriorly along marginal fins (Gerstner and Webb, 1998).

These studies are important to this project because they provide evidence of bedforms being utilized as habitat and instigate questions relating to fish energy savings, feeding, migration and shelter.

Mussels are also known to have associations with bottom types and are usually found on soft sediment environments in dense aggregations at various spatial scales (Snover and Commito, 1998; Kostylev and Erlandsson, 2001). Mussels settle in beds (sand, gravel, mud) ranging in size from tens of meters to kilometers. In high-density patches, mussels form clumps where they are connected with byssal threads.

Van de Koppel et al. (2005) investigated the spatial patterns of young mussel beds on soft sediments in the Wadden Sea located between Germany and the Netherlands. Based on spectral analysis and visual observations, young blue mussels (*Mytilus edulis*) were discovered exhibiting regularly spaced, band-like patterns (Van de Koppel et al., 2005). Mussels showed banded patterns aligned perpendicular to the flow of water and were not associated with underlying structures in the sediment (Van de Koppel et al., 2005).

Van de Koppel et al. (2005) explained that the reason for the banded patterns could be attributed to differentiated settling on sediment structures such as sediment waves. Also, increased turbulence over mussel beds could create mussel aggregation by enhancing the influx of algae from elevated water layers. A critical mechanism for mussel aggregation is a predator-prey interaction (Van de Koppel et al., 2005). Predation leads to reduction of prey causing heterogeneity in the prey population.

Schlining (1999) observed spot prawns inside and outside the Carmel Bay Ecological Reserve (CBER) in California. It was found that spot prawns were electing habitats

characterized by mixed sediment and consolidated substrata, such as gravel, cobble and boulders. High spot prawn densities occurred on a steeply sloping gravel bottom at 200 m water depth. Spot prawns, however, can reach depths of 400 m. There was a significantly larger catch-per-unit effort observed within the CBER when compared to outside locations. Based on video analyses, it was determined that spot prawns are not found on the most commonly available habitat, but are habitat-specific based on depth.

2.3 PHYSICAL OCEANOGRAPHY

The San Juan Archipelago lies in the junction of three major water bodies: Puget Sound, the Strait of Georgia and the Strait of Juan de Fuca. Puget Sound, a lowland connecting the Strait of Juan de Fuca through Admiralty Inlet, is dominated by tidal currents and net flows moving seaward near the surface and landward near the seafloor (Cannon et al., 2001). Currents run in an east-west direction in the broad, eastern part of the Strait of Juan de Fuca and are oriented in a north-south direction near the major channels which lead into the Strait. The tidal currents in the entry passages within the Puget Sound/Georgia Basin region cause strong vertical mixing resulting in weakly-stratified water (Mackas and Harrison, 1997).

The Strait of Juan de Fuca and Haro Strait form the main deep waterways while Rosario Strait is the shallow water body connecting the Puget Sound and Strait of Georgia marine basins with the Pacific Ocean. The Fraser River drainage basin which flows into Georgia Basin encompasses an area of over 234,000 km² and has an average annual discharge of 3,400 m³/s (Roberts and Murty, 1989). The Strait of Georgia, the San Juan Islands and the Strait of Juan de Fuca, is termed the Georgia-Fuca system

(Banas et al., 1999). This waterway serves as the estuarine link between the freshwater runoff of the continent and the saltwater environment of the Pacific Ocean (Banas et al., 1999). Glacial scouring caused by glacier advance from the last ice age is the primary mechanism for the creation of the Georgia-Fuca system which includes deep sills and basins (100 – 420 m) in the coastal ocean (Banas et al., 1999).

Estuarine circulation is the major control of the physical oceanography in the Georgia-Fuca system which has a connection with the open ocean at the west end of the Strait of Juan de Fuca. The Fraser and Skagit Rivers are the main sources of freshwater for the complex Georgia-Fuca system (Banas et al., 1999). The tides in the area consist of mixed-semidiurnal with two high and two low tides of unequal height each tidal period (Figure 2-6).

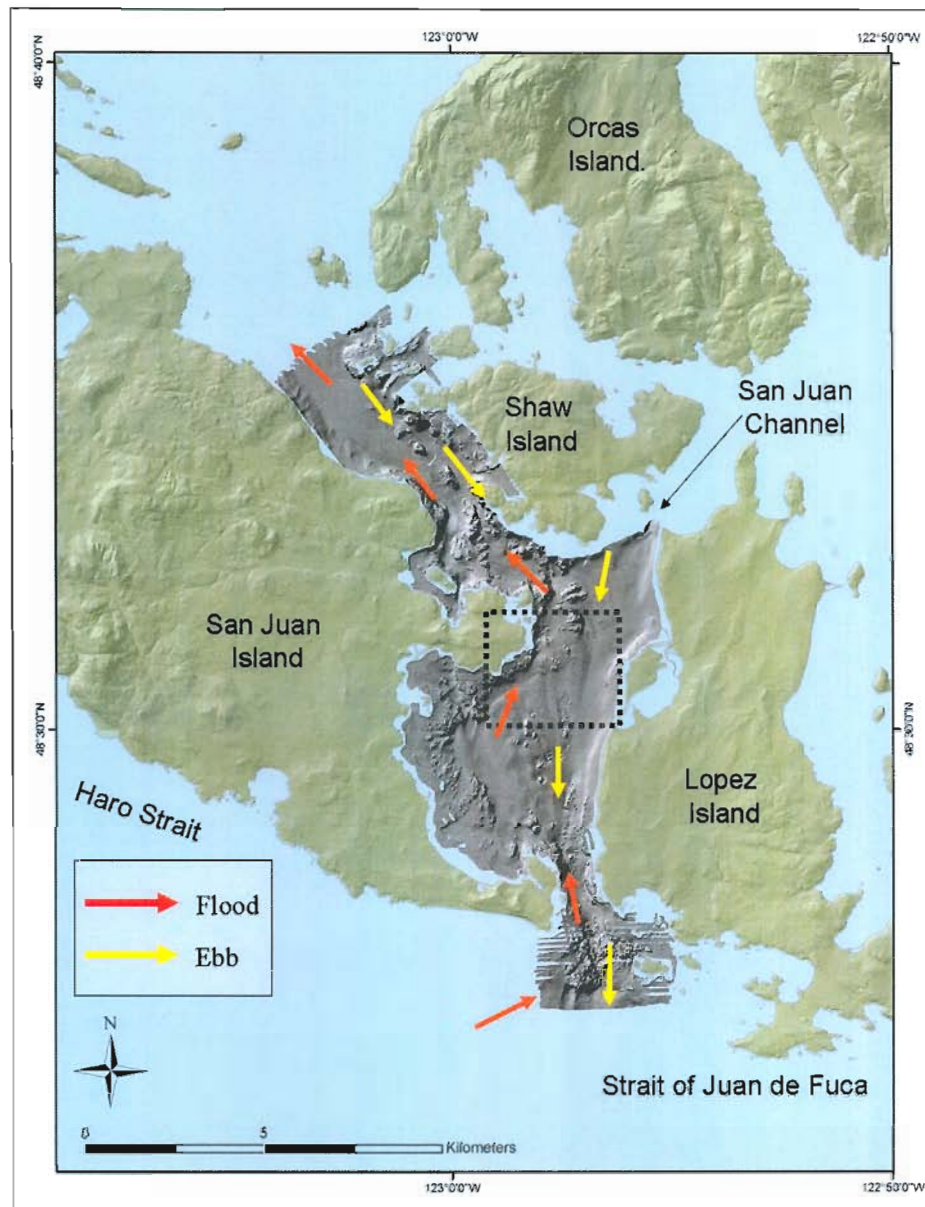


Figure 2-6 Ebbing and flooding directions in Georgia-Fuca system. Hill-shaded multibeam bathymetry and topographic data are shown. Dashed box indicates region where Pacific sand lance were observed emerging from large sand wave field (modified after Charles Endris, written communication, 2006; Banas et al., 1999).

Physical oceanographic processes presently form sedimentary bedforms within the Puget Sound/Georgia Basin region. The estuarine circulation transports water masses up to 0.1 m/s, but speeds may increase during storm events and bottom-water intrusions (Cannon et al., 2001). Daily tidal currents in the eastern Strait of Juan de Fuca have speeds of 0.75 to 1 m/s and have the potential to erode and transport material up to granule size (2-4 mm) (Hewitt and Mosher, 2001). Current velocities have been observed producing shifts in sediment wave structure and shell fragment distributions (Lindholm et al., 2004). Deep flood tides and estuarine circulation during the summer months are also possible mechanisms that can construct the bedforms found in the San Juan Islands region (Hewitt and Mosher, 2001).

A study was conducted at Friday Harbor Laboratories (FHL) exploring the physical oceanographic features of San Juan Channel (Banas et al., 1999). Conductivity temperature and depth recorders (CTDs) were implemented every two kilometers from Cattle Pass to the northern end of San Juan Channel to collect information regarding the presence of stratification along San Juan Channel. In addition, at the midway junction of the San Juan Channel junction near Turn Island, stratification and mixing mechanisms were explored by implementing three survey lines across San Juan Channel hourly over a two-day period. A boat towed a 300 kHz Acoustic Doppler Current Profiler (ADCP) from west to east for current profiling followed by CTD profiles from east to west across the channel (Banas et al., 1999). ADCP observations were recorded during transect data collection.

The Coriolis force, strong southward jets and the topography of the channel influence the behavior of the water movement. High velocities occurred during ebbing and then decreased uniformly. During flooding, the velocity was mostly consistent over the channel (Banas et al., 1999). The flow velocity changed depending on the location in the channel, for instance, both ebb and flood had maximum velocities in the deeper area close to the middle of the channel.

Vertical profiles revealed variations in stratification. Factors influencing this may be due to fresh water flow. For example, stratification existed at the maximum ebb tide. During slack water, the water column became less stratified and homogenous. When ebbing resumed, fresh, low-density water was brought back and vertical stratification began building (Banas et al., 1999).

3 METHODS

3.1 DATA COLLECTION

3.1.1 Multibeam Bathymetry and Backscatter

As a cooperative venture, the Geological Survey of Canada (GSC) and the Canadian Hydrographic Service (CHS) collected multibeam bathymetry and backscatter data for the Center for Habitat Studies at Moss Landing Marine Laboratories (MLML) in 2001 and 2002 using the hull-mounted Simrad® EM 1002 (95 kHz) and Simrad® EM 3000 (300 kHz) multibeam bathymetric sonar systems. Surveys occurred in the waters within the Haro Strait, Strait of Juan de Fuca, San Juan Channel, U.S. and the Boundary Pass region of Canada, utilizing the Canadian Coast Guard Ships (CCGS), *R.B. Young* and *Vector*.

The CHS utilized Simrad® sonar systems for the bathymetric surveys. The Simrad® EM 1002 system has a short to medium range multibeam echosounder designed for high-resolution seabed mapping and can map from the shoreline to a depth of 1,000 m. The system has up to 111 narrow beams of 2x2 degrees and a resolution of 2–8 cm (Simrad 2007a). The total swath width is 150 degrees and across-track coverage can be up to 1,500 m. In shallow water depths, across-track coverage can be 7.5 times the depth beneath the transducer (Simrad 2007a). Data were collected on a 24-hour basis for the Simrad® EM 1002 multibeam bathymetry surveys.

The Simrad® EM 3000 300 kHz echosounder has 127 single beams per ping and 1.5x1.5 degree beam width (Simrad, 2007b). The data were collected during the daytime with this sonar system. The CHS provided the final processed data which included

GEOTIFF files (*.tif and *.tfw), raw (georeferenced *.hdcs files), multibeam bathymetry and grids (*.asc). The CHS compiled the sound velocity data and applied motion and ray-bending corrections to the data.

The hull-mounted Reson 8101 SeaBat® (240 kHz) sonar system was used by the Seafloor Mapping Lab (SFML) at California State University, Monterey Bay (CSUMB) in 2000 using the *R/V MacGinitie*. Multibeam bathymetry and backscatter data were collected within small areas of the San Juan Islands, including Davis Point, Neck Point, Lawson Reef, Pile Point and Turn Island. The CSUMB SFML provided both the raw and final processed multibeam and backscatter data in form of GEOTIFFS and grids for the few small selected areas that they surveyed.

3.1.2 ROV Surveys

In the Fall of 2004 and 2005, a variety of seafloor habitats in northern and southern San Juan Channel (Figure 3-1) were groundtruthed by the WDFW using Deep Ocean Engineering's® Phantom HD2+2 (Figure 3-2). The WDFW provided their 12 m *R/V Molluscan* as an ROV platform. Methods for the ROV survey were devised by the WDFW. Surveys took place during daytime hours.

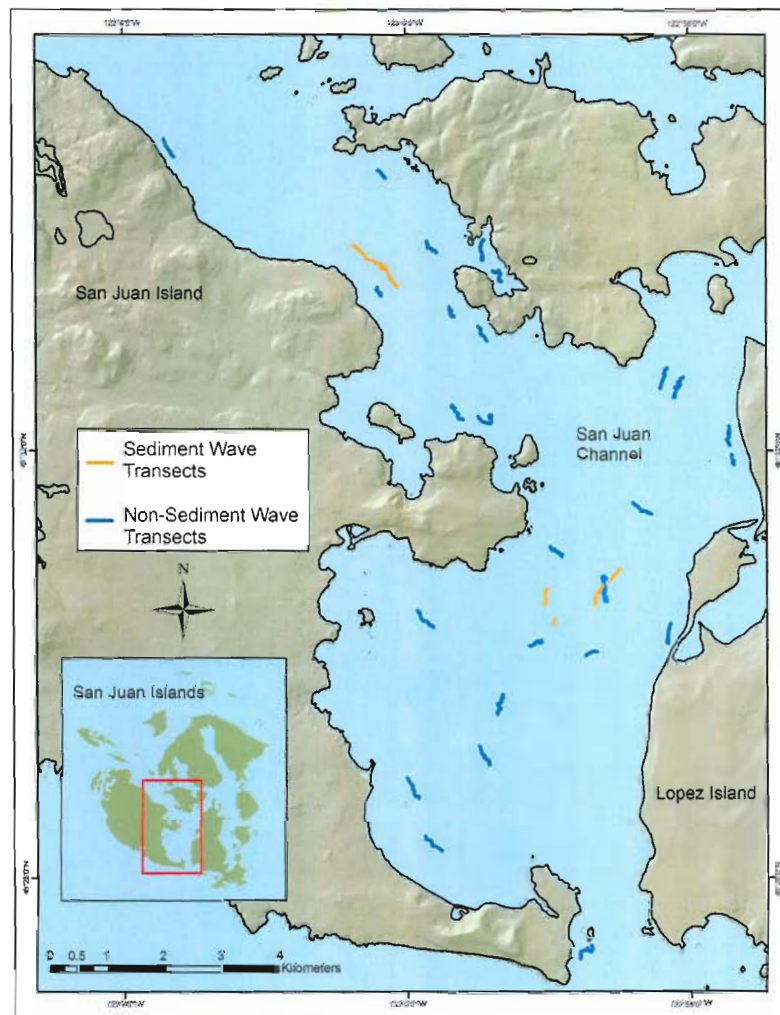


Figure 3-1 Tracklines from 2004 and 2005 ROV surveys in San Juan Channel. Tracklines overlay hill-shaded multibeam bathymetry. Scale 1:85:000.

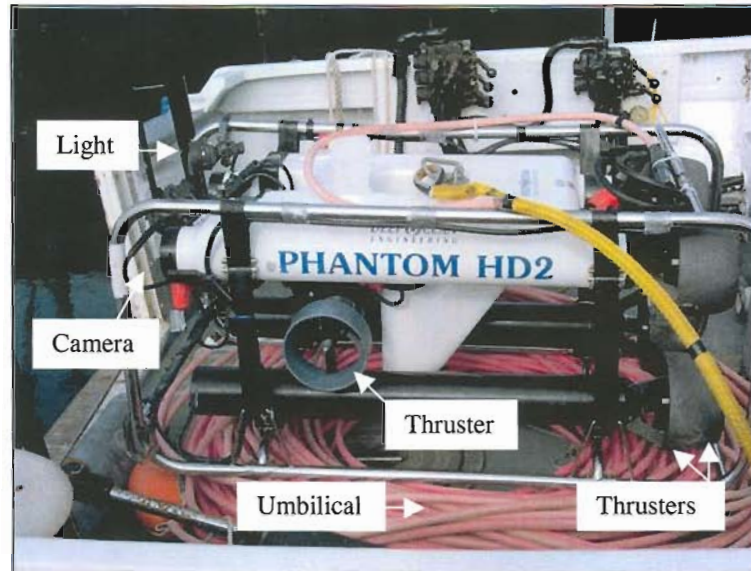


Figure 3-2 Photo of Deep Ocean Engineering's® Phantom HD2 ROV. The ROV umbilical was attached to a line which was attached to a 400 lb. clump weight. The purpose of the weight is to take strain off the umbilical.

The purpose of the ROV survey was to collect information regarding bottom fish habitat associations funded by Washington Sea Grant as well as to groundtruth marine benthic habitat maps produced at the Center for Habitat Studies at MLML. Transects were categorized based on depth and bottom type and included shallow/deep, soft/coarse and smooth/complex. Video data were also collected in areas characterized as sediment waves in San Juan Channel. Transect lengths were not uniform although the goal of the survey was to run transects with a minimum length of 400 m during a predicted slack tide. The bedform transects were longer because the WDFW crew of the R/V *Molluscan* wanted to allocate as much time as possible to collect high-quality video data for this thesis project.

Transects were conducted parallel to depth contours and maneuvered into the current to maintain vessel and ROV steerage. The ROV dives were divided by strata. The salient strata for this study included soft seafloor. To determine starting locations, random areas were chosen in ArcGIS 9.0 using the random line generator in Hawth's Analysis Tools (Hawth's Analysis Tools, www.spatial ecology.com, 2007). A minimum of three transects were designed for each strata. For each stratum, ten starting locations were created where the first three were chosen as primary points and the remaining seven were secondary points. Secondary points were selected when conditions prohibited ROV deployment including fishing activity, vessel traffic, obstructions and weather.

The ROV was equipped with four $\frac{1}{2}$ HP horizontal thrusters, two $\frac{1}{4}$ HP lateral thrusters, and one $\frac{1}{4}$ HP vertical thruster providing directional control. The ROV had a Sony EVI-330 high-resolution color zoom camera (>460 lines, wide end FOV = 48.8 deg. H, 37.6 deg. V), a fluxgate compass and a pressure sensor for computing ROV depth. The ROV's field of view had a forward viewing angle of $\sim 45^\circ$ below horizontal that maximized coverage of the seafloor during data collection and allowed the pilot an optimal driving view (Robert Pacunski, personal communication, 2006).

The ROV operated with two DeepSea Power and Light (DSPL) 250 W floodlights providing consistent lighting. One of the fixed lights is forward-directed and another is mounted to the camera, which pivots with the camera (Robert Pacunski, personal communication, 2004). The ROV is equipped with 10 cm spaced parallel lasers which aided in estimating measurements of sediment wave wavelengths in the videos. The laser spacing is proportional to the height of the ROV off the bottom. A video monitor was

installed on the bridge of the R/V *Molluscan* and enabled a live-feed from the ROV to an observer taking notes of habitat and organisms viewed in real-time. Additionally, while surveying, the pilot paused the vehicle occasionally to count and identify fishes and invertebrates.

An Offshore Research Engineering (ORE) TrackPoint II Ultra-Short Baseline (USBL) acoustic tracking system interfaced with a Northstar 952 DGPS system was installed on the vessel and was used to track the location of the ROV on the seafloor. An ORE 4330B multibeacon transponder mounted on the ROV was used to relay signals to the USBL system (Robert Pacunski, personal communication, 2004). To navigate the ROV, the USBL/DGPS system was connected to a KVH digital azimuth compass and a laptop computer running Hypack®MAX navigation software on the ship. Real-time positions of the vessel and ROV were recorded in one-second intervals.

To encode the time, depth, and calculated ROV location (input from Hypack®MAX) to the video signal, a PISCES video-text overlay system was used. The ROV's height off the seafloor varied between $\frac{1}{4}$ to $\frac{1}{2}$ m. The ROV speed varied during individual transects and ranged between 0.5 and 2 m/s. The average speed of each transect was calculated by dividing the transect length by the time.

When the ROV was used in depths less than 30 m, the ROV was driven by hand-feeding the umbilical cable over the support vessel's stern. At depths greater than 30 m, a 400 pound clump/(depressor) weight attached to a $\frac{3}{8}$ " braided Kevlar line was lowered with a winch and attached to the line every 6 m. The purpose of the weight was to take the strain off the umbilical and reduce roll affects. The ROV was driven 34 m astern of

the vessel and the umbilical was attached to the Kevlar line. The ROV was then driven back to the vessel and continued down the Kevlar line until it came in contact with the clump weight. The ROV pilot kept the clump weight in view of the ROV at all times. As the weight was deployed, the umbilical was attached to the Kevlar line at 25 m intervals until the clump weight was ~5 m off the seafloor. At that time, the ROV was positioned between 0.25 m and 1 m above the seafloor and a position fix was recorded. The ROV only dragged a small amount of umbilical at depth. Sometimes the clump weight influenced ROV positioning so the ROV was disoriented off the seafloor.

Video imagery collected in 2004 was supplied to the Center for Habitat Studies by the WDFW. The final transect data files were processed at the WDFW and provided in the form of Shape Files as Generalized Tracklines (GT). Positional errors (> 10m/sec) recorded in the navigation data were removed using Hypack®MAX single-beam editing software. Under Washington Sea Grant project #R/ES-59, the WDFW provided the Center for Habitat Studies with the ROV video data of each individual transect. These videos were copied onto Mini DV digital videocassettes which were compatible for viewing on the video system at the Center for Habitat Studies.

3.1.3 Sediment Sampling

A Peterson® grab sampler was used by the GSC to collect sediment samples in the Boundary Pass region in 2005. These samples were taken in the trough, crest and side of a sediment wave (Figure 3-3). This bedform field was identified based on multibeam bathymetry previously collected in the area and were characterized in marine benthic habitat maps at the Center for Habitat Studies at MLML.

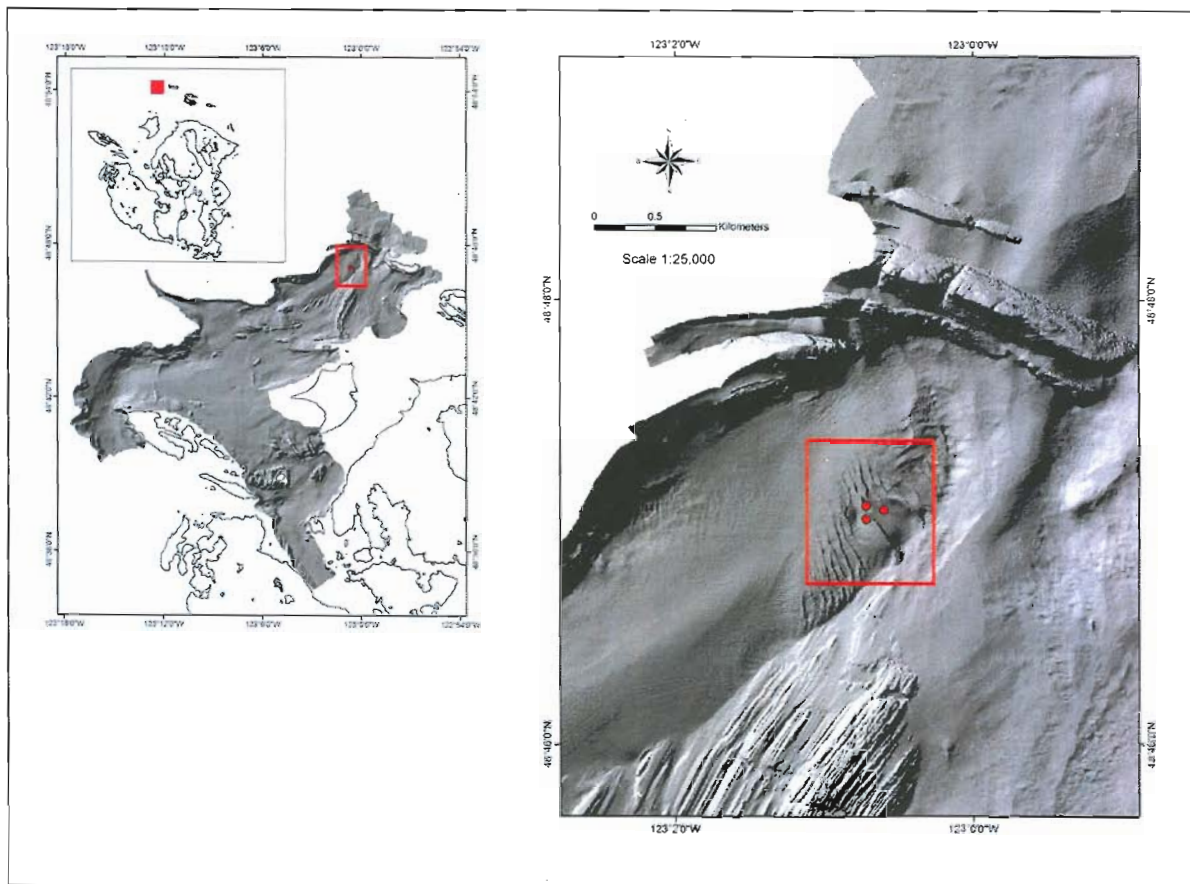


Figure 3-3 Location map of multibeam bathymetry showing location of three sediment grab samples (red points) collected in the crests and troughs of a sediment wave field in the Boundary Pass region. Samples provided by the GSC.

3.2 DATA ANALYSIS

3.2.1 Multibeam Bathymetry and Backscatter

3.2.1.1 MARINE BENTHIC HABITAT MAPS

Multibeam bathymetry and backscatter data collected in the areas of Boundary Pass, Haro Strait, San Juan Channel and Strait of Juan de Fuca, were analyzed with the GIS programs, ArcGIS 8.2® and ArcGIS 9.0®. Using these programs, the surface analyses of the multibeam bathymetry and grids produced including artificially sun-illuminated relief at varying angles and azimuths, slope-shaded relief, contours at varying

intervals depths and grids. These varying datasets were created to maximize data quality and define geologic features. Multibeam bathymetric data were gridded at a 2 m horizontal resolution indicating there is one sounding per 2 m x 2 m cell when viewed in a GIS. Therefore, these data cannot resolve seafloor features that are less than 2 m (horizontal). Multibeam bathymetric backscatter data were processed at 0.2 m resolution using a variety of programs, including ISIS®, DelphMap®, TnT Mips® and ArcView®. Multibeam bathymetric and backscatter data were projected in Universal Transverse Mercator (UTM), Zone 10, with a World Geodetic System (WGS) 84 datum and spheroid (*see* Appendix A for complete description of multibeam bathymetric backscatter processing procedures).

The remote sensing datasets were used in the interpretation and characterization of marine benthic habitat maps based on the Deep-Water Habitat Classification Scheme by Greene et al. (1999) (*see* Appendix B for descriptions for creating marine benthic habitat maps and Appendix C for Deep-Water Habitat Classification Scheme and Explanation). Individual habitats were assigned codes corresponding to a specific macro- or micro-habitat classification. All available data including multibeam bathymetry, multibeam backscatter, ROV video and sediment samples as well as the knowledge of the geologic history and physical oceanographic conditions of the region were used to make the characterizations for the creation of marine benthic habitat maps. Habitat characterizations entailed experienced knowledge of geologic and remote sensing principles.

In addition to interpreting geology from multibeam bathymetric and backscatter maps, a slope analysis was conducted using ArcGIS®. Varying slope values were assigned to bedforms identified in the multibeam bathymetry data. Slope was categorized as flat (0-5°), flat/sloping (5-30°), sloping (30-45°) and steep (45-90°). The category “flat/sloping” was used if the area viewed in the video was a combination of alternating flat and sloping seafloor.

3.2.1.2 SEDIMENTARY BEDFORMS

For this study, the characterization and classification system for coarse-grained bottom current sediment waves was used (Wynn et al., 2002b; Wynn and Stow, 2002, Wynn et al., 2000) and included the terminology from a classification scheme of bedforms (Reineck and Singh, 1980) as they related to the sedimentary bedforms identified in the Puget Sound/Georgia Basin region.

Various morphologies and sizes for bedforms was created and modified based on wave height and wavelength classifications by Wynn et al., 2002b; Wynn and Stow, 2002; and Wynn et al., 2000 (Table 3-1). Codes were assigned to bedform types for analysis. For sedimentary bedform analyses, grain sizes were calculated based on the Wentworth scale (Wentworth, 1922) (Table 3-2). Additionally, dune shape was measured using the ratio of wavelength to height, which is termed ripple index or vertical form index, according to Allen (1968). Low values (10–30) indicate steep dunes and high values (100–400) represent flat dunes.

Table 3-1 Sedimentary bedform classification scheme table displaying varying bedform types based on wave heights and wavelengths. Sedimentary bedform classification scheme modified from Wynn et al., 2002b, Wynn and Stow, 2002 and Wynn et al., 2000. Codes are applicable to characterization of sedimentary bedforms.

Code	Bedform Type	Wave Height (m)	Wavelength (m)
1	<i>Sand ripples</i>	< 0.006	< 0.6
2	<i>Sediment wave</i>	several	10s m - few kms
3	<i>Fine-grained bottom current</i>	up to 150	up to 10 km
4	<i>Coarse-grained bottom current</i>	few	up to 200
5	<i>Dunes</i>	0.2 - 25	1 - 200
6	<i>Ripples superimposed on dunes</i>	< 0.006 - 25	< 0.6 - 200

Table 3-2 Beach grain size categories table displaying beach grain size categories called the Wentworth scale of particle diameters. The ϕ scale is based on the negative logarithm (to base 2) of the particle diameter in millimeters [$\phi = \log_2 d$]. The coarser particles have negative values (after Bird, 2000).

Wentworth scale category	Particle diameter	ϕ scale
Boulders	> 256 mm	below - 80
Cobbles	64 mm - 256 mm	- 60 to - 80
Pebbles	4 mm - 64 mm	- 20 to - 60
Granules	2 mm - 4 mm	- 10 to - 20
Very coarse sand	1 mm - 2 mm	00 to - 10
Coarse sand	$\frac{1}{2}$ mm - 1 mm	10 to 00
Medium sand	$\frac{1}{4}$ mm - $\frac{1}{2}$ mm	20 to 10
Fine sand	$\frac{1}{8}$ mm - $\frac{1}{4}$ mm	30 to 20
Very fine sand	$\frac{1}{16}$ mm - $\frac{1}{8}$ mm	40 to 30
Silt	$\frac{1}{256}$ mm - $\frac{1}{16}$ mm	80 to 40
Clay	< $\frac{1}{256}$ mm	above 8

The multibeam bathymetry and backscatter data collected in San Juan Channel in Washington and the Boundary Pass region, Canada, were examined to identify sedimentary bedform structures. To gather information that would be used to determine average depth (m), wavelength (m) and height (m) of the bedforms in San Juan Channel and Boundary Pass, multibeam bathymetric grids were viewed in ArcGIS®. To determine which bedforms would be measured, Hawth's Analysis Tools was used to generate ten random points in the form of a Shape File (*.SHP) format within the bedform fields of San Juan Channel (Figure 3-4) and Boundary Pass (Figure 3-5). If a randomly generated point was located in the trough of the bedform, it was not used in the analysis.

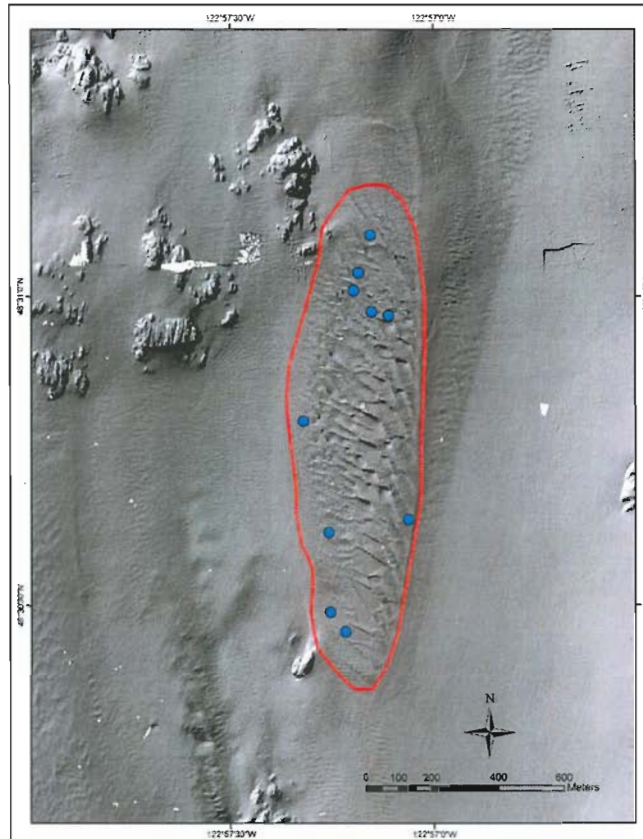


Figure 3-4 Image of multibeam bathymetry outlining bedform field in San Juan Channel showing randomly generated points which were used to determine bedform size including wavelength (m), height (m) and depth (m). Points were produced using Hawth's Analysis Tools.

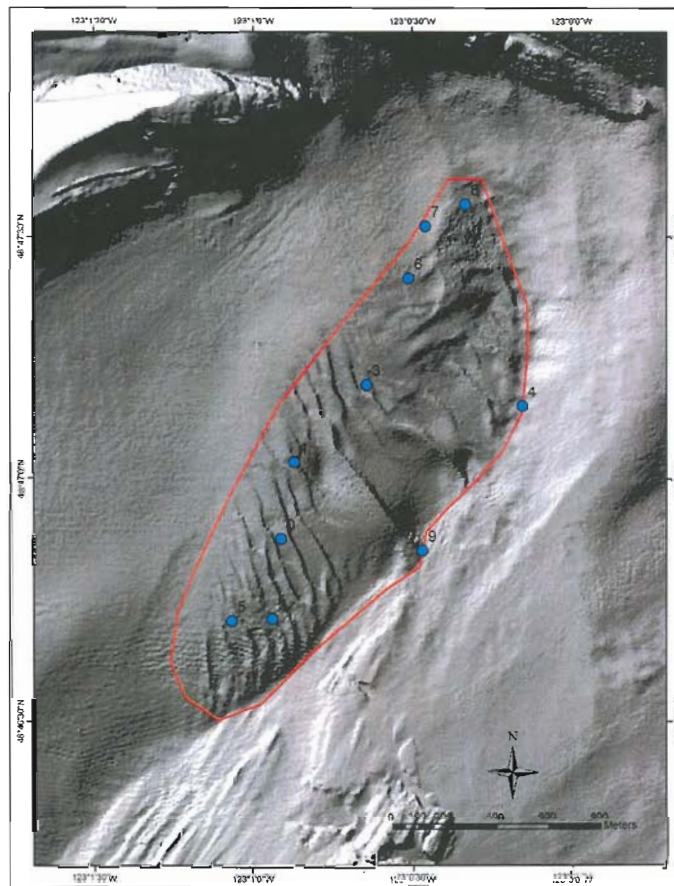


Figure 3-5 Image of multibeam bathymetry outlining bedform field in Boundary Pass region, Canada, showing randomly generated points which were used to determine bedform size including wavelength (m), height (m) and depth (m). Points were produced using Hawth's Analysis Tools.

In ArcGIS®, a tool created to measure features in the hill-shaded multibeam bathymetry was used to determine the wavelengths and heights (in meters) of the bedforms. Also, a tool was used to create profiles of the bedforms (Figure 3-6). The ID tool was used in ArcGIS® to acquire depth information from the grids.

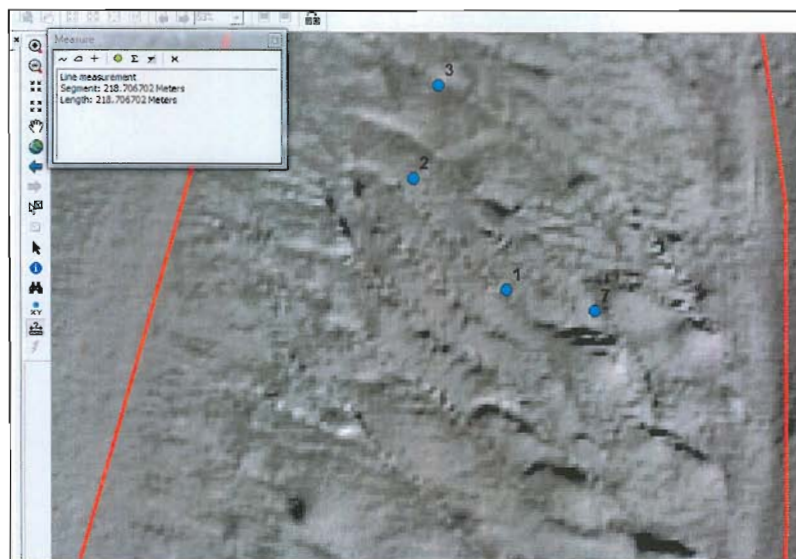


Figure 3-6 Example of bedforms measured in ArcGIS® in San Juan Channel where bedforms were measured using the measuring tool (in meters).

A multibeam bathymetric survey of a sediment wave field in the Boundary Pass region, Canada, was conducted both in 2001 and in 2003. The data from the two different years were compared in ArcGIS® and examined for sediment migration. Additionally, multibeam bathymetry data were collected in San Juan Channel in 2002 and 2006. These two datasets were also visually compared in ArcGIS®.

Tool marks have been identified in multibeam bathymetric data collected in the Puget Sound/Georgia Basin region. Tool marks are either objects lying in the path of currents or are objects moved by currents that produce markings on the sediment surface (Reineck and Singh, 1980). Tool marks can be divided into stationary tool marks, obstacle marks and moving tool marks. According to Reineck and Singh (1980), stationary tool marks are temporarily resting passive objects lying on the seafloor including wood, pebbles and shells. These types of tool marks are created when objects

come to rest on the seafloor and leave an imprint in the soft surface sediment. The shape of the moving tool mark is influenced by the mode in which the object is moved by dragging, rolling, or saltation. Moving tool marks refer to objects moving along the seafloor based on current flow. Markings differ based on the shape and size of the objects, the mode of transportation and the composition of the sediment surface (Reineck and Singh, 1980).

As objects such as pebbles or shells rest on the seafloor, obstacle marks are formed by currents that deflect around the object as a result of the object deflecting the flow lines. Obstacle marks are the product of the current flow. As sand collects on the downcurrent side of small objects, such as pebbles in the path of a current, small sand ridges form which narrow downcurrent. On the upcurrent side of the obstacle, a semicircular depression is produced. These features are called current crescents (Figure 3-7).

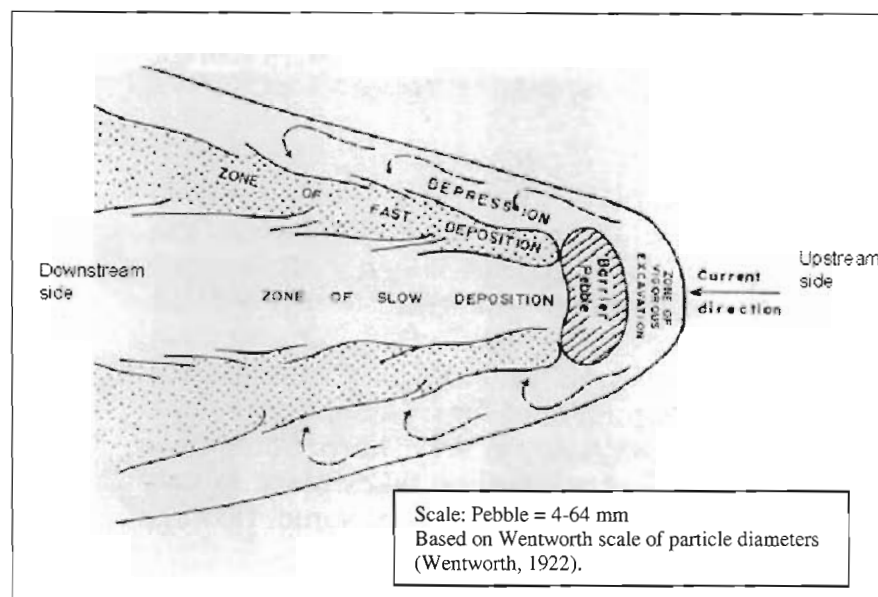


Figure 3-7 Illustration of development of a current crescent's pattern of flow and sedimentation mechanism (after Sengupta, 1966).

3.2.2 ROV Survey

3.2.2.1 Habitat

For this study, videos collected in 2004 and 2005 solely in soft sediment areas including sedimentary bedforms in San Juan Channel were used in the analysis. Transects were separated into sand wave and non-sand wave habitats. The sand wave habitats were further classified in a GIS and divided into crest and trough categories based on time bins taken from the ROV transects.

The methods for analyzing ROV videos, including area swept, was estimated based on methods of Pacunski and Palsson (written communication, 2006). Videos were first viewed by the WDFW and annotations were made. ROV video collected in sediment wave habitats was not viewed in WDFW analysis. For this project, ROV videos in all soft sediment areas were viewed again, including newly analyzed sediment

waves transects. Transect width was estimated every 60 seconds by measuring the plane of the lasers (10 cm) in relation to the measured distance of the dots on the video monitor to the width of the video monitor. The screen width was 27 cm. The laser dot width on the screen was measured physically with a ruler in millimeters, (e.g. 18 mm). To determine the center width (m), the screen width (cm) was divided by laser dot width (mm) (e.g. $27/20 = 1.35$). Average transect widths were summed and the total was divided by the number of bins in each transect. Distance traveled by the ROV for each transect was using Hawth's Analysis Tools' Table Tools function using ArcGIS®. This tool automatically calculated the length of each transect. Total area swept (km^2) for each transect was estimated by averaging the width estimates (m) and multiplying by transect length (m).

When viewing each individual transect, the tape was paused every 60 seconds and the primary geological information was recorded into a spreadsheet. No trackline editing was needed as it did not affect the overall distance traveled by the ROV. Habitat types were recorded for every 60-second time bin based on the overall geological feature of the area. Within each 60-second time bin, continuous habitat areas that included a minimum of 75% of one habitat type were documented and analyzed in the ROV video.

If the ROV flew above $\frac{1}{4}$ to $\frac{1}{2}$ m from the bottom, video collected during those transect lines, or parts of transect lines, were excluded from the analysis. When the ROV was off the seafloor for <10 seconds, there were no edits made to the trackline or video database. For time periods >10 seconds, the one-minute bin was categorized as "off transect" and the GT length was shortened based on the average speed of the ROV.

3.2.3.2 Fishes and Invertebrates

All commercially and recreationally important fishes and invertebrates were counted and identified to the lowest taxonomic level. Tapes were analyzed for the purpose of recording the fishes and invertebrates seen during each of the dives, accrued into 60 second time bins and recorded into a spreadsheet.

Densities were calculated to determine the average number of individuals per transect per km² for each of the families observed in the sand wave and non-sand wave habitats based on video analysis. For this analysis, transect width, length and area swept were calculated. Transects were first smoothed in ArcGIS® using a smoothing tool. Lengths were adjusted at the WDFW depending on tracking inconsistencies. For instance, if the ROV drifted off-transect and the ROV hovered off the seafloor for greater than 10 seconds and traveled too quickly to make accurate counts, or, if the ROV followed a fish for identification and traveled off-track, that particular length was omitted from the final length calculation (Robert Pacunski, personal communication, 2007).

Each transect and species count was weighted by area of each transect in both sand wave and non-sand wave habitats and substrate types. For each 60-second time bin, each count in each bin was normalized by the area of each transect and were summed on a per transect basis. A two-tailed T-Test was performed to determine statistically significant differences in means between the non-sand wave and sand wave habitats. Percent composition for each transect was calculated for fish and invertebrate families observed in the ROV videos in the gravel, mixed, rock and sand substrates. Hard and soft substrates were distinguished based on the deep-water classification scheme for

marine benthic habitats (Greene et al., 1999). Percent compositions were also calculated for families observed in the ROV videos among differing slopes.

Family level was used as not all organisms were identified to genus/species level. Observed numbers were determined from direct observations from the ROV video transects where the number of individuals of each fish and invertebrate family for each substrate type was calculated. To compute expected values for the fishes and invertebrate families, the total number of individuals observed in each substrate type was divided by the total number of individuals observed throughout all substrate types.

The observed and expected values were used in a two-tailed Chi-Square analysis using G-test statistics to test for differences among sand, gravel, mixed and rock habitat types in sand wave and non-sand wave transects. The G-Test was used to test the null hypothesis that the Poisson distribution supplies a sufficient fit to the observed data (Krebs, 1999). P-values were calculated using the following formula:

$$G = 2 \sum \{(\text{Observed frequency} [\log_e (\text{Observed frequency} / \text{Expected frequency})])\}$$

where G = Test statistic for log-likelihood ratio

To establish where fishes and invertebrates were located in the sediment waves (i.e., crest or trough), a Bathymetric Position Index (BPI) created in a GIS was incorporated into the multibeam bathymetric dataset. BPI is a measure of relative elevation which indicates the position of a given point in the overall surrounding landscapes using a Digital Elevation Model (DEM) (Figure 3-8). BPI can be used to identify different features such as peaks and valleys at specific scales (Figure 3-9). BPI

was used to identify areas of varying slope (for example, troughs and crests). BPI uses fine and broad scales to identify features. When using a BPI, a fine scale (large map scale) dataset allows users to identify smaller features within the benthic environment whereas in a broad scale (small map scale), larger features are identified.

In a GIS, the several layers were displayed, including hill-shaded and slope-shaded multibeam bathymetry and gridded BPI data shape files showing transect tracklines. The tracklines were attributed with information such as time and position information which was created while the ROV was traversing the seafloor. This information corresponded to the fish and invertebrate information recorded in a spreadsheet created during analysis of the ROV videos. For example, when fishes or invertebrates were identified during a 60-second time bin, the time at which the organisms were identified was recorded into a spreadsheet. The time stamp was obtained from the ROV video screen. Within each 60-second time bin and among time bins, the BPI was used to analyze where fish and invertebrate occurrences took place according to transect line files with corresponding time stamps. While utilizing the spreadsheet with time stamp information for fish and invertebrate occurrences, the line files with time stamp information in a GIS and the BPI grids, it was possible to estimate if organisms were occurring within the troughs or crests of sand waves.

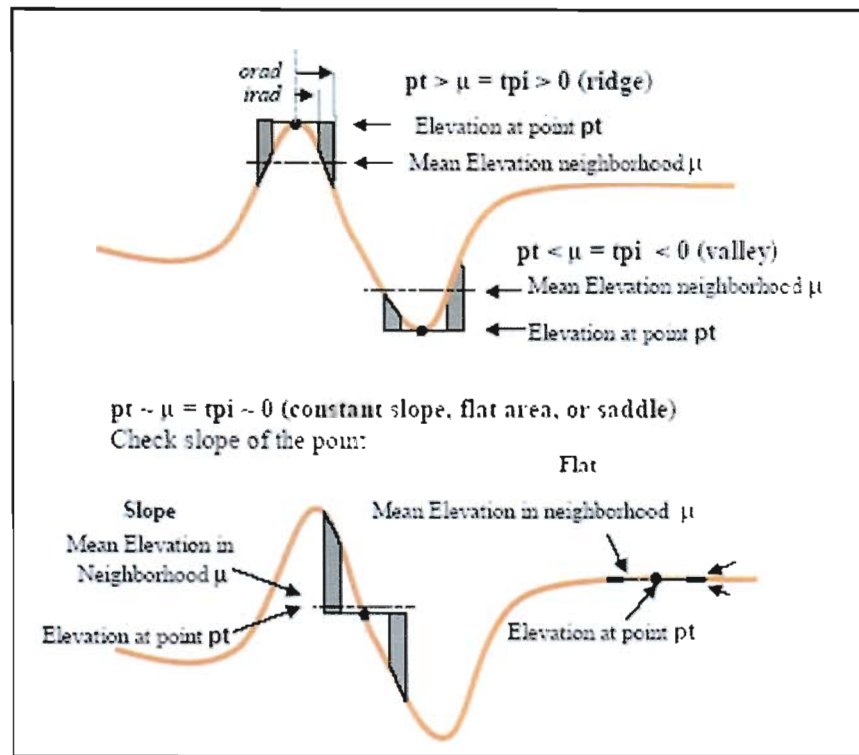


Figure 3-8 Illustration of Bathymetric Position Index (BPI). In a GIS, BPI measures relative elevation, which indicates the position of a given point in the overall surrounding landscapes using a Digital Elevation Model (DEM). BPI identifies different topographic highs and lows, such as peaks and valleys (after Weiss, 2001).

Several DEMs were produced to determine the appropriate values for the BPI analysis. BPI DEMs with neighborhood sizes of 10 and 50 m were created using a 2 m DEM. The BPI fine scale factor of BPI_{10} and broad scale factor of BPI_{50} were most appropriate for the analysis based on visual comparisons to the slope and hill-shaded imagery. To assess accuracy of habitat type, the BPI values were also compared to habitat data observed during the ROV video analysis.

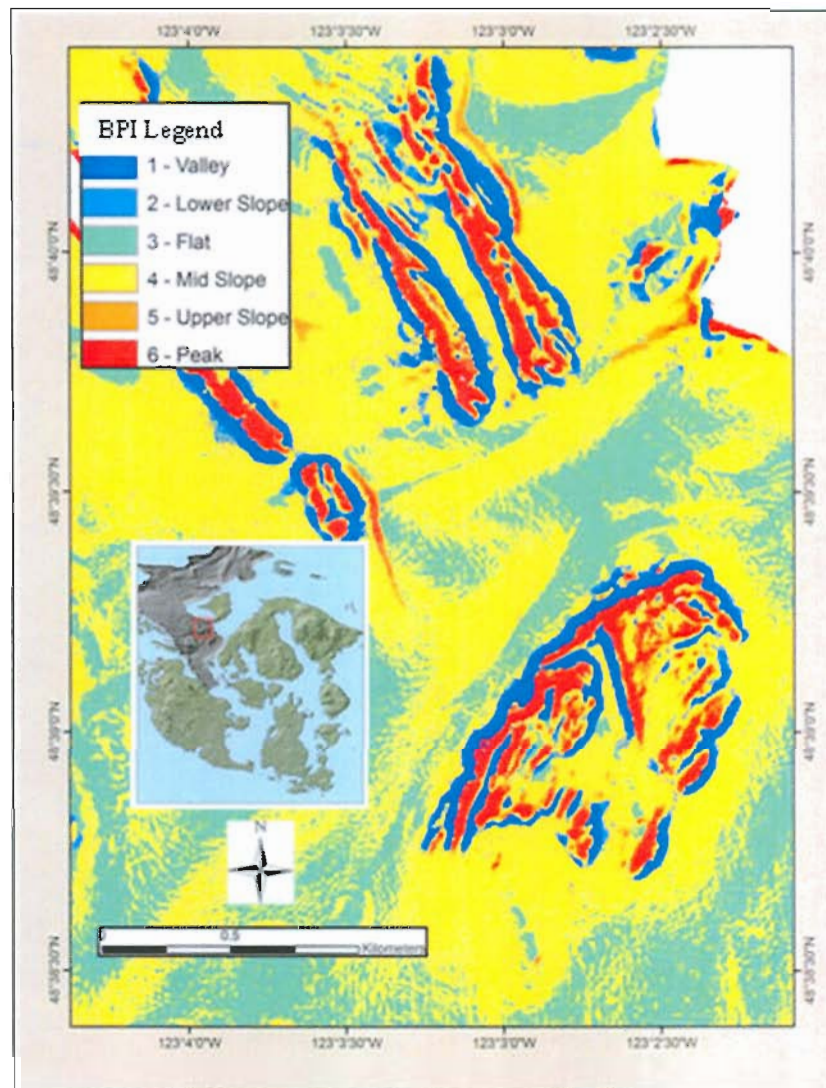


Figure 3-9 Example of 5 m DEM with BPI analysis for the Boundary Pass region of Canada. Values were generated using multibeam bathymetric dataset. Positive BPI values are shown in red colors indicating topographic highs and negative BPI values are illustrated in blue colors showing topographic lows.

3.2.3 Sediment Sampling

Substrate type was determined based on interpretations and analyses of geophysical and remote sensing data. For example, grain size was qualitatively determined from backscatter data based on backscatter intensity (light and dark shades), which indicated fine- and coarse-grained sediment. Also, grain size was determined from sieve analyses of sediment samples collected in sediment wave fields in the Boundary Pass region and San Juan Channel.

Sediment grab samples collected by the GSC in the Puget Sound/Georgia Basin region in 2004 were analyzed to determine the substrate type of bedforms that were previously mapped with multibeam bathymetry. Samples were processed using the mechanical Ro-Tap® sieving analyzer. In this procedure, three sediment samples were analyzed at MLML. The technique for the sieve analysis process was based on the methods of Folk (1974).

4 RESULTS

4.1 MULTIBEAM BATHYMETRY AND BACKSCATTER

4.1.1 Marine Benthic Habitat Maps

A unique, contiguous multibeam bathymetric dataset has been collected since 2000 (Figure 4-1). Multibeam bathymetric survey depths ranged from ~14 to 327 m in Haro Strait, ~18 to 266 m in the Strait of Juan de Fuca, and ~15 to 169 m in San Juan Channel. In the Boundary Pass region, depths ranged from ~10 to 377 m. Areas calculated from the multibeam bathymetry are ~182,000 km² for Haro Strait, ~ 206,000 km² for the Strait of Juan de Fuca, and ~ 23,000 km² for San Juan Channel. Boundary Pass encompassed ~ 258,000 km².

Multibeam backscatter data processed from the multibeam sonar data in Haro Strait (Figure 4-2) and Juan de Fuca Strait (Figure 4-3), for example, provided textural information for the seafloor sediment and exhibited a variety of geologic features. These included hummocky sediment, bedforms of varying sizes and fractured and faulted rocky outcrops. The darker-colored tones of the backscatter data denote coarse-grained sediment, whereas, the lighter-colored tones represent finer-grained sediment.

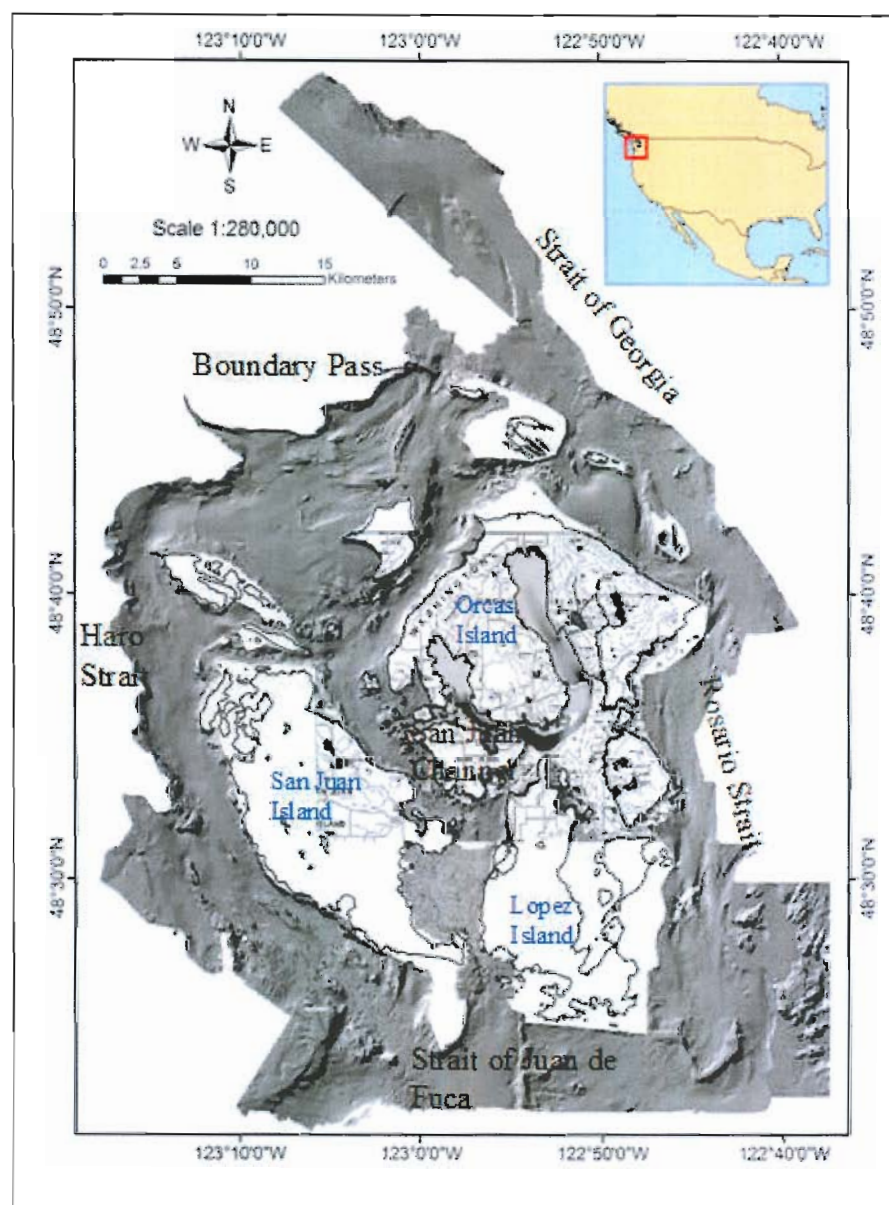


Figure 4-1 Overview of multibeam bathymetry collected from 2000 to 2007 in the San Juan Archipelago region.

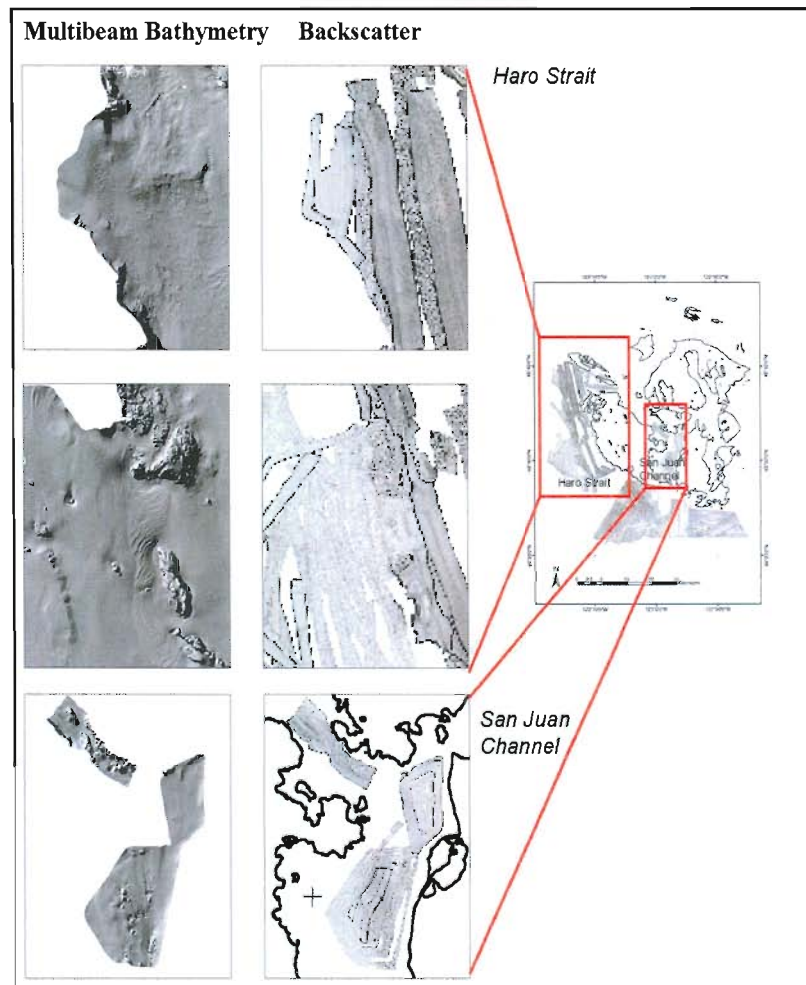


Figure 4-2 Examples of multibeam bathymetry and backscatter data where red boxes are highlighting examples of multibeam bathymetry and backscatter data collected with a Simrad® EM 1002 (95 kHz) sonar system in Haro Strait and San Juan Channel. The images on the left-hand side are illustrating multibeam bathymetry and the images on the right-hand side are depicting the backscatter data extracted from the multibeam bathymetry for the same area. Images created in ArcGIS®.

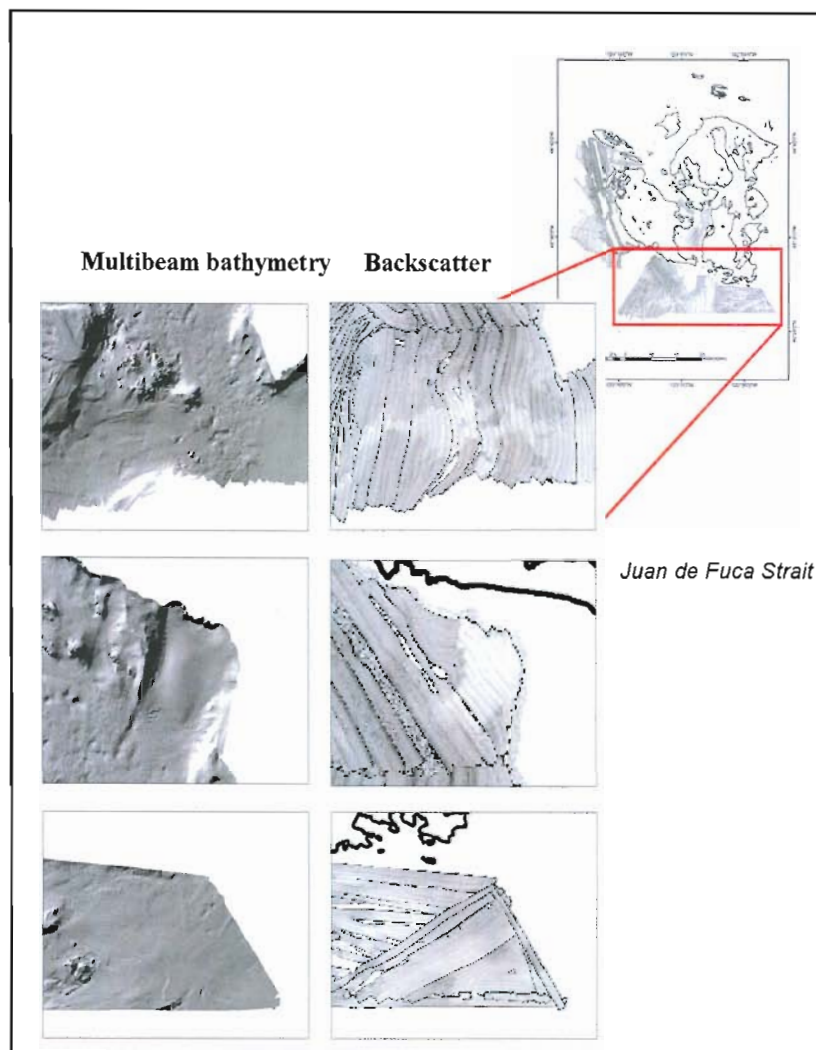


Figure 4-3 Examples of multibeam bathymetry and backscatter data where red box is highlighting examples of multibeam bathymetry and backscatter data collected with a Simrad® EM 1002 (95 kHz) sonar system in the Strait of Juan de Fuca. The images on the left-hand side are illustrating multibeam bathymetry and the images on the right-hand side are depicting the backscatter data extracted from the multibeam bathymetry for the same area. Images created in ArcGIS®.

Marine benthic habitat maps were created based on the interpretation of remote sensing imagery collected in the Puget Sound/Georgia Basin region (Figure 4-4). Habitat maps display codes that were color-coded based on age. For example, yellow and orange colors represented younger sediment while darker colors such as red and purple indicate older sediment. The maps also included descriptions that were produced for the following areas with their associated scales of interpretation: San Juan Channel (scales 1:5,000, 1:7,000 and 1:8,500) (Figure 4-5 and Figure 4-6), Strait of Juan de Fuca (scale 1:10,000) (Figure 4-7 and Figure 4-8), Haro Strait (scale 1:10,000) (Figure 4-9 and Figure 4-10) and Boundary Pass (scale 1:10,000) (Figure 4-11 and Figure 4-12). Data included multibeam bathymetry and backscatter, available groundtruthing information, as well as applying knowledge of the geological and physical oceanographic characteristics of the area. The products derived from the surficial analyses of multibeam bathymetric datasets in a GIS aided in the interpretation and characterization of marine benthic habitat maps by revealing diverse seafloor topography, enhancing areas varying in slope and providing lines of constant depth (*see* Appendix B for complete descriptions of marine benthic habitat map production).

Habitat characterizations were created collaboratively by MLML's Center for Habitat Studies students. Specifically, Holly Lopez created habitat maps for San Juan Channel, Haro Strait, Strait of Juan de Fuca and Boundary Pass. Charles Endris collaboratively created maps for San Juan Channel and Bryan Dieter contributed to the interpretation of Boundary Pass. Janet Tilden produced interpretations for Davis Point, Neck Point, Lawson Reef, Pile Point and Turn Island.

Using a GIS, habitat maps of San Juan Channel were created from multibeam bathymetry data sets collected in both 2000 and 2002. There were 25 habitat types identified ranging from soft depressions in unconsolidated sediment; soft (sand/mud) scour; mixed consolidated glacial mounds; and, hard bedrock pinnacles or boulders. Based on habitat interpretations of the Strait of Juan de Fuca, 22 habitat types were derived including soft, unconsolidated (sand/mud) deposits; sediment waves; scarps; mixed, hard consolidated glacial mounds; mixed unconsolidated (sand/gravel) levee deposits; and, hard, ice-scoured bedrock exposure. In Haro Strait, 11 habitat types were identified and included unconsolidated sediment, mixed glacial mounds and fractured and glacially scoured bedrock. In the Boundary Pass region, there were 18 habitat characterizations which included hummocky sediment waves, unconsolidated (sand/mud), mixed glacial mounds, scarps and bedrock pinnacles.

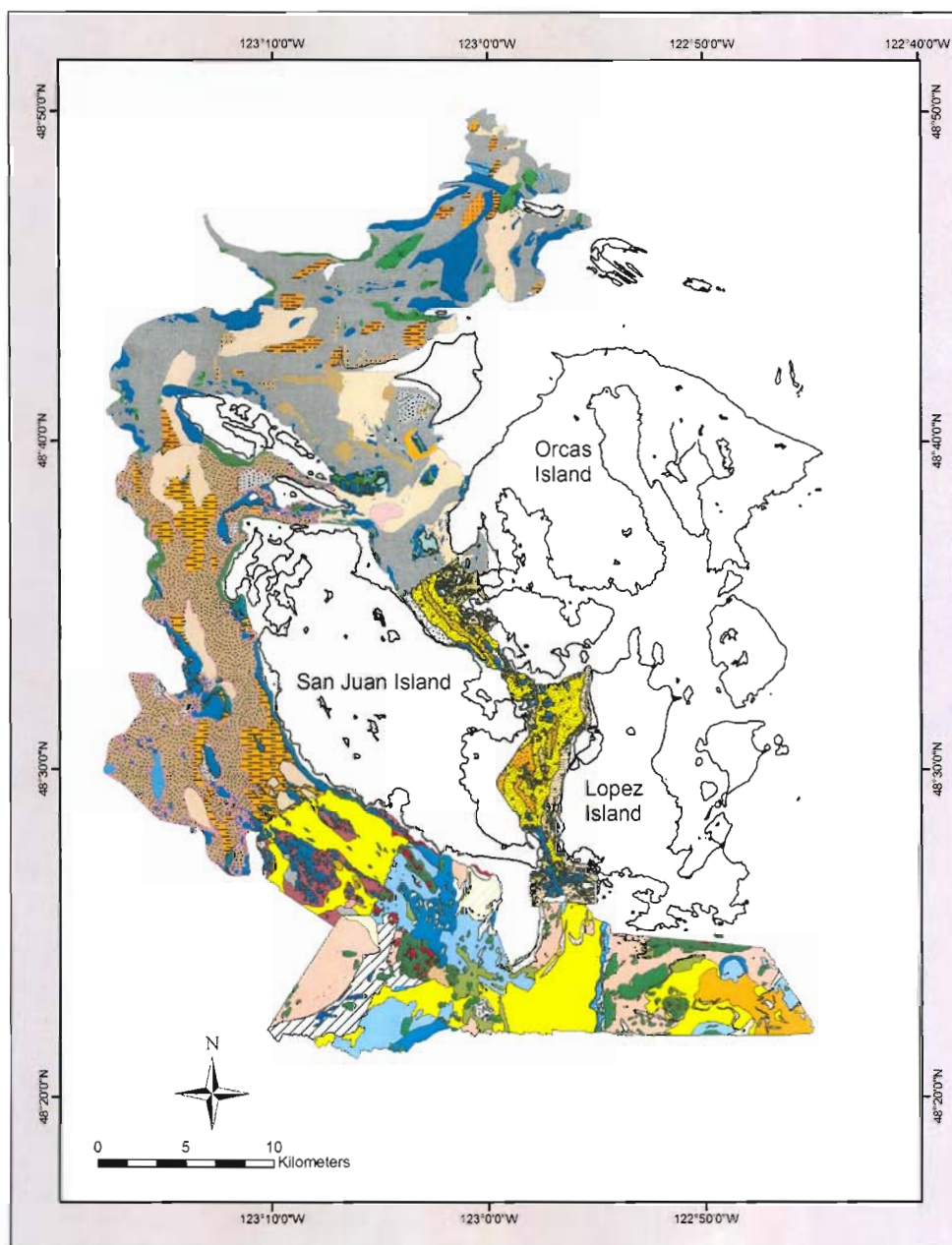


Figure 4-4 Marine benthic habitat maps based on remote sensing data including multibeam bathymetry, backscatter and sediment samples collected in the Boundary Pass, Haro Strait, San Juan Channel, and Strait of Juan de Fuca regions in the San Juan Archipelago, Washington, and Georgia Basin, British Columbia.

San Juan Channel Habitat Map

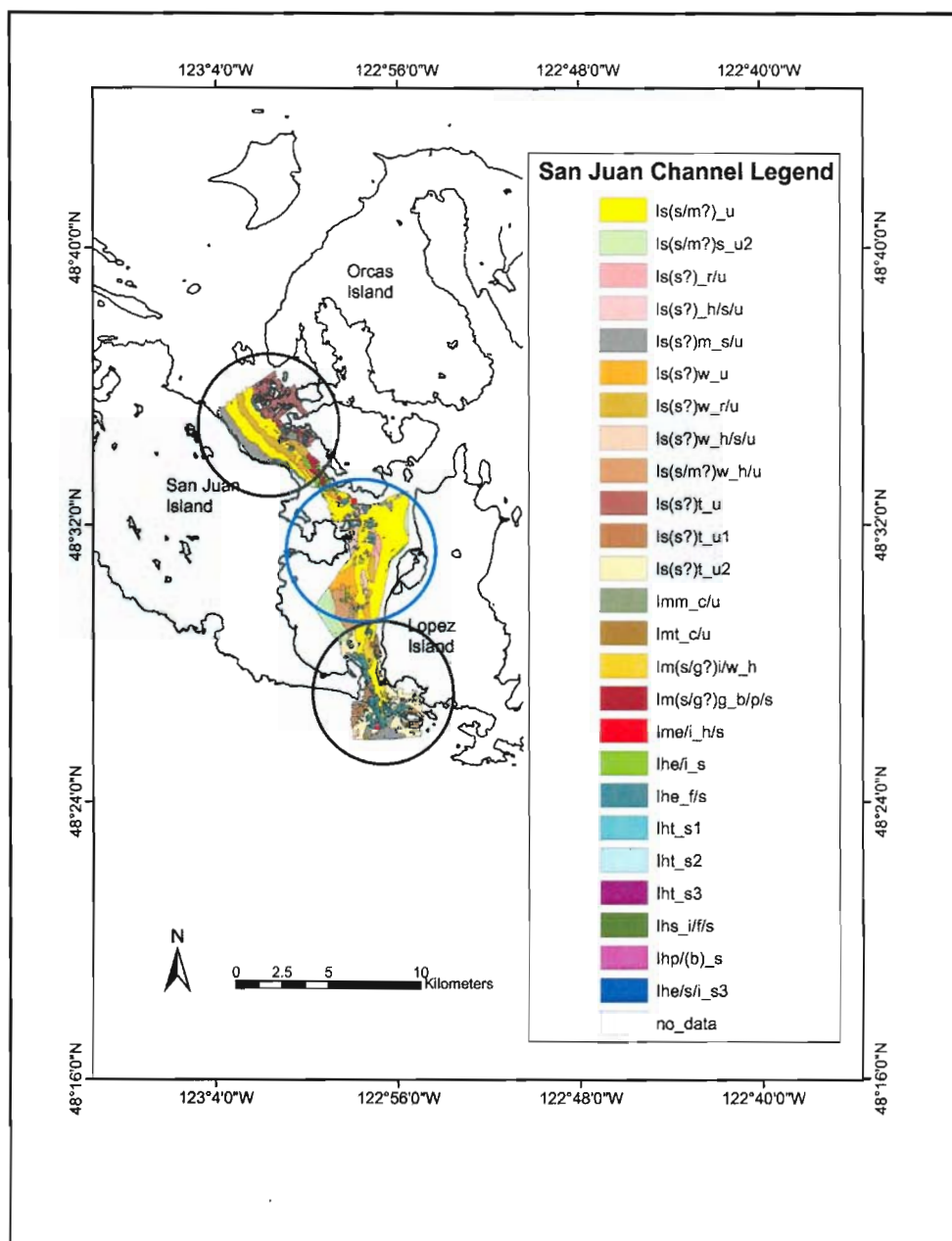


Figure 4-5 Marine benthic habitat map of San Juan Channel created by combining interpretations made from two different multibeam bathymetry datasets collected in 2000 (black circles – habitat maps interpreted at 1:5,000 and 1:7,000) and 2002 (blue circle – habitat map interpreted at 1:8,500). Overall map scale 1:225,000.

San Juan Channel Habitat Map Legend












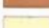


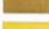




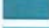






San Juan Channel Legend		Habitat Description
	ls(s/m?)_u	Soft unconsolidated (sand/mud?) deposit in inland sea (fjord)
	ls(s/m?)s_u2	Soft (sand/mud?) sloping (1-30°) scarp of unconsolidated sediment in inland sea (fjord)
	ls(s?)_r/u	Soft unconsolidated (sand?) ripples in inland sea (fjord)
	ls(s?)_h/s/u	Soft unconsolidated (sand?) scoured irregular relief in inland sea (fjord)
	ls(s?)m_s/u	Soft depression or mound in unconsolidated sediment in inland sea (fjord)
	ls(s?)w_u	Soft unconsolidated (sand?) sediment waves in inland sea (fjord)
	ls(s?)w_r/u	Soft unconsolidated (sand?) sediment waves with ripples in inland sea (fjord)
	ls(s?)w_h/s/u	Soft unconsolidated (sand?) sediment waves with scoured, hummocky sediment in inland sea (fjord)
	ls(s/m?)w_h/u	Soft unconsolidated (sand/mud?) sediment waves with hummocky sediment in inland sea (fjord)
	ls(s?)t_u	Soft unconsolidated (sand?) sediment deposit on terrace in inland sea (fjord)
	ls(s?)t_u1	Soft unconsolidated (sand?) sediment deposit on terraced slope in inland sea (fjord)
	ls(s?)t_u2	Soft (sand?) covered sloping (1-30°) terrace with unconsolidated sediment in inland sea (fjord)
	lmm_c/u	Mixed hard consolidated subcrop mound locally covered with soft unconsolidated sediment in inland sea (fjord)
	lmt_c/u	Mixed hard consolidated terrace bedrock locally covered with unconsolidated sediment in inland sea (fjord)
	lm(s/g?)i/w_h	Mixed (sand/gravel?) sediment in ice-scoured, hummocky wave field in inland sea (fjord)
	lm(s/g?)g_b/p/s	Mixed hard (sand/gravel?) pavement scoured channel with local unconsolidated sediment cover in inland sea (fjord)
	lme/i_h/s	Mixed hard bedrock exposures locally covered with unconsolidated sediment with scoured, irregular relief in inland sea (fjord)
	lhe/i_s	Hard ice-scoured bedrock exposure in inland sea (fjord)
	lhe_f/s	Hard bedrock exposure with clearly defined fractures in inland sea (fjord)
	lht_s1	Hard sloping terrace in inland sea (fjord)
	lht_s2	Hard, gently sloping terrace (1-30°) in inland sea (fjord)
	lht_s3	Hard, steeply sloping terrace (30-60°) in inland sea (fjord)
	lhs_i/f/s	Hard, glacially scoured and fractured bedrock scarp in inland sea (fjord)
	lhp/(b)_s	Hard bedrock pinnacles or boulders in inland sea (fjord)
	lhe/s/i_s3	Hard steeply sloping (30-60°) ice-formed bedrock scarp in inland sea (fjord)
	no_data	No data

Figure 4-6 Legend of marine benthic habitat map of the San Juan Channel where habitat characterizations were based on classification scheme for deep seafloor habitats (Greene et al., 1999).

Strait of Juan de Fuca Habitat Map

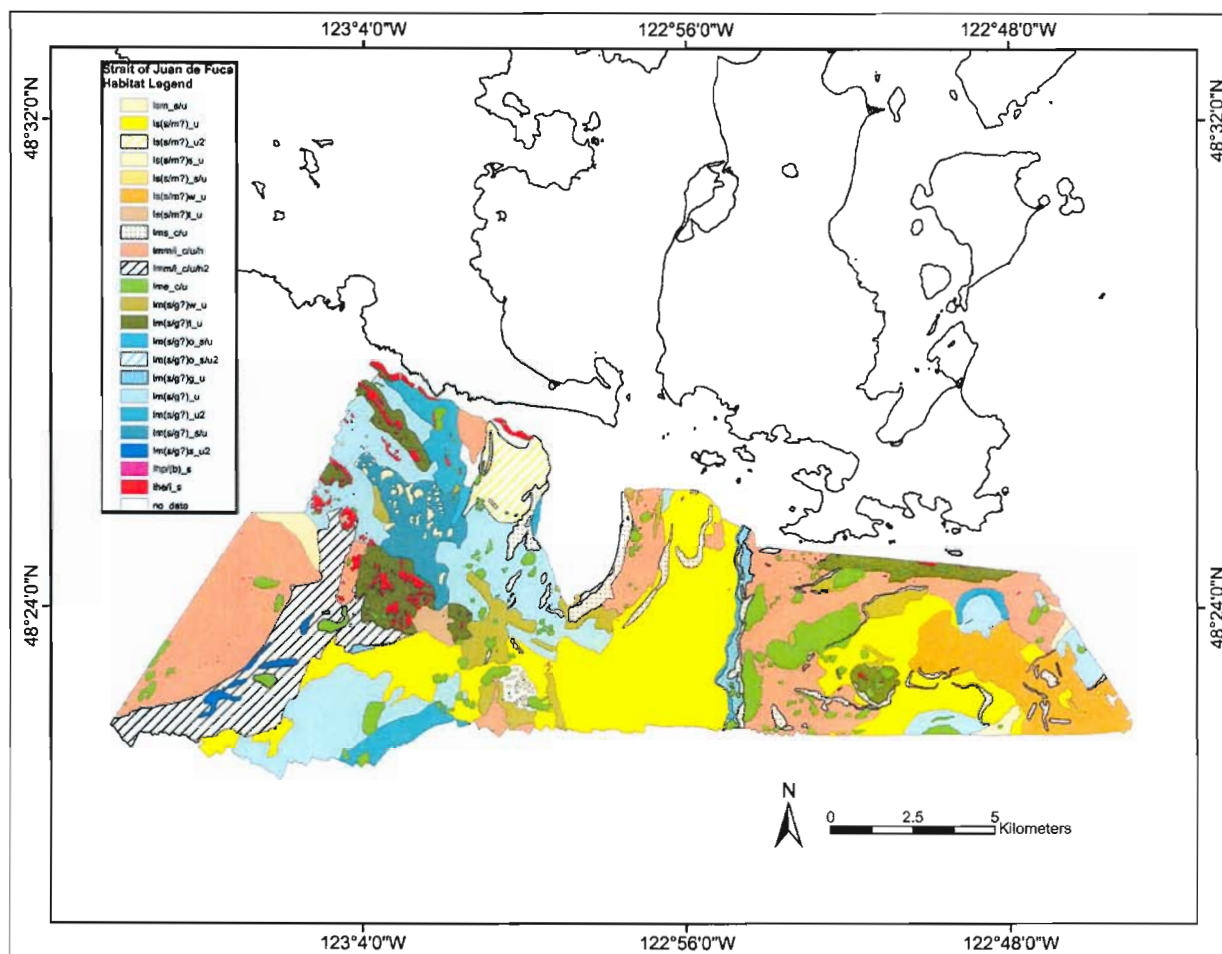


Figure 4-7 Marine benthic habitat map of the Strait of Juan de Fuca where habitat map was interpreted using multibeam bathymetry and backscatter data at a scale of 1:10,000. Overall map scale 1:175,000.

Strait of Juan de Fuca Habitat Map Legend

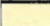


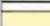


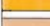
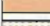


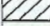

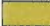




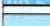





Strait of Juan de Fuca Legend	Habitat Description
 lsm_s/u	Soft depression in unconsolidated sediment in inland sea (fjord)
 ls(s/m?)_u	Soft unconsolidated (sand/mud?) deposit in inland sea (fjord)
 ls(s/m?)_u2	Soft (sand/mud?) sloping (1-30°) with unconsolidated sediment in inland sea (fjord)
 ls(s/m?)_s_u	Soft (sand/mud?) scarp with unconsolidated sediment in inland sea (fjord)
 ls(s/m?)_s/u	Soft (sand/mud?) scour locally covered with unconsolidated sediment in inland sea (fjord)
 ls(s/m?)_w_u	Soft (sand/mud?) sediment waves locally covered with unconsolidated sediment in inland sea (fjord)
 ls(s/m?)_t_u	Soft (sand/mud?) terrace locally covered with unconsolidated sediment in inland sea (fjord)
 lms_c/u	Mixed hard consolidated scarp locally covered with soft unconsolidated sediment in inland sea (fjord)
 lmm/i_c/u/h	Mixed hard consolidated glacial mounds locally covered with unconsolidated sediment in inland sea (fjord)
 lmm/i_c/u/h2	Mixed hard consolidated glacial mounds on slope (1-30°) locally covered with unconsolidated sediment in inland sea (fjord)
 lme_c/u	Mixed hard consolidated outcrop locally covered with soft unconsolidated sediment in inland sea (fjord)
 lm(s/g?)_w_u	Mixed (sand/gravel?) unconsolidated sediment waves in inland sea (fjord)
 lm(s/g?)_t_u	Mixed unconsolidated (sand/gravel?) terrace deposit in inland sea (fjord)
 lm(s/g?)_o_s/u	Mixed unconsolidated (sand/gravel?) levee overbank deposit in inland sea (fjord)
 lm(s/g?)_o_s/	Mixed unconsolidated (sand/gravel?) levee overbank deposit on slope (1-30°) in inland sea (fjord)
 lm(s/g?)_g_u	Mixed (sand/gravel?) gully locally covered with unconsolidated sediment in inland sea (fjord)
 lm(s/g?)_u	Mixed unconsolidated (sand/gravel?) deposit in inland sea (fjord)
 lm(s/g?)_u2	Mixed unconsolidated (sand/gravel?) deposit on slope (1-30°) in inland sea (fjord)
 lm(s/g?)_s_u	Mixed unconsolidated (sand/gravel?) scarp in inland sea (fjord)
 lm(s/g?)_s_u2	Mixed unconsolidated (sand/gravel?) scarp on slope (1-30°) in inland sea (fjord)
 lhp/(b)_s	Hard bedrock pinnacles or boulders in inland sea (fjord)
 lhe/i_s	Hard ice-scoured bedrock exposure in inland sea (fjord)
 no_data	No data

Figure 4-8 Legend of marine benthic habitat map of the Strait of Juan de Fuca where habitat characterization was based on classification scheme for deep seafloor habitats (Greene et al., 1999).

Haro Strait Habitat Map

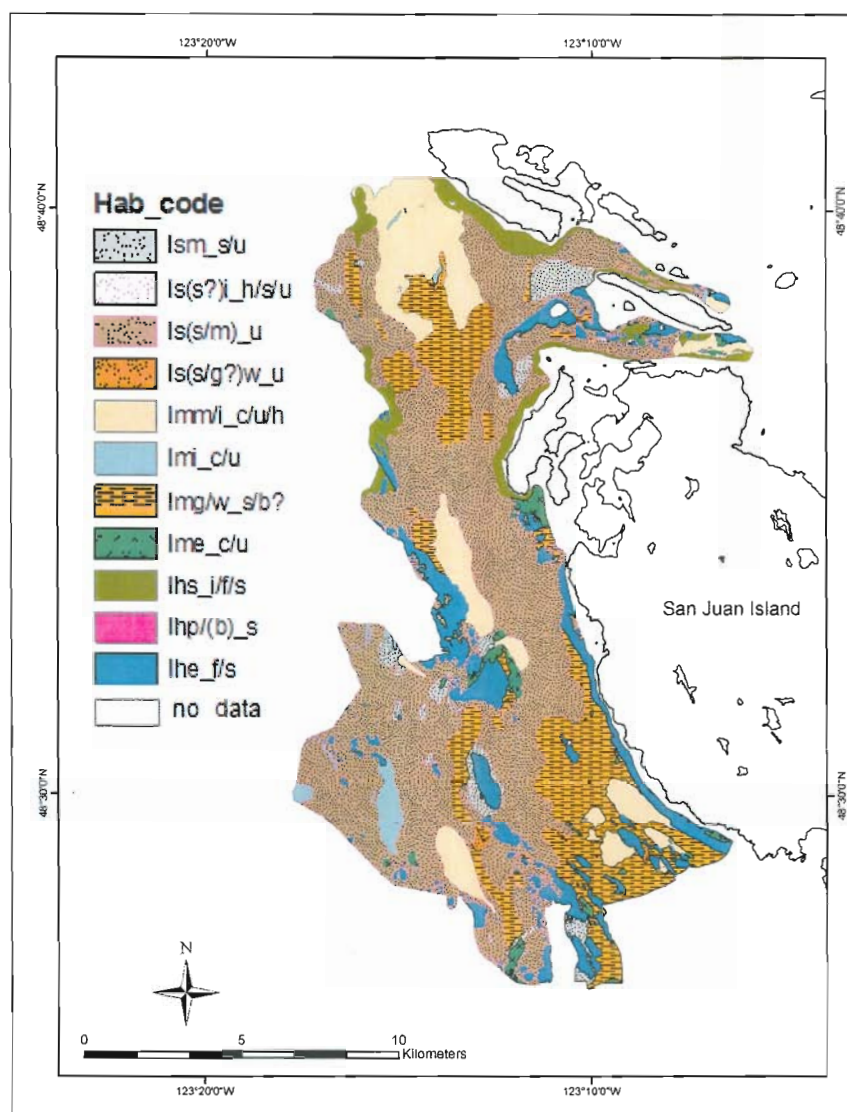


Figure 4-9 Marine benthic habitat map of Haro Strait interpreted at a scale of 1:10,000. Overall map scale 1:225,000.

Haro Strait Habitat Map Legend













Hab_code		
	lsm_s/u	Soft depression in unconsolidated sediment in inland sea (fjord)
	ls(s?)_h/s/u	Soft unconsolidated sediment (sand/mud) in inland sea (fjord)
	ls(s/m)_u	Soft unconsolidated (sand/gravel?) sediment waves in inland sea (fjord)
	ls(s/g?)w_u	Mixed hard consolidated glacial mounds locally covered with soft unconsolidated sediment in inland sea (fjord)
	lmmv_l_c/w/h	Mixed hard consolidated glacial mounds locally covered with unconsolidated sediment in inland sea (fjord)
	lmi_c/u	Mixed gullies and bimodal sediment waves and scouring in inland sea (fjord)
	lmg/w_s/b?	Mixed hard consolidated outcrop locally covered with soft unconsolidated sediment in inland sea (fjord)
	lme_c/u	Hard, glacially scoured and fractured bedrock scarp in inland sea (fjord)
	lhs_i/f/s	Soft unconsolidated hummocky scoured sediment (sand?) and ice-formed features or deposits in inland sea (fjord)
	lhp/(b)_s	Hard bedrock pinnacles or boulders in inland sea (fjord)
	lhe_f/s	Exposed bedrock, fractured and glacially scoured in inland sea (fjord)
	no data	No data

Figure 4-10 Legend of marine benthic habitat map of Haro Strait where habitat characterization was based on classification scheme for deep seafloor habitats (Greene et al., 1999).

Boundary Pass Habitat Map

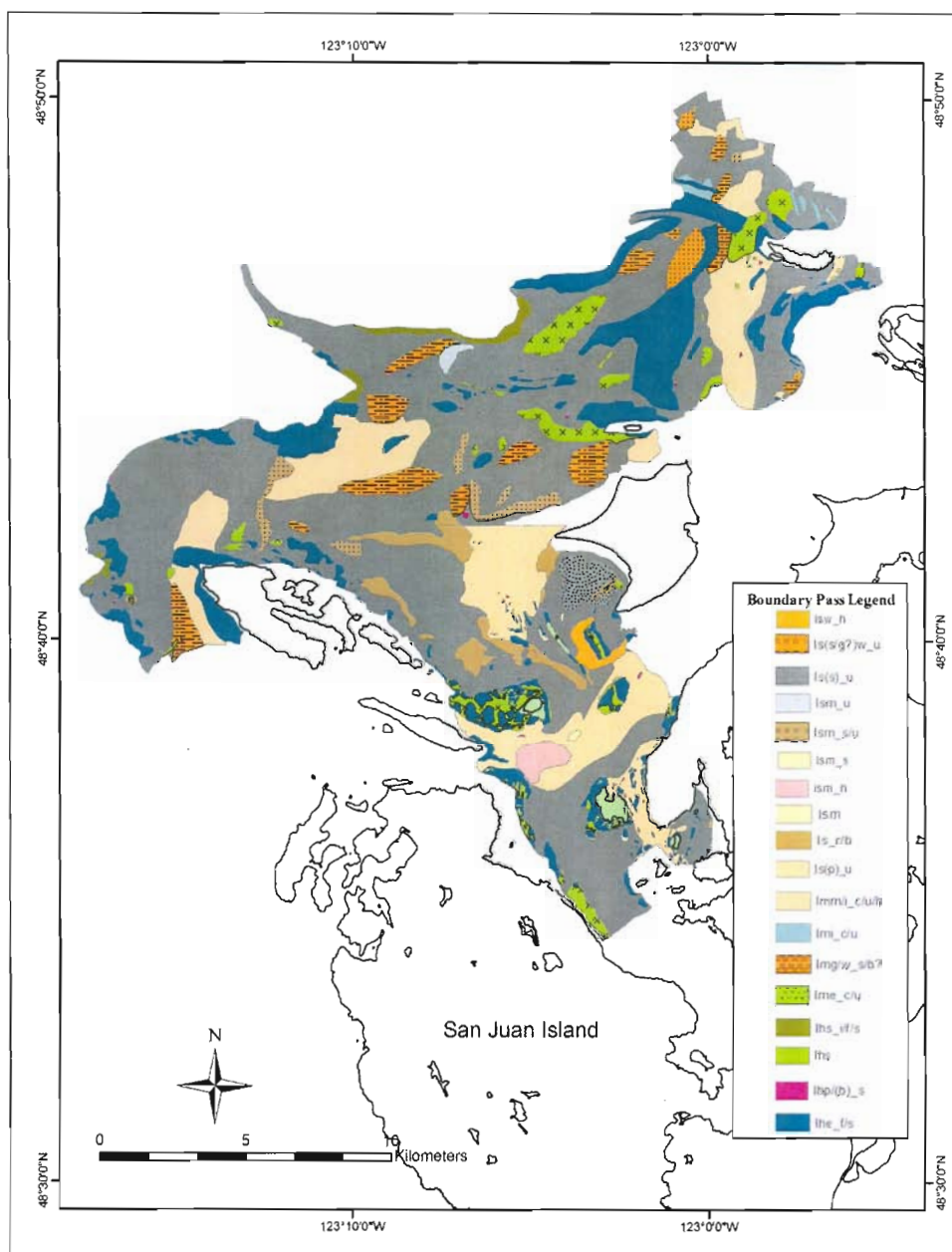


Figure 4-11 Legend of marine benthic habitat map of the Boundary Pass region of the U.S. and Canada interpreted at 1:10,000. Overall map scale 1:150,000.

Boundary Pass Habitat Map Legend








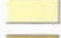










	lsw_h	Hummocky sediment waves in inland sea (fjord)
	ls(s/g?)w_u	Soft unconsolidated (sand/gravel?) sediment waves in inland sea (fjord)
	ls(s)_u	Soft unconsolidated (sand) sediment deposit in inland sea (fjord)
	lsm_u	Soft unconsolidated (mud) in inland sea (fjord)
	lsm_s/u	Soft depression in unconsolidated sediment in inland sea (fjord)
	lsm_s	Soft sediment with mounds and depressions and scouring in inland sea (fjord)
	lsm_h	Soft hummocky sediment with mounds and depressions in inland sea (fjord)
	lsm	Soft sediment with mounds and depressions in inland sea (fjord)
	ls_r/b	Soft unconsolidated bimodal ripples in inland sea (fjord)
	ls(p)_u	Soft unconsolidated sediment (pebbles) in inland sea (fjord)
	lmm/i_c/u/h	Mixed hard consolidated glacial mounds locally covered with soft unconsolidated sediment in inland sea (fjord)
	lmi_c/u	Mixed hard consolidated glacial mounds locally covered with unconsolidated sediment in inland sea (fjord)
	lmg/w_s/b?	Mixed gullies and bimodal sediment waves and scouring in inland sea (fjord)
	lme_c/u	Mixed hard consolidated outcrop locally covered with soft unconsolidated sediment in inland sea (fjord)
	lhs_i/f/s	Hard, glacially scoured and fractured bedrock scarp in inland sea (fjord)
	lhs	Hard, scarps in inland sea (fjord)
	lhp/(b)_s	Hard bedrock pinnacles or boulders in inland sea (fjord)
	lhe_f/s	Exposed bedrock, fractured and glacially scoured in inland sea (fjord)

Figure 4-12 Legend of marine benthic habitat map of the Boundary Pass region of the U.S. and Canada where habitat characterization was based on classification scheme for deep seafloor habitats (Greene et al., 1999).

Habitat features were characterized as soft, mixed or hard. Habitat interpretations from all surveyed areas yielded 76 habitat types ranging from soft, unconsolidated (sand/mud) deposits and scours; sediment waves; scarps; mixed consolidated glacial mounds; mixed unconsolidated (sand/gravel) levee deposits; hard, ice-scoured bedrock exposure and hard bedrock pinnacles or boulders.

4.1.2 Sedimentary bedforms

Sedimentary bedforms of varying sizes (ripples, waves, ripples overlying waves and dunes) in the Puget Sound/Georgia Basin region have been identified and characterized in marine benthic habitat maps based on multibeam bathymetry, multibeam backscatter, ROV video observations and sediment grab samples. Bedform shapefiles were queried in a Geographic Information System (GIS) from marine benthic habitat maps (Figure 4-13).

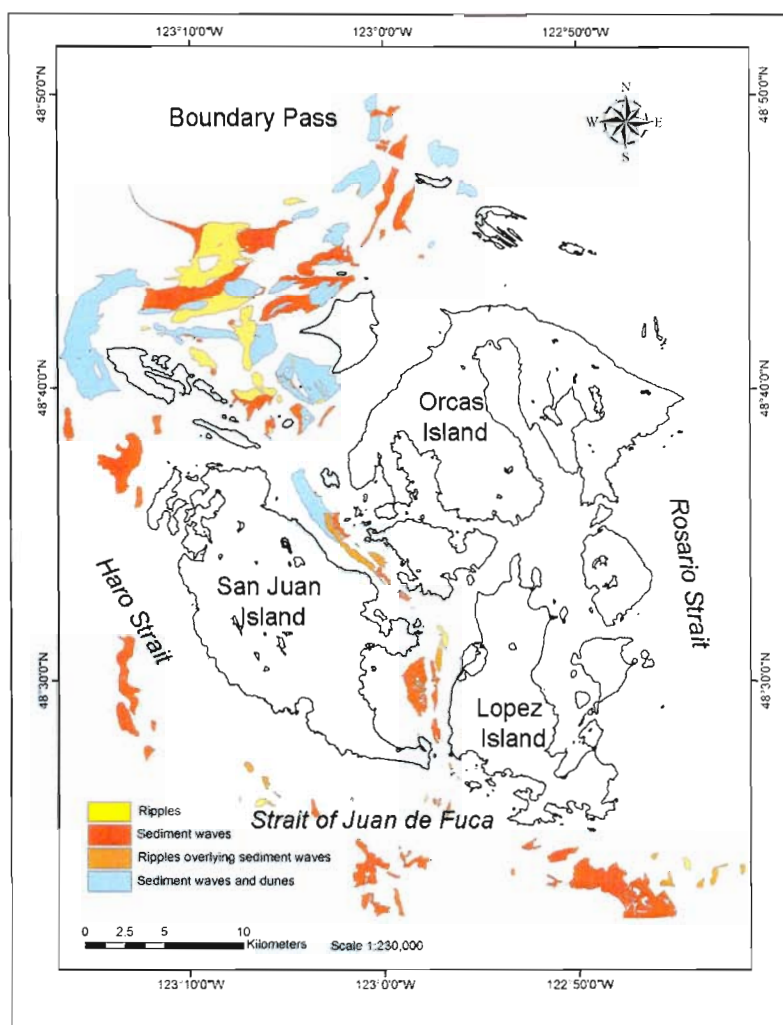


Figure 4-13 Distribution of bedforms of varying sizes (ripples, sediment waves, ripples overlying sediment waves and dunes) in the San Juan Archipelago, Washington, and Georgia Basin, Canada.

In San Juan Channel, the ten random points that were generated using Hawth's Analysis Tools to identify individual bedforms for measurement yielded a mean depth of 67 m in the sediment wave field. The mean wavelength (m) of the individual bedforms measured was 264 m and the mean height of the bedforms was 13 m. In the sediment wave field in the Boundary Pass region, the individual bedforms measured resulted in a

mean depth of 188 m and bedforms with a mean wavelength of 555 m and a mean height of 10 m.

When comparing multibeam bathymetric DEMs in a GIS from data collected in the Boundary Pass region between 2001 and 2003 (Figure 4-14) and in San Juan Channel from 2002 to 2006 (Figure 4-15), it was determined that these bedforms migrate and are dynamic. Between the two surveys of the bedform field in the Boundary Pass region, the bedform sediment underwent erosion and deposition resulting in movement ranging from ~0.5 m to ~2 m. In San Juan Channel, erosion and deposition occurred between the two surveys and sediment movement ranged between ~0.35 m to ~8 m.

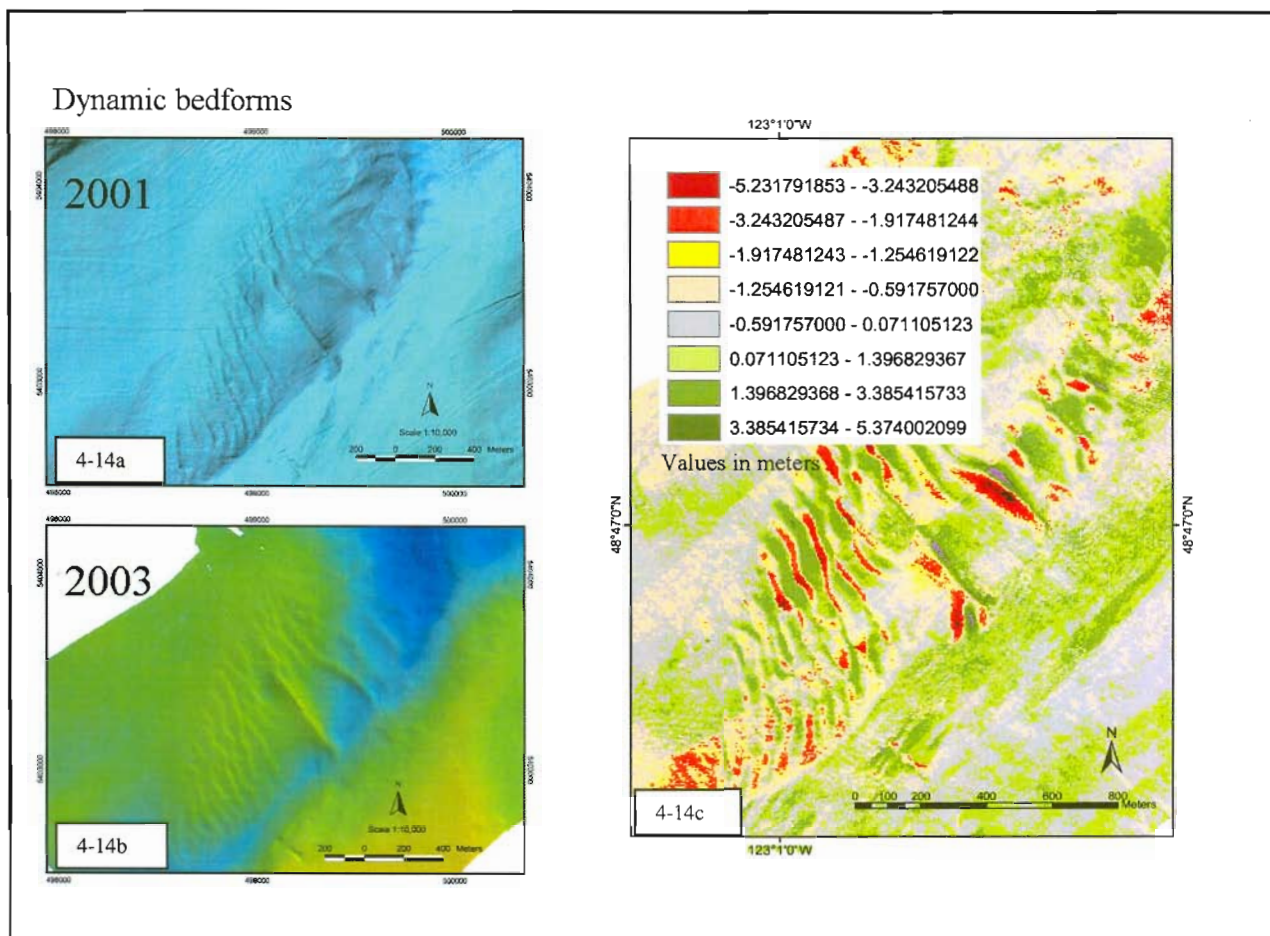


Figure 4-14 Multibeam bathymetry collected in 2001 and 2003 in Boundary Pass region as seen in Figures 4-14 a and b. Figure 4-14c shows the raster difference map created in ArcGIS® showing erosion and deposition in sedimentary bedforms between the 2001 and 2003 surveys.

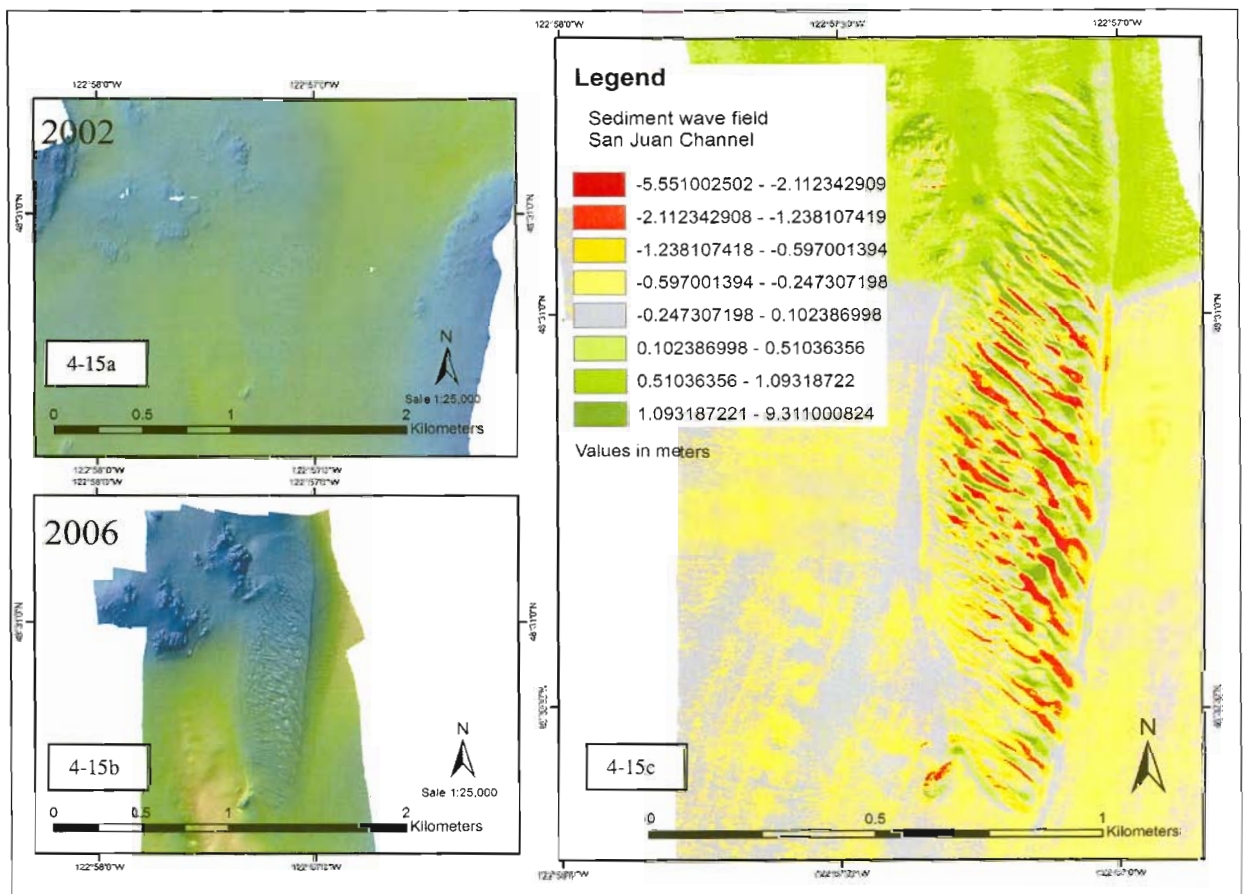


Figure 4-15 Multibeam bathymetry collected in 2002 and 2006 in San Juan Channel as seen in Figures 4-15 a and b. Figure 4-15c shows the raster difference map created in ArcGIS® showing erosion and deposition in sedimentary bedforms between two surveys.

Obstacle marks are present in the multibeam bathymetric datasets analyzed in this study (Figure 4-16). These marks indicate that bottom currents are shaping the seafloor sediment. The currents are causing the sediment to travel around the bottom features, such as rocks and pebbles, and are indicators of the ebbing or flooding direction of the current. The marks are a sign of a dynamic underwater environment.

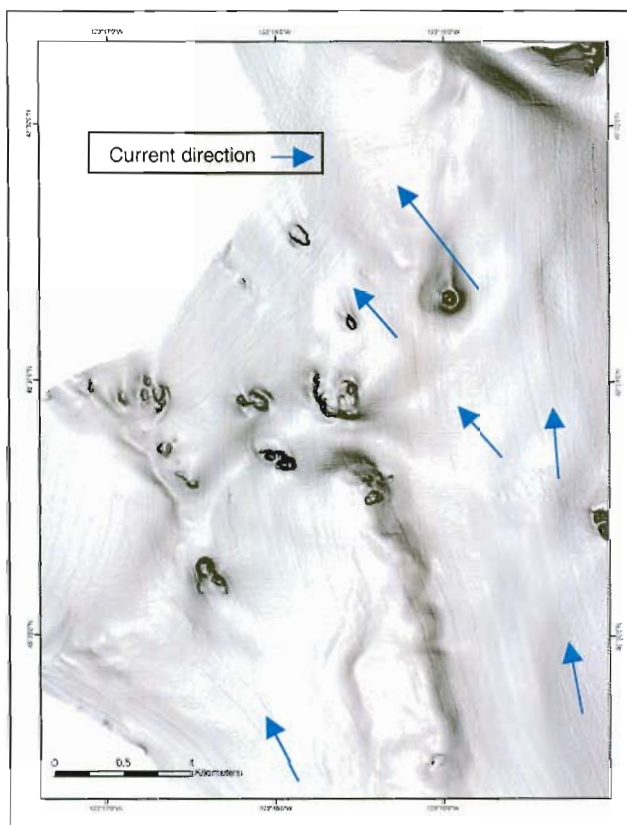


Figure 4-16 Obstacle marks identified in multibeam bathymetric data collected in Haro Strait. Bathymetry is displayed in slope shade in ArcGIS®. Current is from the northwest. Depth varies from 50 to 105 m.

Sediment waves formed in high-energy environments were mapped with multibeam bathymetry and viewed in ROV videos in San Juan Channel (Figure 4-17). Sand waves as well as ripples superimposed on waves were observed and were composed of both fine-grained sediment (sand) and coarse-grained sediment (cobbles and pebbles) in troughs of waves and coarse-grained sediment along crests of bedforms.

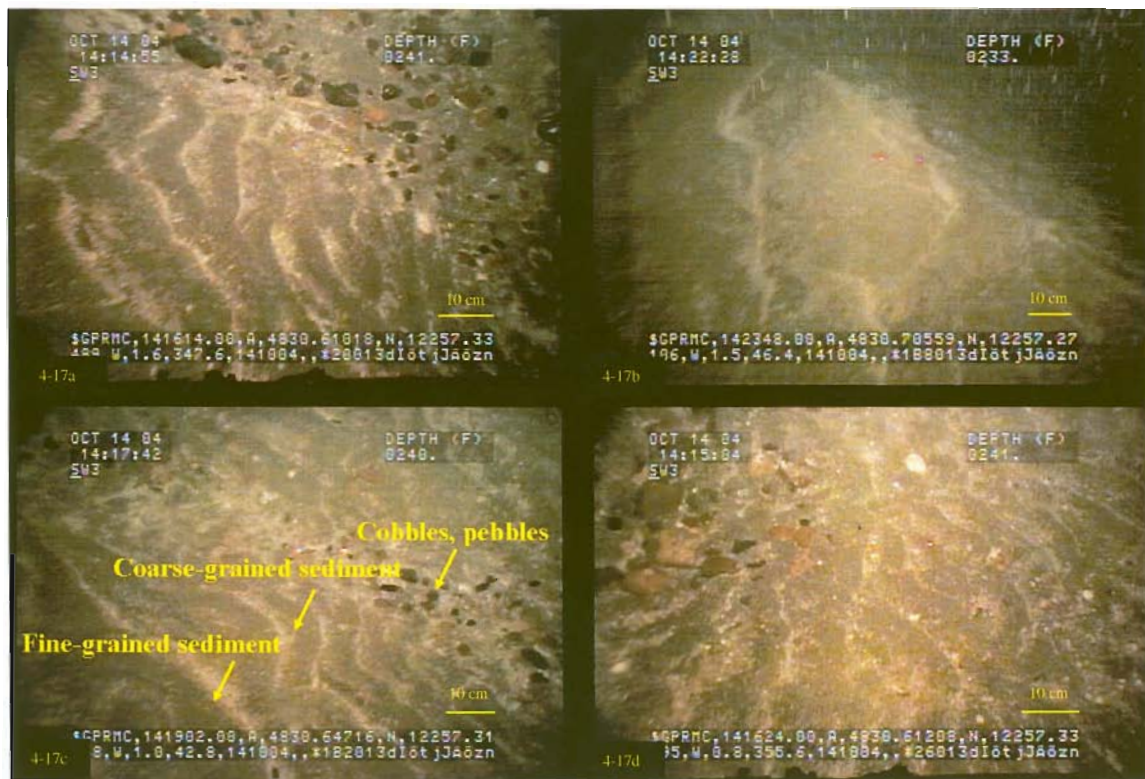


Figure 4-17 Screen grabs taken from dive in San Juan Channel using Phantom HD2+2 ROV. Lasers indicate 10 cm spacing. Depth in feet is shown in top right corner of each image.

4.2 ROV SURVEY

4.2.1 Habitat

Based on characterizations of geologic structures from multibeam bathymetric and backscatter data collected in the Puget Sound/Georgia Basin region, a variety of habitats was identified. These included bedrock outcrops, sandy and muddy seafloor and sediment waves. The ROV transects generally confirmed the habitat maps created from the multibeam bathymetric and backscatter data. Based on definitions from Greene et al. (1999), substrate types included mud, sand, gravel, pebble, cobble, shell-hash, hardpan, boulder and bedrock. While the focus of this study was on soft sediment habitats, the

ROV transited areas that included rock. Therefore, rocky areas were included in the substrate analysis. The habitats of San Juan Channel are the main area of study for this project (Figure 4-18). The sediment wave field in San Juan Channel was characterized by smaller ripples overlying the larger waves in the marine benthic habitat maps.

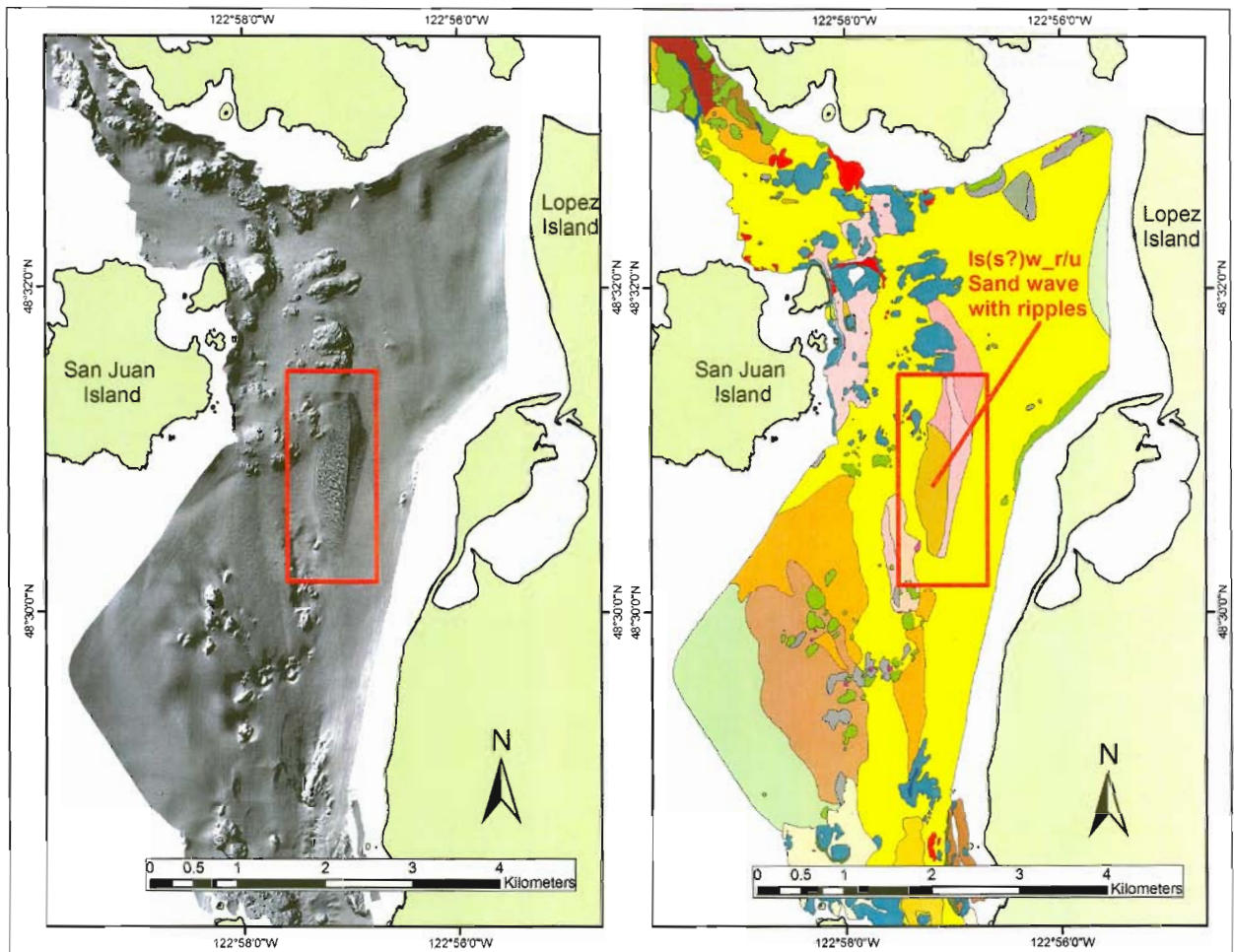


Figure 4-18 Multibeam bathymetry and associated marine benthic habitat map of San Juan Channel shown on left-hand side. Marine benthic habitat map interpreted from multibeam imagery. Red box highlights sand wave field where Pacific sand lance were observed with an ROV emerging from sediment. Both images have a scale of 1:50,000. Marine benthic habitat map characterizations based on classification scheme by Greene et al. (1999).

The 2004 and 2005 ROV San Juan Channel survey transect lengths ranged from 192 to 1,266 m. Depths ranged from 6 to 163 m. In total, 65 dives were conducted. Each transect was considered as an independent sample and each species identified was weighted by the area covered by the transect. A total of 39 transects covering an

estimated 21 km² was investigated for this study, in which there were 29 transects collected in non-sand wave habitats and 10 transects collected in the sand wave areas. Some transects were divided into parts for various reasons, such as the video tape ran out during a dive or the ROV was moved off the seafloor due to currents, but were considered the same transect number in the analysis.

4.2.2 Fishes and Invertebrates

Twenty-two fish taxa representing fourteen families were observed and counted from all the ROV video collected in soft sediment habitats (Table 4-1). Fishes identified to the genus/species level included Pacific sand lance (family Ammodytidae), ratfish (family Chimaeridae), Pacific cod (family Gadidae), kelp greenling (family Hexagrammidae), Puget Sound rockfish (family Scorpaenidae) and quillback rockfish (family Scorpaenidae).

Table 4-1 List tabulating total estimated number of individuals counted for each fish family and genus/species in San Juan Channel. Organisms were identified to species level as could be determined. Family names were used in the analysis.

Fish Family and Common Name	Species	Family	Total Number Individuals Observed
Agonidae			
Sturgeon poacher	<i>Podothecus accipenserinus</i>	Agonidae	1
Unidentified poacher	n/a	Agonidae	4
Ammodytidae			
Pacific sand lance	<i>Ammodytes hexapterus</i>	Ammodytidae	114
Chimaeridae			
Spotted ratfish	<i>Hydrolagus coliei</i>	Chimaeridae	17
Cottidae			
Great sculpin	<i>Myoxocephalus polyacanthocephalus</i>	Cottidae	4
Unidentified sculpin	n/a	Cottidae	4
Embiotocidae			
Striped seaperch	<i>Embiotoca lateralis</i>	Embiotocidae	1
Unidentified perch	n/a	Embiotocidae	2
Gadidae			
Pacific cod	<i>Gadus macrocephalus</i>	Gadidae	1
Unidentified gadid	n/a	Gadidae	827
Hexagrammidae			
Kelp greenling	<i>Hexagrammos decagrammus</i>	Hexagrammidae	27
Whitespotted greenling	<i>Hexagrammos stelleri</i>	Hexagrammidae	7
Lingcod	<i>Ophiodon elongatus</i>	Hexagrammidae	8
Painted greenling	<i>Oxylebius pictus</i>	Hexagrammidae	2
Unidentified hexagrammid	n/a	Hexagrammidae	2
Liparidae			
Snailfish	n/a	Liparidae	2
Pholidae			
Unidentified gunnel	n/a	Pholidae	8
Pleuronectidae			
Rex sole	<i>Glyptocephalus zachirus</i>	Pleuronectidae	2
Rock sole	<i>Lepidopsetta bilineata</i>	Pleuronectidae	8
Dover sole	<i>Microstomus pacificus</i>	Pleuronectidae	10
English sole	<i>Parophrys vetulus</i>	Pleuronectidae	1
Unidentified flatfish	n/a	Pleuronectidae	34
Rajidae			
Big skate	<i>Raja binoculata</i>	Rajidae	1
Salmonidae			
Unidentified salmon	n/a	Salmonidae	1
Scorpaenidae			
Brown rockfish	<i>Sebastes auriculatus</i>	Scorpaenidae	1
Puget Sound rockfish	<i>Sebastes emphaeus</i>	Scorpaenidae	596
Yellowtail rockfish	<i>Sebastes flavidus</i>	Scorpaenidae	1
Quillback rockfish	<i>Sebastes maliger</i>	Scorpaenidae	36
Tiger rockfish	<i>Sebastes nigrocinctus</i>	Scorpaenidae	3
Unidentified rockfish	n/a	Scorpaenidae	2
Stichaeidae			
Snake prickleback	<i>Lumpenus sagitta</i>	Stichaeidae	7
Unidentified prickleback	n/a	Stichaeidae	5
Unidentified fish			
Unidentified fish	Unidentified fish		46
Total			<i>N=1,785</i>

For all fish families, after the data were log transformed, there were no differences in densities [total number of fish individuals divided by transect area (m^2)] between sand wave and non-sand wave habitats using a two-sample T-Test for all fish families ($P=0.863$) (Table 4-2). There was an average of 6 ± 4.10 SE fish per km^2 based on ROV video analysis in non-sand wave transects and an average of 6 ± 4.44 SE fish per km^2 in sand wave transects. Sand lance, gadid and flatfish densities were 0 ± 0.32 SE, 5 ± 0.08 SE and 4 ± 0.57 SE fish/ km^2 in non-sand wave transects and were not statistically different from their densities where they occurred in 1 ± 1.06 SE, 6 ± 4.16 SE and 4 ± 1.66 SE fish / km^2 in the sand wave fields, respectively. Test probabilities were Ammodytidae $P=0.103$, Gadidae: $P=0.688$, and Pleuronectidae: $P=0.469$. However, there were statistically significant density differences between Hexagrammidae ($P=0.004$) and Scorpaenidae ($P=0.001$) families between non-sand wave and sand wave transects. Kelp greenling densities were 4 ± 0.49 SE fish/ km^2 in non-sand wave transects and were higher than the 0 fish/ km^2 found in non-sand wave transects. Rockfish densities were 6 ± 1.24 SE fish/ km^2 in non-sand wave transects and were higher than the 0 fish/ km^2 found in sand wave transects.

Table 4-2 List of transect area and fish density calculations from ROV survey in San Juan Channel showing area calculations (m²) for each transect conducted in both non-sand wave and sand wave habitats with associated fish densities (km²).

<i>Non-Sand Wave</i>		Density (# per km ²)	
	Transect #	Transect Area (m ²)	All fish
	1116	315.4	6
	1149	659.4	4
	1213	362.3	5
	1222	273.8	8
	1234	602.6	6
	1238	520.0	6
	1308	500.9	6
	1335	443.9	6
	1355	483.1	4
	1359	855.0	7
	1414	557.7	0
	1449	585.1	4
	1458	457.5	8
	1503	772.2	4
	1518	785.3	6
	1607	747.9	8
	1610	484.3	7
	1619	420.0	4
	1636	336.5	9
	1700	319.4	6
	1706	430.8	9
	1801	444.8	6
	1811	431.7	6
	1831	671.4	5
	1850	800.1	6
Mean			6
Two-tailed T-Test			0.86301

<i>Sand Wave</i>		Density (# per km ²)	
	Transect #	Transect Area (m ²)	All fish
	1133	604.9	7
	1300	327.0	7
	1342	407.4	8
	1357	347.4	7
	1440	679.1	6
	1532	548.5	6
	1548	504.0	7
	1617	909.5	5
	1624	490.0	6
	1705	640.8	6
	1838	1151.6	5
Mean			6

The observed frequencies of fish families were compared to their expected frequencies if the fishes occurred in direct proportion to the frequencies of sand, gravel, rock, or mixed substrates tallied from the non-sand wave and sand wave transects. The Chi-Square Analysis resulted in a significant difference between observed and expected frequencies, and the null hypothesis was rejected stating that species occurrences are independent of habitat types. For fish families, the G-test statistic yielded 519.67 with a two-tailed P-value of 2.60E-112 (DF=3) (Table 4-3).

Table 4-3 Results of the Log-Likelihood Ratio for Goodness-of-Fit for fishes. The P-value ensues that the null hypothesis is rejected and that there is a utilization of substrate type among the fish families observed in the ROV video data collected in San Juan Channel.

Substrate Type Category	G-Test Statistic	DOF	P-Value (Two-Tailed)
Gravel	519.67	3	2.60E-112
Mixed		3	
Rock		3	
Sand		3	

There were variations in percent composition of fish families between non-sand wave areas and sand wave areas in San Juan Channel (Figure 4-19). In non-sand wave habitats, individuals in the families Gadidae and Scorpaenidae dominated. In sand wave habitats, individuals in the family Gadidae were most frequent, while the family Ammodytidae was the second-most frequent family and occurred in higher frequency than in non-sand wave habitats. Furthermore, in the crests of sedimentary bedforms, the families Ammodytidae and Gadidae dominated, while in the troughs, there was a higher

percent composition of individuals in the family Gadidae. There was a higher percent composition of individuals in the family Pleuronectidae in the troughs than in the crests.

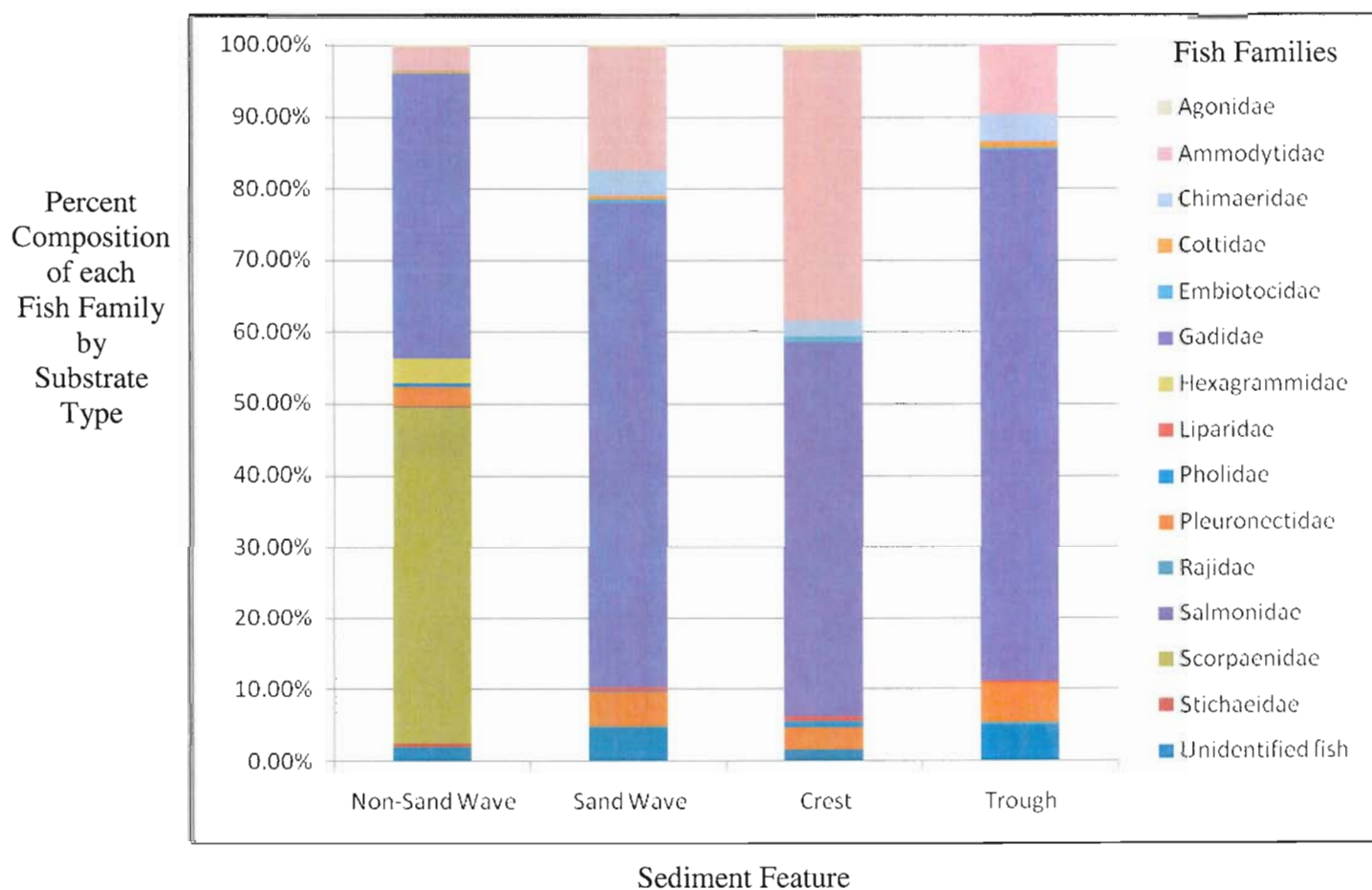


Figure 4-19 Descriptive graph of percent composition of fish families in non-sand wave versus sand wave habitats and crest and trough morphologies based on analyzed ROV video collected in San Juan Channel. Crest and trough characterizations were based on slope and BPI data using a GIS. Percent of total number of fish families observed is on the y-axis and sediment feature based on geomorphologic type is on the x-axis. Names of families are shown in different colors. N=5,056.

The percent composition of fishes varied among the different substrate types tallied from the time bin observations among all transects (Figure 4-20). Family frequencies were calculated from fish observations for each substrate type, and for the gravel substrate category, virtually all fish were gadids. For the mixed substrate category, the family Gadidae dominated while there were occurrences of Ammodytidae, Liparidae and Scorpaenidae. In areas where the ROV transited soft sediment that had occurrences of rock, individuals in the family Hexagrammidae and Scorpaenidae were present. In habitats composed of sand, individuals in the family Ammodytidae and Gadidae had the highest compositions; however, considerable percent compositions of the family Chimaeridae and Pleuronectidae existed.

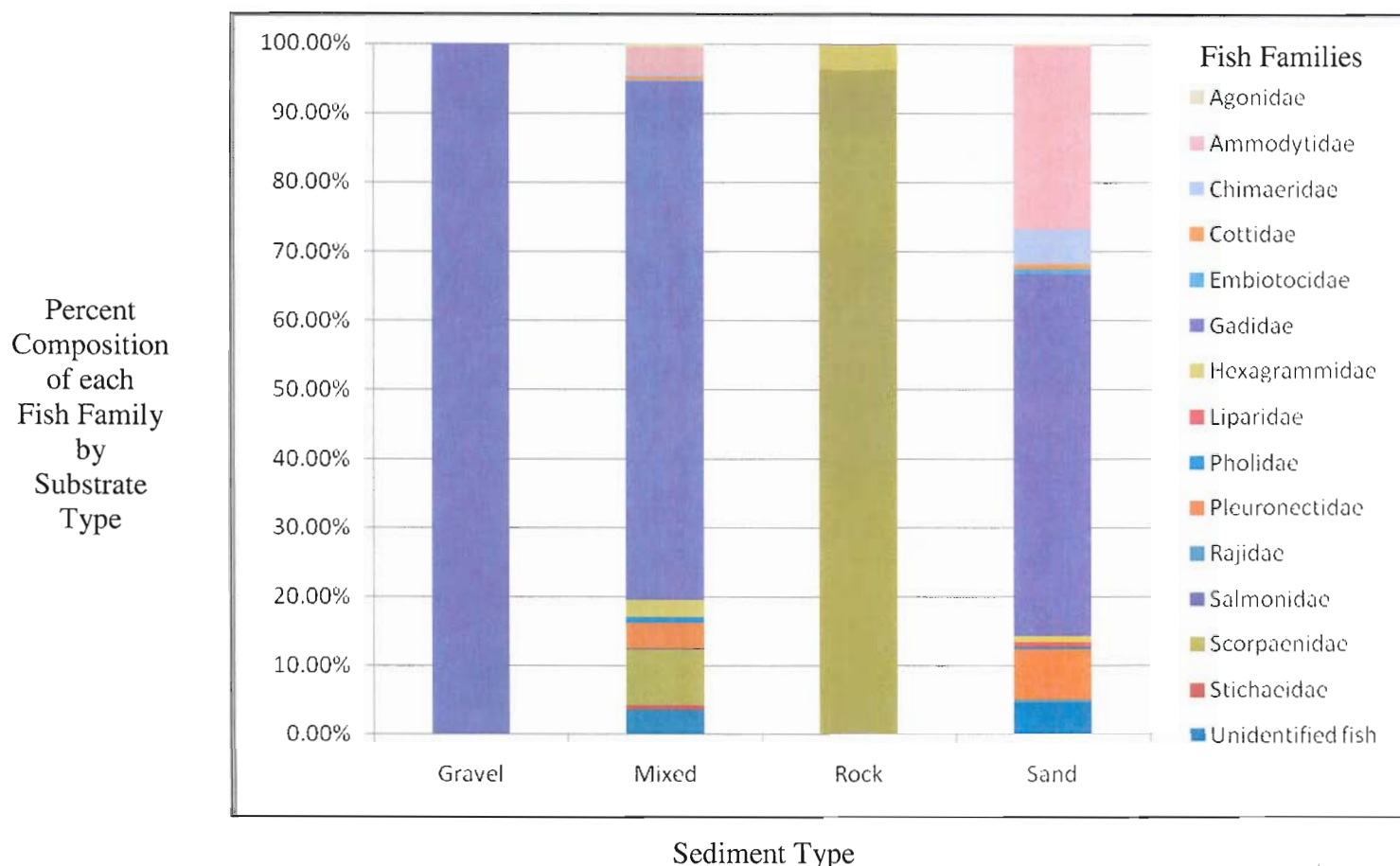


Figure 4-20 Graph of percent composition of fish families in gravel, mixed, rock and sand substrates with percentage on the y-axis and substrate type on the x-axis. Substrates include non-sand wave and sand wave habitat types. Names of families are shown in different colors. N=5,056.

The relative percent composition of fish families among varying slope values was calculated (Figure 4-21). Steep areas are included in the analysis as ROV transects contained both soft sediment and rock time bins. There were similarities between the varying slope categories. The Gadidae was the most dominant family in flat and flat/sloping areas. In sloping and steep areas, the family Scorpaenidae had the highest percent composition. Individuals in the family Hexagrammidae were also present in both

of these categories. Individuals in the family Ammodytidae was seen in all slope variations except those categorized as steep.

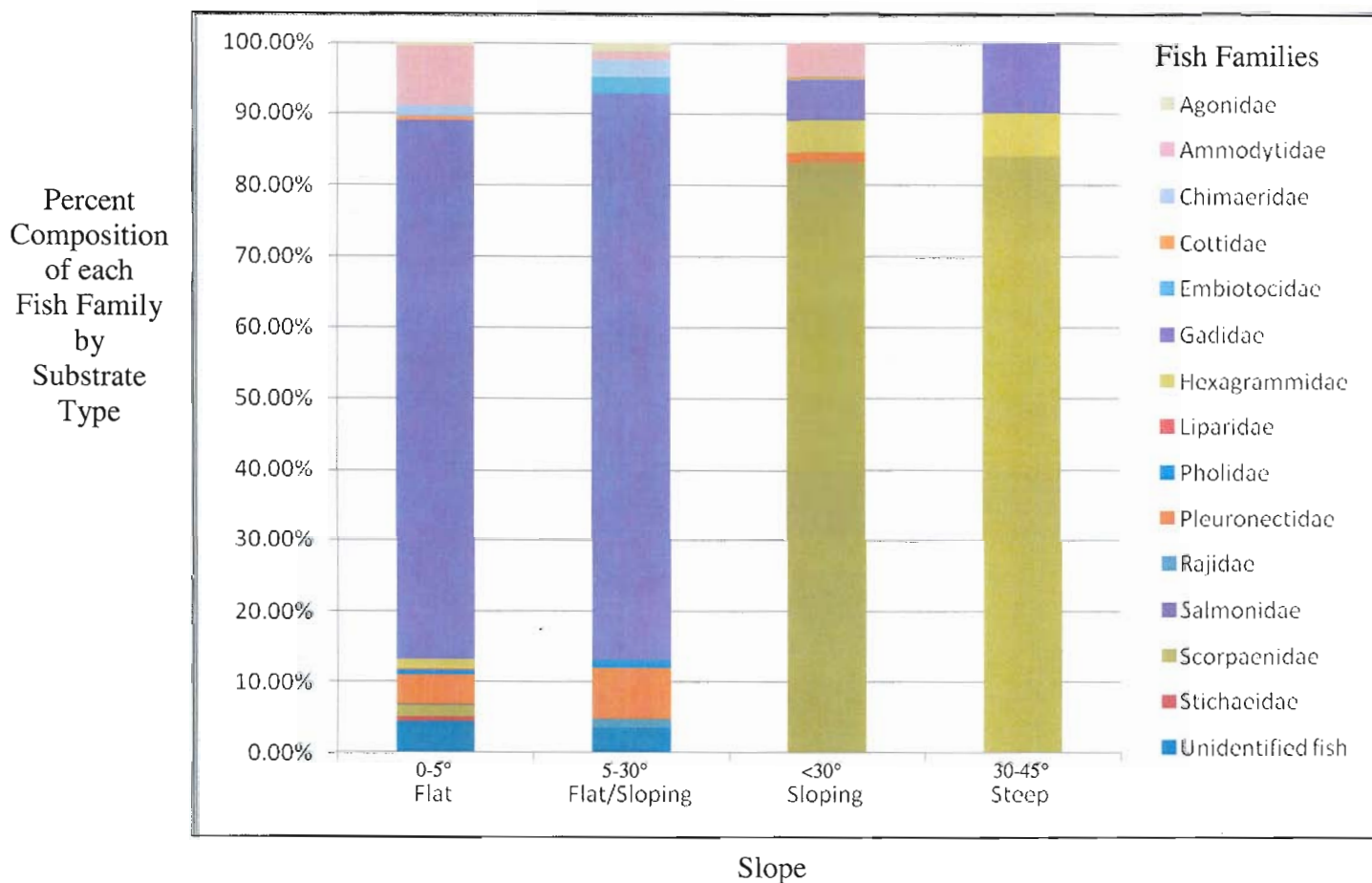


Figure 4-21 Descriptive graph of percent composition of fish families in flat, flat/sloping, sloping and steep areas. Note: while soft sediment habitats were the focus of the study, transects transited areas where rock occurred. Percentage is on the y-axis and morphologic type is on the x-axis. Names of families are shown in different colors. N=5,056.

On the ROV survey in San Juan Channel in 2004, sand lance were viewed emerging from sediment waves as the ROV transited the seafloor (Figure 4-22). The depth at which the sand lance were observed was about 75 m. They were situated within the ripples on top of coarse-grained sediment waves and startled, swam out of the ripples.



Figure 4-22 Screen grab taken from dive in San Juan Channel using Phantom HD2+2 ROV. Note sand lance emerging from sediment waves (outlined by yellow circle). Lasers indicate 10 cm spacing. Depth in feet is shown in top right corner of each image.

Invertebrates were identified to genus and species level and included spot prawn (family Pandalidae) and red sea cucumber (family Stichopodidae) (Table 4-4). Northern horse mussels were also observed in the ROV video. The mussels were too numerous and cryptic to count, but their presence or absence was quantified. Mussel shells were observed on both the ridges and crests of the sediments waves (Figure 4-23). Mussels were not seen in the 2004 videos, but were observed in the 2005 videos. The shells were

observed in depths between approximately 75 m and 125 m. In areas where mussel shells were present in the crest of the bedform, the substrate type varied from sand to mixed gravels, pebbles and coquina. Mussel shells observed in the trough of a bedform were characterized as having both sand and mixed gravel, pebble and mud substrate and on a flat/sloping bottom. All observations of mussel shells were seen in sand wave transects. It is not known if there were living mussels seen in the ROV videos in San Juan Channel in 2004; however, it is postulated that the observations are of mussel shells amongst living mussels. Previous trawls in the area resulted in living mussels.

Table 4-4 List tabulating total estimated number of individuals counted for each fish family in San Juan Channel. Organisms were identified to species level as could be determined. Family names were used for analysis.

Invertebrate Family and Common Name	Species	Family	Total Number Individuals Observed
Pandalidae			
Spot prawn	<i>Pandalus platyceros</i>	Pandalidae	2611
Stichopodidae			
Red sea cucumber	<i>Parastichopus californica</i>	Stichopodidae	660
Total			<i>N</i> =3,271



Figure 4-23 Screen grab taken from dive in San Juan Channel using Phantom HD2+2 ROV. Yellow circle is highlighting mussel shells in bedform troughs. Lasers indicate 10 cm spacing. Depth in feet is shown in top right corner.

There were no differences in densities [total number of fish individuals divided by transect area (m^2)] between sand wave and non-sand wave habitats after the data were log transformed using a two-sample T-Test for all invertebrate families ($P=0.491$) (Table 4-5). There was an average of six invertebrates per km^2 based on ROV videos analyses for non-sand wave transects and an average of seven invertebrates per km^2 in sand wave transects. Spot prawn and sea cucumber densities were 6 ± 2.25 SE and 5 ± 3.01 SE fish/ km^2 in non-sand wave transects and were not statistically different from their densities where they occurred in 7 ± 4.63 SE and 4 ± 2.31 SE fish / km^2 in the sand wave fields, respectively. Test probabilities were Pandalidae: $P=0.567$ and Stichopodidae: $P=0.110$.

Table 4-5 List of transect area and invertebrate density calculations from ROV survey in San Juan Channel showing area calculations (m^2) for each transect conducted in both non-sand wave and sand wave habitats with associated invertebrate densities (km^2).

Non-Sand Wave		Density (# per km^2)	
Transect #	Transect Area (m^2)	All fish	
1116	315.4	6	
1149	659.4	5	
1213	362.3	4	
1222	273.8	4	
1234	602.6	7	
1238	520.0	7	
1308	500.9	5	
1335	443.9	7	
1355	483.1	4	
1359	855.0	6	
1414	557.7	5	
1449	585.1	0	
1458	457.5	9	
1503	772.2	0	
1518	785.3	9	
1607	747.9	6	
1610	484.3	0	
1619	420.0	5	
1636	336.5	8	
1700	319.4	7	
1706	430.8	6	
1801	444.8	4	
1811	431.7	7	
1831	671.4	6	
1850	800.1	5	
Mean		6	
Two-tailed T-Test		0.49076	

Sand Wave		Density (# per km^2)	
Transect #	Transect Area (m^2)	All fish	
1133	604.9	9	
1300	327.0	4	
1342	407.4	6	
1357	347.4	6	
1440	679.1	4	
1532	548.5	6	
1548	504.0	9	
1617	909.5	6	
1624	490.0	7	
1705	640.8	8	
1838	1151.6	8	
Mean		7	

The observed frequencies of invertebrates in the four substrate categories were compared to the frequencies of these substrate categories among the transects. For invertebrate families, the G-test statistic yielded 867.09 with a two-tailed P-value of $1.22\text{E-}187$ (DF=3) (Table 4-6). Therefore, the observed values were significantly different than the predicted values. Therefore, invertebrates observed in the ROV videos in San Juan Channel are not randomly distributed along gravel, mixed, rock and sand substrates.

Table 4-6 Results of the Log-Likelihood Ratio for Goodness-of-Fit for invertebrates. The P-value ensues that the null hypothesis is rejected and that there is a utilization of substrate type among the invertebrate families observed in the ROV video data collected in San Juan Channel.

Substrate Type Category	G-Test Statistic	DOF	P-Value (Two-Tailed)
Gravel	867.09	3	1.22E-187
Mixed		3	
Rock		3	
Sand		3	

For transects that were separated into categories based on occurrence in sand wave and non-sand wave habitats, individuals in the family Pandalidae had the highest percent composition in sand wave habitats (Figure 4-24). Individuals in the family Stichopodidae were frequent in both sand wave and non-sand wave habitats; however, in non-sand wave habitats, individuals in the family Stichopodidae dominated and had the highest percent composition. In the bedforms where number of individuals were counted and analyzed based on their presence in the crest or trough, individuals in the family Pandalidae had the highest percent composition in both parts of the bedform; however, a slightly higher percent composition was observed in the trough. Individuals in the family Stichopodidae had a low percent composition in both crest and trough.

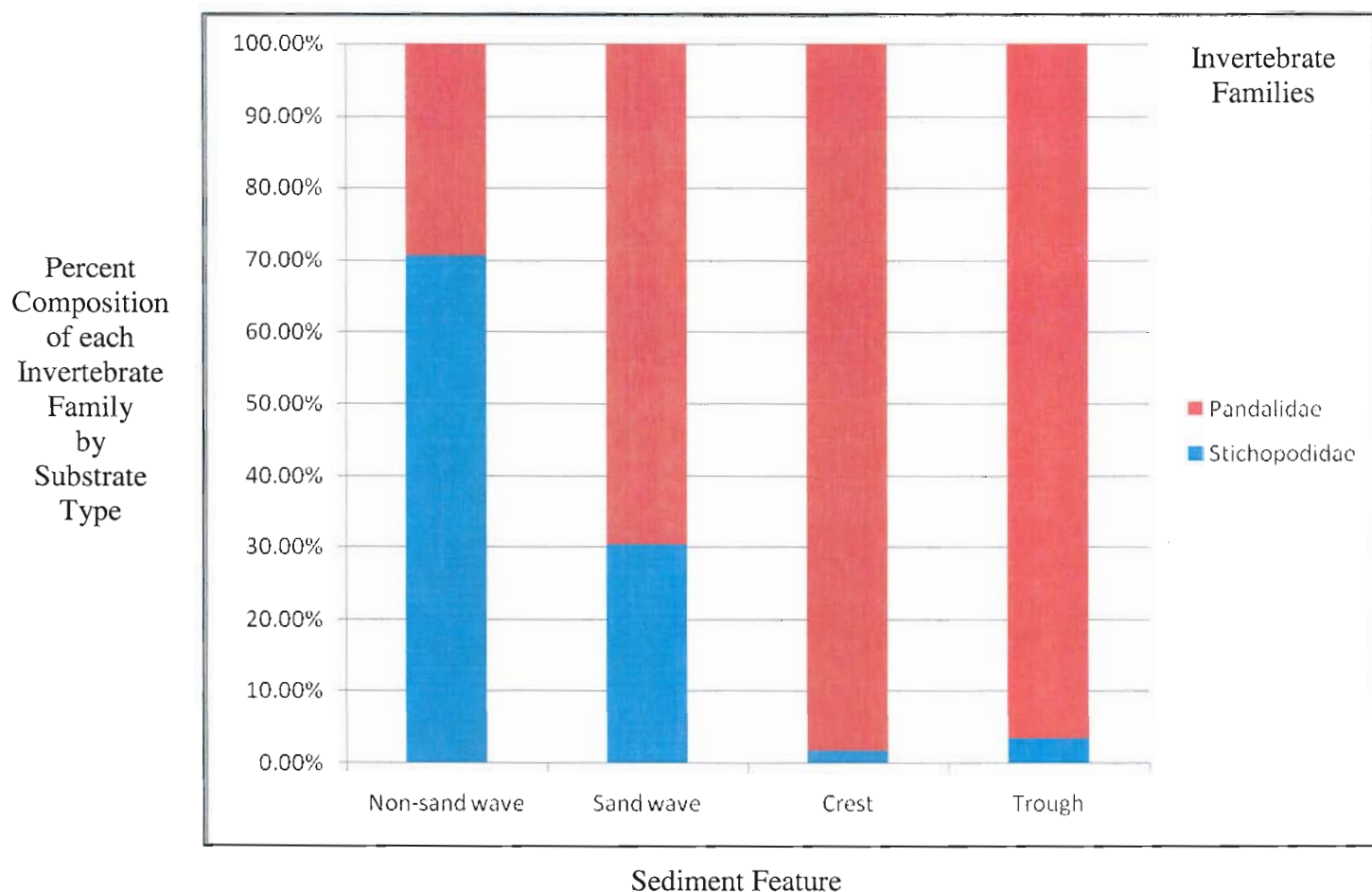


Figure 4-24 Descriptive graph of percent composition of invertebrate families in non-sand wave versus sand wave habitats and crest and trough morphologies based on analyzed ROV video collected in San Juan Channel. Crest and trough characterizations were based on slope and BPI data using a GIS. Percent of total number of fish families observed is on the y-axis and sediment feature based on geomorphologic type is on the x-axis. Names of families are shown in different colors. N=5,056.

Variations in percent composition of invertebrate families among substrate types were revealed (Figure 4-25). In the gravel and sand categories, spot prawns dominated. There were mostly spot prawns in mixed sediment type, but there was a high percent

composition of red sea cucumbers. In soft sediment areas where the ROV encountered areas of rock, red sea cucumbers were the majority.

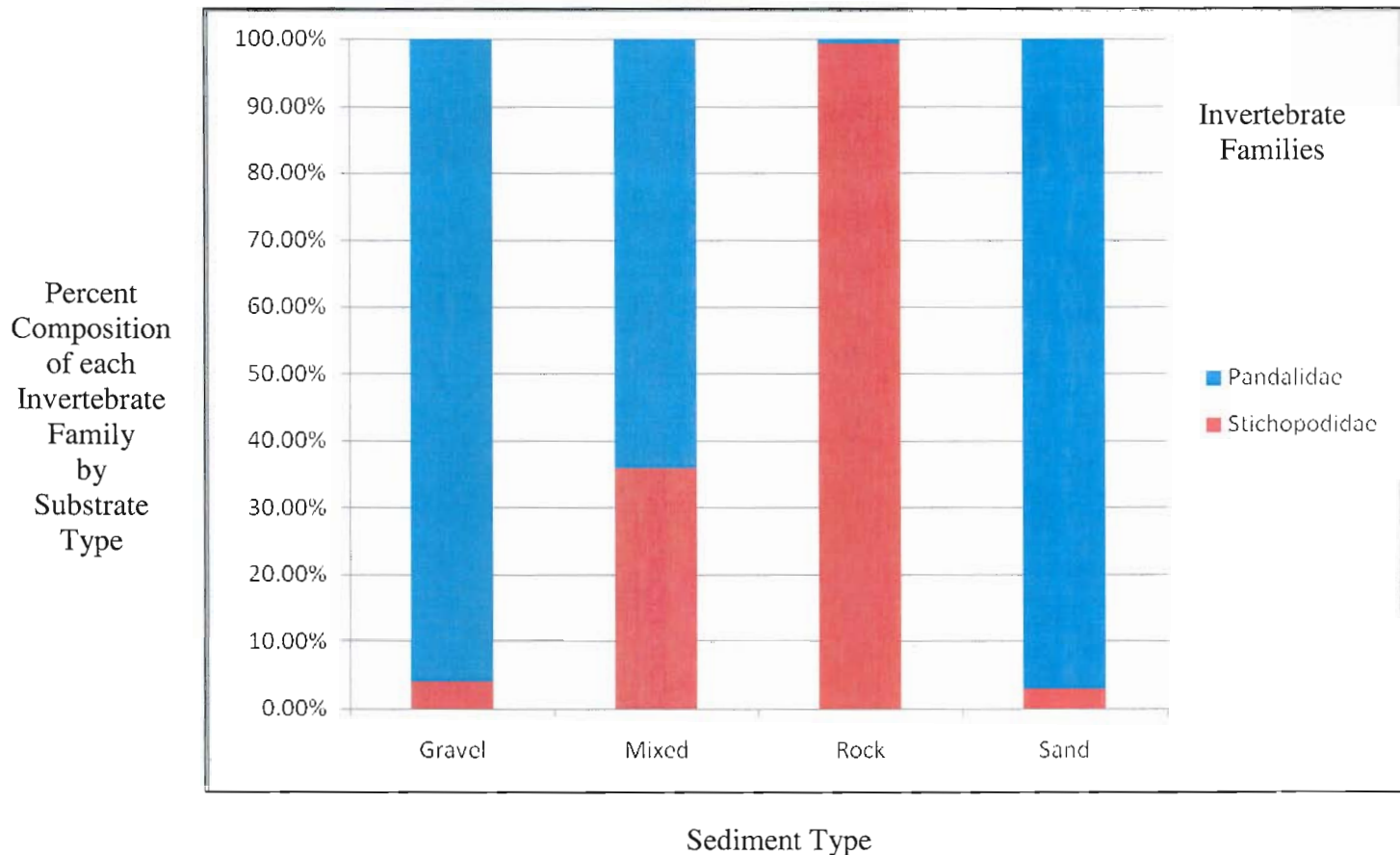


Figure 4-25 Graph of percent composition of invertebrate families in gravel, mixed, rock and sand substrates with percentage on the y-axis and substrate type on the x-axis. Names of families are shown in different colors. N=5,056.

Differences in percent composition of invertebrate families were observed among varying slope values (Figure 4-26). Spot prawns were present in all slope categories, but had the highest percent composition in flat/sloping areas ranging from 0-30°. Red sea cucumbers were viewed in all the slope variations, but dominated the areas categorized as steep.

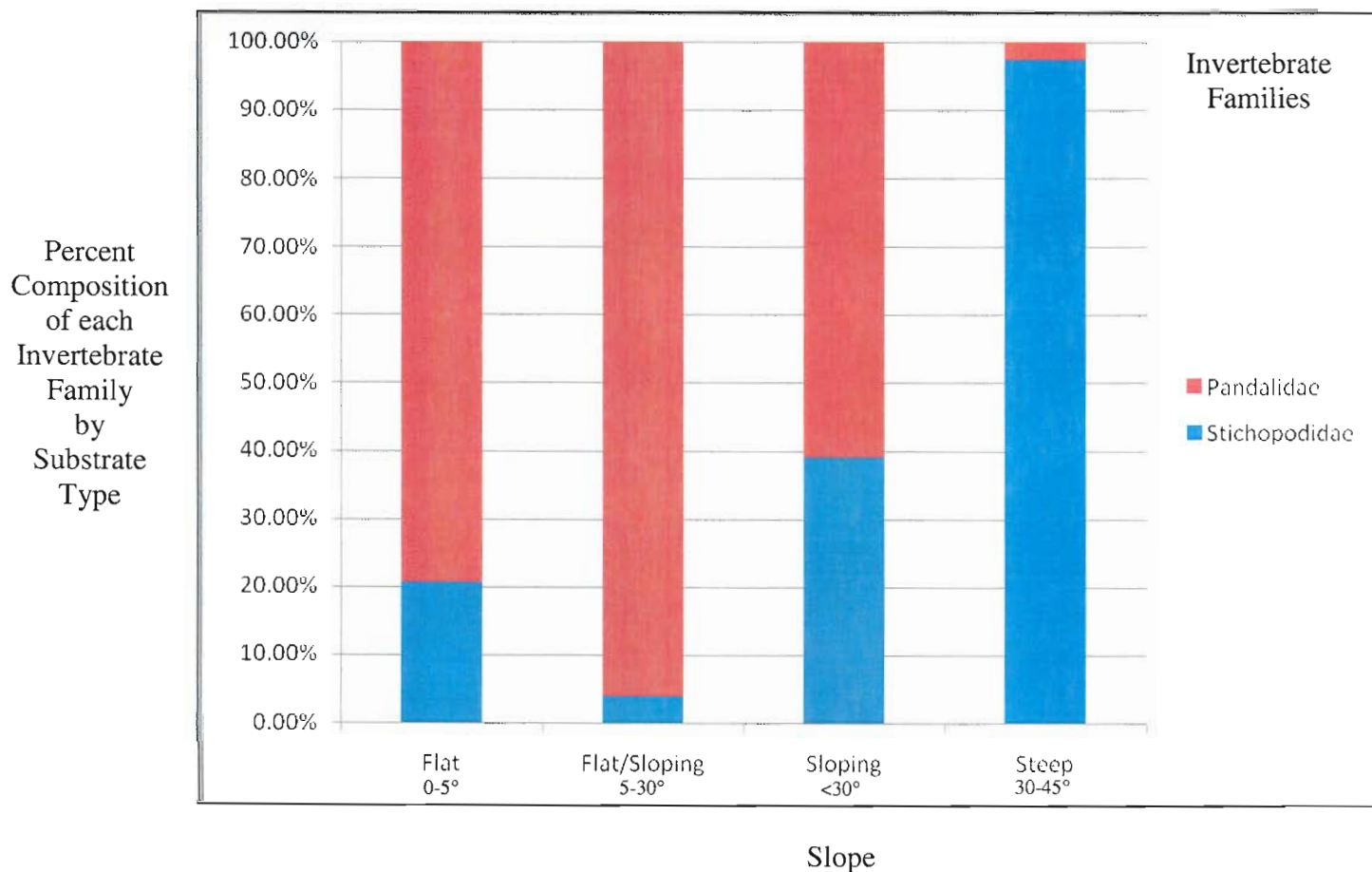


Figure 4-26 Descriptive graph of percent composition of invertebrate families in flat, flat/sloping, sloping and steep areas. Note: while soft sediment habitats were the focus of the study, transects transited areas where rock occurred. Percentage is on the y-axis and morphologic type is on the x-axis. Names of families are shown in different colors. N=5,056.

4.2.3 BPI and Slopes

A Bathymetric Position Index (BPI) was used for the analysis of crest and troughs resulting from ROV transects in San Juan Channel (Figure 4-27). This map identified the bathymetric highs and lows of the seafloor and colored them accordingly. The areas of seafloor categorized as bathymetric lows are shaded in blue and the areas of seafloor categorized as bathymetric highs were assigned orange and red colors. A slope map was additionally used to further identify areas of varying seafloor elevation (Figure 4-28). In the GIS, slope values were assigned to areas of the seafloor with varying slopes. In regions where there was relatively flat seafloor, green and yellow colors were assigned. Orange and red colors were used to designate areas displaying a high slope.

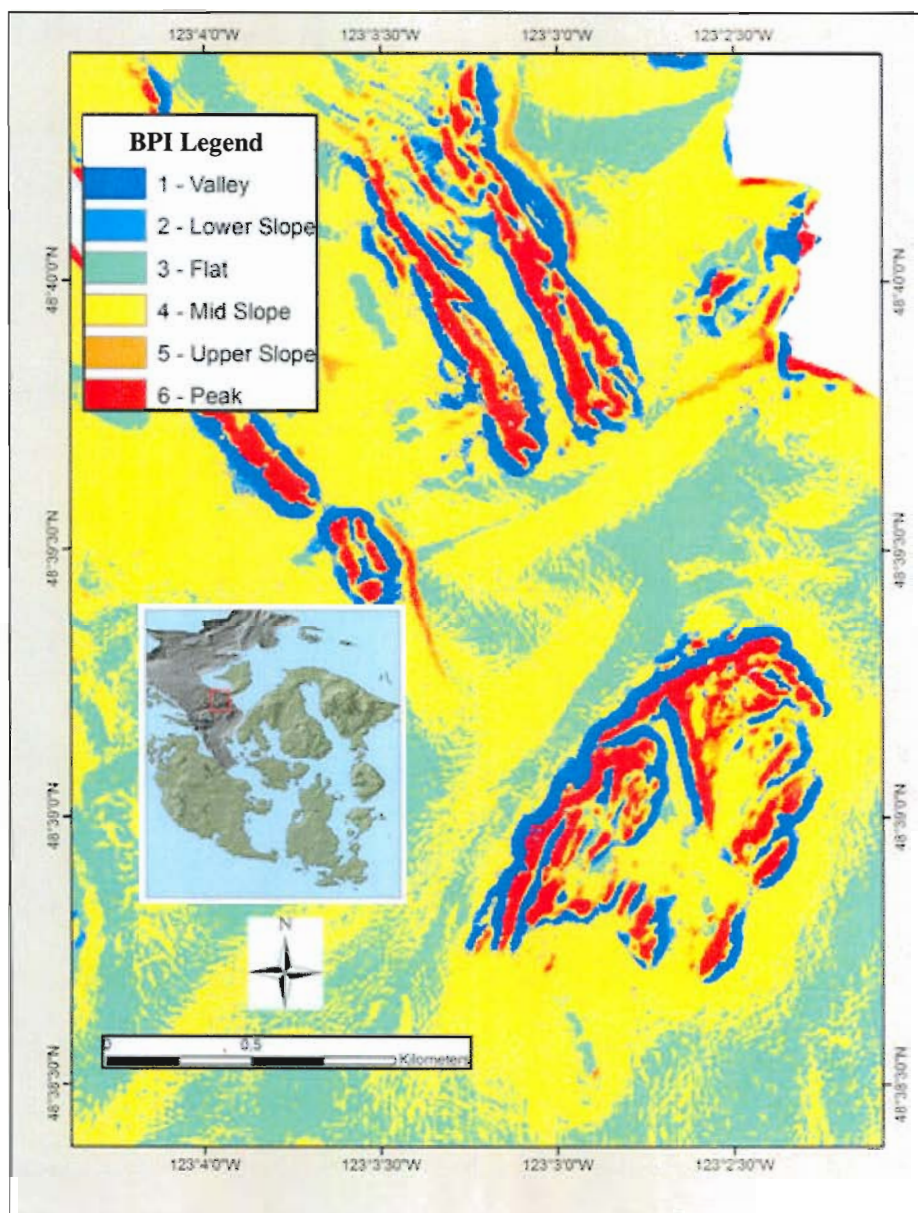


Figure 4-27 Image of BPI DEM overlaying multibeam bathymetry. BPI with values of 50 were used for ROV analysis in San Juan Channel. Orange and red colors indicate topographic highs or peaks, or in this dataset, crests, and blue colors illustrate topographic lows, or troughs. Scale 1:15,000.

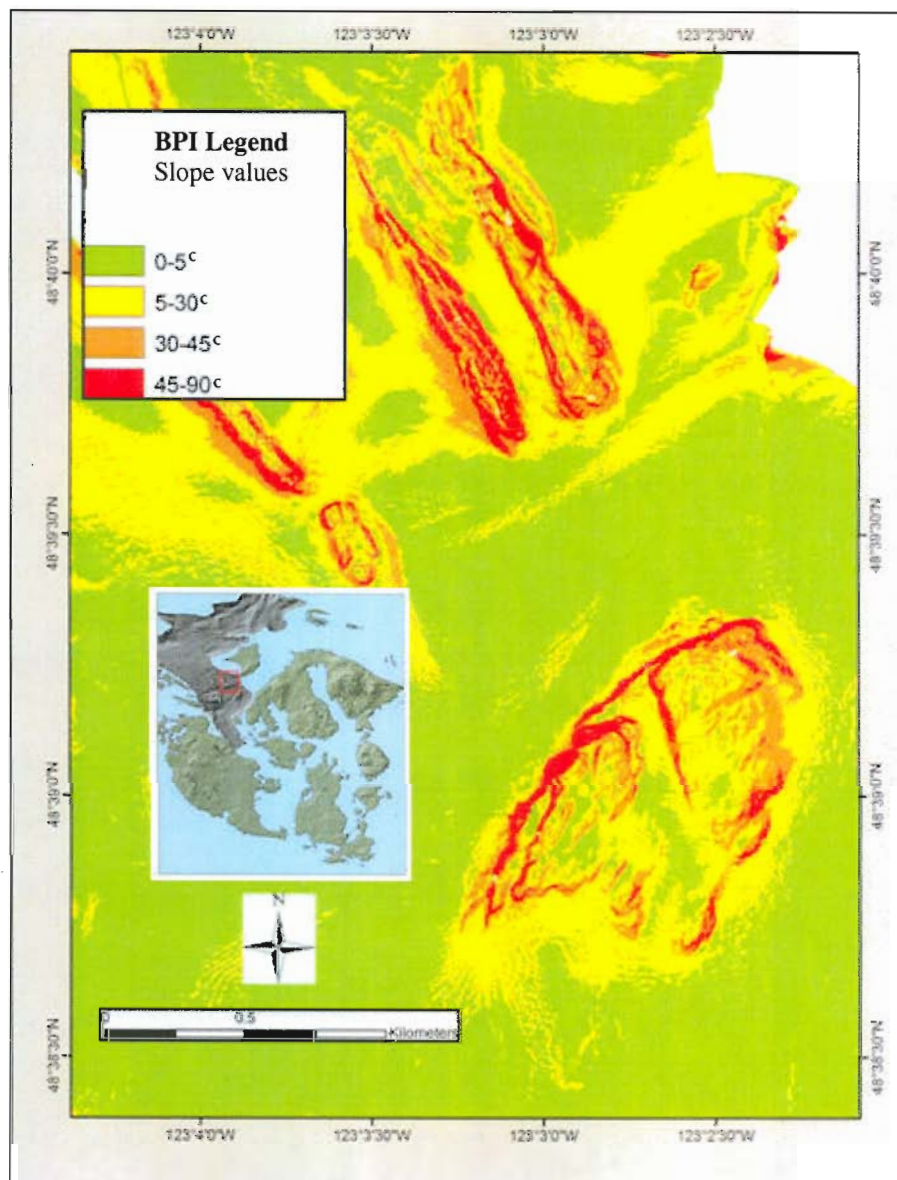


Figure 4-28 Image of slope map derived from multibeam bathymetry. Slope levels of 0-30 degrees are colored green and yellow and values of 30-45 degrees are shown in orange and red colors. The slope map was used in conjunction with BPI DEM for ROV video analysis in San Juan Channel. Scale 1:15,000.

4.3 SEDIMENT SAMPLING

The grain size analysis of sediment taken from a bedform field in the Boundary Pass region, Canada, was composed mostly of sand with gravel. Samples 1, 2 and 3 were collected in the crest, trough and boundary separating adjacent bedforms (Figure 4-29). Sample 1 (crest) consisted of 80.5% sand, 19.5% gravel and 0.1% silt. In Sample 2 (trough), 65.5% was sand, 34.4% was gravel and 0% was silt. In the bedform boundary in Sample 3, sand dominated with 90.7% followed by 9.3% gravel and 0.1% silt. The mean particle diameter in Sample 1 was 0.551 mm and the mean ϕ was 0.86. For Sample 2, the mean particle diameter was 0.708 mm and the mean ϕ was 0.50. Sample 3 had a mean particle diameter of 0.507 mm and a mean ϕ of 0.98. Sediment samples were coarse-grained (Figure 4-30).

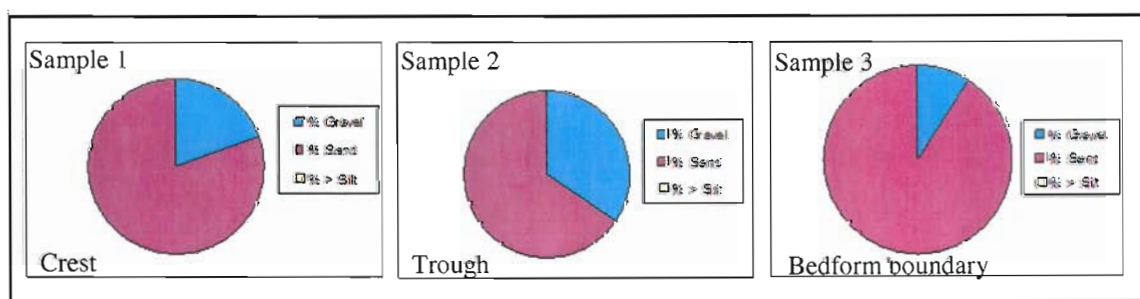


Figure 4-29 Results of grain size analysis show that the crest of the bedform field in Boundary Pass, Canada, is composed of mostly sand. The trough is also composed mostly of sand but also contains gravel. The boundary between the bedforms is mostly sand.



Figure 4-30 Example of sediment sample collected in Boundary Pass. Sample is coarse-grained sediment from the trough of a bedform field collected by the Geological Survey of Canada (GSC).

5 DISCUSSION

The main objective of this study was to investigate fish and invertebrate habitat associations with soft sediment and sand wave fields in the Georgia Basin and Northwest Straits region. There were significant differences in densities for individuals in the families Hexagrammidae and Scorpaenidae. This is most likely due to habitat type differences as fish from these families are generally associated with rocky habitats (Matthews, 1990a,b; Pacunski and Palsson, 2001; Tilden, 2004; Murie et al., 1994; Richards, 1986, 1987; West et al., 1995; Buckley, 1997). There were no differences in densities for the remaining fish families identified in the ROV videos in San Juan Channel. Also, there were no density differences in invertebrates observed between non-sand wave and sand wave habitats. There was a higher number of transects in the non-sand wave areas than in sand wave areas which played a role in the differences between fish and invertebrate densities.

This study is important in that it shows a relationship between substrate type and abundance of fishes and invertebrates. Furthermore, it is necessary to study the Puget Sound/Georgia Basin region because this area and its dynamic and varied geological features provide habitats for a variety of fishes and invertebrates. Small-scale changes in abundance and distribution can be credited to variation within assemblages (Auster et al, 1995). These habitat changes are related to bathymetric changes. The results of this study indicate that fish and invertebrate families are utilizing different habitat types.

Multibeam bathymetric and backscatter data combined with ROV video and sediment samples are viable tools for understanding the abundance and associations of demersal fishes and invertebrates in the Puget Sound/Georgia Basin region. Seafloor mapping technology enabled the creation of high-resolution maps that provide a view into the benthic environment that previous methods were unable to uncover. These datasets are unique to the region as they are a contiguous compilation of both shallow and deepwater data and provide extensive seafloor information about the region. These data exhibit varying geological seafloor features and structures, such as sediment waves, bedrock outcrops, mounds, depressions and areas affected by current and glacial scour. These features are the result of tectonic uplift, glacial scouring, and daily tides and currents in the area.

The waters surrounding and within the Puget Sound/Georgia Basin region experience the effects of the daily tides, freshwater runoff, winds and along-channel atmospheric pressure differences. These physical oceanographic conditions contribute to the creation of marine benthic habitats, specifically sedimentary bedforms. Analysis of multibeam bathymetric datasets collected at two different time periods in San Juan Channel, Washington, and the Boundary Pass region, Canada, demonstrated that these bedforms are actively-migrating seafloor features. The continuous monitoring of these ephemeral structures will aid fisheries biologists in managing the wildlife associated with these habitats. As information databases grow regarding fishes and invertebrates distribution, there will also be an increase in understanding the commercially and recreationally important fishes and invertebrates in the region.

Sediment composition of sedimentary bedform fields observed in San Juan Channel and in the Boundary Pass region in the ROV video was similar to the sediment composition of bedforms studied in the Strait of Juan de Fuca as described by Mosher and Thomson (2000; 2002). Based on knowledge of currents in the San Juan Archipelago and my experience collecting ROV video in San Juan Channel, I am in agreement with Mosher and Thomson (2000) that currents within the islands contribute to bedform construction. The raster difference maps created from the multibeam bathymetric datasets for the San Juan Channel and Boundary Pass areas supported the idea that sediments are being shifted. While this coincides with the views of Hewitt and Mosher (2001), there needs to be short term studies to determine if these bedforms are actively migrating in contrast to just moving back and forth.

By investigating the relationship between bedform size and depth, a relationship between wavelength (m), height (m) and depth (m) was determined. This corresponds to research from previous studies (Yalin, 1964, 1977, 1987; Allen, 1982; Ashley, 1990; Southard and Boguchwal, 1990; Dalrymple and Rhodes, 1995). However, more samples are needed to determine a statistical relationship between bedform size and depth. Also, more research on flow velocities in the regions surrounding bedform fields in the area would be helpful.

The erosion and deposition of sediment is evident from analyzing the multibeam bathymetric datasets. Creating a BPI from a DEM was a useful technique in that it aided in identifying the varying sizes of the bedform features which were correlated with fish and invertebrate occurrences seen in the ROV video. Also, by analyzing slope in

multibeam bathymetry data, the angle of repose and the lee and stoss-side slopes of bedforms can be determined. Additionally, the tool marks observed in the multibeam bathymetric data are evidence that currents are modifying the seafloor sediment.

Methodologies used in previous studies that explored fish and their associations with bedforms varied from this project. For instance, investigations were conducted in laboratories in flumes and tanks under controlled conditions where filtered seawater was continuously flushed and aerated (Gerstner and Webb, 1998; Gerstner, 1998; Stoner and Titgen, 2003). Additionally, other studies occurred seasonally (Stoner, 2003), while in this study, data were collected during the Fall only. Further data collection conducted during the seasons in addition to Fall would increase information in the Puget Sound/Georgia Basin about fishes and invertebrates and the environment since marine organisms change habitats seasonally and with age or size (Langton et al. 1996; Able 1999; Stoner et al. 2001).

Groundtruthing tools such as ROVs and sediment grabs made direct observations of the seafloor and surrounding environment possible. The use of an ROV revealed macrohabitat relationships between geologic structures and fishes and invertebrates. The 2004 and 2005 ROV surveys provided crucial documentation of marine benthic habitats including soft-sediment areas such as bedforms as well as the presence or absence of fishes and invertebrates within the bedforms.

The waters of the Puget Sound/Georgia Basin region are diverse in habitat type and fauna. While many studies have been conducted in areas of high relief, there was a lack of research in low relief environments. While soft-sediment areas are not considered

variable habitats, they support high diversity (Etter and Grassle, 1992; Coleman et al., 1997; Gray et al., 1997; Snelgrove, 1999). Soft to mixed-sediment substrate include glaciomarine sediment consisting of silt, sands and gravel, consolidated or unconsolidated sand and gravel, and sedimentary bedforms comprised of sand and gravel. Due to past episodes of glaciation, geologic processes and tidal variation, the availability of coarse-grained sediment in the channels and waterways enclosed by the San Juan Islands provide a place of refuge and shelter for Pacific sand lance and other fishes and invertebrates.

Sand lance are commonly found within sandy substrates which act as a place of refuge. Currents were evident while collecting the ROV data and occasionally impacted the movement of the ROV. The oceanographic processes in the San Juan Archipelago are evidence that oceanographic conditions provide necessary elements for the sand lance to thrive. The currents can arrange loose sediments and deposit shells and cobbles to provide a temporary habitat for small fishes and invertebrates (Auster, 1998).

Results from the ROV survey in San Juan Channel demonstrated a high density of Pacific sand lance. This information coincides with a study by Blaine (unpublished report, 2006) who also observed a high density of Pacific sand lance in the same wave field. Since strong tidal currents exist in the region of the bedform field, it is possible that high concentrations of zooplankton are attracting the sand lance to feed.

The sandeel, a member of the family Ammodytidae, was observed burrowing in the sand in the North Sea (Wright and Tuck, 2000). This behavior was perceived as a method of avoiding predators and as a strategy for energy conservation. The habitats in

which the sandeels thrive were characterized as coarse sand or sand mixed with gravel or shell fragments. Also, ripples on the seafloor were positioned tangential to the tidal stream. In San Juan Channel, sand lance were observed in sand waves composed of mixed and sand substrates in areas of strong currents.

Wright and Tuck (2000) contend that sediment composition, such as pure sand, is not the only contributing factor towards sandeel distribution. Rather, the sediment grain size and physical oceanographic conditions of the area could also influence their presence. For example, sandeels ventilate their gills with interstitial water while burrowing in tidally active areas where ripples exist. Ripples are generally associated with an abundant sand supply and currents up to 1 m/s (Stride, 1982). In San Juan Channel where sand lance were observed burrowing in sand waves, 1-2 m/s currents exist in the area and were likely a contributing factor for the formation of the sand waves. Stoner et al. (2007) postulated that habitats with enhanced structural complexity, such as bedforms, provide higher densities of prey items. The sand waves observed in San Juan Channel may also contain prey items that attract sand lance and other fishes and invertebrates.

Stoner et al. (2007) demonstrated that juvenile flatfish distribution at a nursery ground in Alaska is not only based on environmental variables such as depth, temperature and sediment characteristics, but also sediment surface bedforms, emergent invertebrates and vegetation. It was found that rock sole abundance was associated with the non-traditional habitat variables, including worm tubes and sediment surface bedforms. For northern rock sole and Pacific halibut, positive correlations have been reported between

fish catch and the bycatch of shells and echinoderms in beam trawl collections (Stoner and Titgen, 2003). Additionally small flatfishes were observed in ROV surveys in association with troughs of sand waves (Norcross and Mueter, 1999). Additionally, sex segregation of English sole was associated with grain-size characteristics in Puget Sound, Washington (Becker, 1988). Results were similar among a variety of sampling conditions, years, seasons, embayments and depths.

In San Juan Channel, there were higher abundances of individuals in the Pleuronectidae family in geomorphologies characterized as wave and in mixed and sand substrate types. Rock sole were observed in mixed sediment and sand bedforms with small ripples and waves. Individuals in the Ammodytidae, Embiotocidae, Gadidae, Pleuronectidae, Pandalidae and Stichopodidae family were found where mussel shells were positioned in the crests and troughs of sediment waves. Individuals in the Ammodytidae, Gadidae and Pleuronectidae families were also observed among the troughs and crests of sediment waves where no mussel shells were found.

Macro-invertebrate and groundfish assemblages were studied at Heceta Bank, Oregon (Tissot et al., 2007). Abundances among fish species and macro-invertebrates were compared to seafloor types which were based on the geological definitions of habitat types of Greene et al. (1999). These included shallow rock ridges, mid-depth boulder-cobbles, deep cobbles and deep mud slope. Shallow water was defined as less than 100 m and deeper areas were greater than 150 m. Some organisms that were found in the Heceta Bank study were the same as those observed in San Juan Channel. These included dover sole, rex sole, ratfish, lingcod, Puget Sound rockfish and sea cucumbers.

At Heceta Bank, dover sole were abundant in mud that consisted of boulders, cobbles and pebbles while rex sole inhabited mud void of boulders. Lingcod were associated with shallow rock ridges, cobbles and large boulders. These geologic substrates and geomorphologies provide a source of food and shelter. Puget Sound rockfish were found in boulder-cobble habitat. Ratfish and sea cucumbers were found in habitat characterized as deep mud slope.

In San Juan Channel, Hexagrammidae were found mostly on rocky substrates with an irregular geomorphology. Individuals observed in the Pleuronectidae family were observed in mixed and sand substrate types. Individuals in the Chimaeridae family were seen in sand and ripples. Stichopodidae were seen in a mixed substrate type and in both regular and irregular geomorphologies. High velocity habitats provide greater food resources and opportunities for cod migration (Gerstner, 1998). Lough et al. (1989) discovered widespread aggregations of juvenile cod in pebble-gravel deposits on the Georges Bank. The presence of these young organisms in this type of substrate was related to the supply of settlement-stage affected by water circulation. Gadids were found throughout the gravel, mixed and sand substrates in San Juan Channel. Pacific cod were observed in a mixed gravel and cobble environment and sediment waves in San Juan Channel. The sediment wave field is situated in an area designated by higher current velocities and was characterized by smaller ripples overlying the larger waves.

Mussels are found on rocky shores where larvae and postlarvae can attach to a bare, hard substrate (Commito, et al., 2006). Mussels do not generally attach to bare, soft substrate because the larvae cannot connect to small sediment particles that may

potentially be transported by currents. Commito, et al. (2006) studied the mechanisms that control mussel distribution and related them to soft sediment environments. There was a positive correlation between greater abundance of mussels and water flow. Since only the shells of mussels were found in the bedforms in San Juan Channel, it is difficult to determine if live mussels were originally inhabiting the sand wave areas, or if currents transported them, but should be explored further in future studies in the San Juan Archipelago.

Spot prawns were observed mostly on gravel and sand substrate types. This coincides with observations of spot prawn habitat at the Carmel Bay Ecological Reserve (CBER) in California (Schlining, 1999). In San Juan Channel, spot prawns were found at depths ranging from about 45 to 165 m. In the CBER, spot prawns were found around 200 m water depth. Additional studies on spot prawn distribution would enhance knowledge about spot prawn distribution based on depth and available habitat.

Possible explanations for the distributions of fishes and invertebrates in San Juan Channel in the varying substrate, geomorphology and slope habitats include predator avoidance and prey availability, varying life stages of the organisms, water circulation, season and geographic scale. Gray (2002) suggests that available food resources control population densities at various scales. This influences species richness determined by spatial and temporal heterogeneity. Futures studies should research effects of habitat type on fish distribution among the surrounding regions of San Juan Channel as well as varying seasons. A previous study by Palsson and Tsou (2005) found fish community density differences from bottom trawl surveys data collected in Puget Sound.

It is possible that there may be an effect of organisms on the substrate. The mussel beds may be stabilizing the sediment waves which is beneficial for procuring food sources in the current-driven environment. Additionally, the potential influence of sand lance and sea cucumbers on the sedimentary substrate should be further investigated.

6 CONCLUSION

This study demonstrated that multibeam bathymetric sonar systems are effective technologies for generating a variety of products including hill-shaded, slope and marine benthic habitat maps in a GIS. Combining these datasets with groundtruthing information including ROV videos and sediment grain samples provide a comprehensive dataset necessary for identifying seafloor characteristics and biological associations.

The ROV is a useful tool for collecting observational data of the seafloor and its inhabitants given the proper bathymetry and physical oceanographic conditions. The Phantom HD2+2 ROV proved appropriate for collecting small scale video data in the sediment bedform and soft sediment areas of San Juan Channel. However, limitations included swift bottom currents causing the ROV to drift off the seafloor as well as technical problems associated with tracking and recording. The ROV effectively collected data needed to create fish and invertebrate abundance and density calculations.

The results of this study provide fish and invertebrate habitat association information necessary for making marine resource management decisions in the Georgia Basin and Northwest Straits region. These results contribute to the understanding of the geological, biological and physical oceanographic characteristics of the area and consequently aid in the protection of these habitats by the potential designation of Marine Protected Areas (MPAs). Additionally, the results presented in this study suggest that the uses of geophysical and remote sensing data are effective in studying fish/invertebrate-substrate associations in geologically diverse areas. Watching ROV videos were beneficial for verifying marine benthic habitat maps and determining habitat associations.

Marine benthic habitat maps act as a critical aid to scientists as they make informed decisions about Marine Protected Areas and Reserves. For example, by illustrating where soft, mixed and hard substrates are located, fisheries biologists and managers can use their expertise to identify where future population estimates and trawls could be conducted.

Mapping and observational methods such as video collected from ROVs and the collection of sediment samples from grabs are critical aids which foster habitat-related research. As the technology advances, scientific methodologies for understanding underwater habitats improve. High-resolution and groundtruthing datasets enable researchers to build a scientific database in a GIS regarding an environment's geological, biological and physical oceanographic characteristics.

7 LITERATURE CITED

- Able, K.W., 1999. Measures of juvenile fish habitat quality: examples from a National Estuarine Research Reserve, *in* Benaka L (Ed.) Fish habitat: essential fish habitat and rehabilitation. American Fisheries Society, Symposium 22, Bethesda, MD: 134-147.
- Allen, J.R.L., 1968. Current ripples: their relation to patterns of water and sediment motion. North-Holland Publishing Company, Amsterdam, 433p.
- Allen, J.R.L., 1982. Sedimentary Structures – Their Characteristics and Physical Basis, Vol. 1. Developments in Sedimentology, Vol. 30A Elsevier, New York, 593p.
- Ashley, G.M., 1990. Classification of large-scale subaqueous bedforms: a new look at an old problem. SEPM Bedforms and Bedding Structures Research Symposium. Journal of Sedimentary Petrology, 60: 160-172.
- Auster, P.J. 1985. Some observations of fish orientation to current direction and effects on predator-prey interactions. NAFO Scientific Council Studies, 8: 53-55.
- Auster, P.J., 1998. A conceptual model of the impacts of fishing gear on the integrity of fish habitats. Conservation Biology 12: 6, 1198-1203.
- Auster, P.J. and Stewart, L.L., 1986. Sand lance. Species profiles: life histories and environmental requirements of coastal fishes and invertebrates (North Atlantic) sand lance. U.S. Fish and Wildlife Service Biological Report. U.S. Army Corps of Engineers, TR EL-82-4, 82: 1-11.
- Auster, P.J.; Lindholm, J.; Schaub, S.; Funnell, G.; Kaufman, L.S.; and Valentine, P.C., 2003. Use of sand wave habitats by silver hake. Journal of Fish Biology, 62: 143-152.
- Auster, P.J.; Malatesta, R.J.; and LaRosa, S.C., 1995. Patterns of microhabitat utilization by mobile megafauna on the southern New England (USA) continental shelf and slope. Marine Ecology Progress Series, 127: 77-85.

- Banas, N.; Bricker, J.; Carter, G.; Gerdes, F.; Martin, W.; Nelson, E.; Ross, T.; Scansen, B.; Simons, R.; and Wells, M., 1999. Flow, stratification, and mixing in San Juan Channel. Coastal and Estuarine Geophysical Fluid Dynamics Oc590b, Friday Harbor Laboratories, University of Washington, 1-89.
- Barnard, P.L.; Hanes, D.M.; Rubin, D.M.; and Kvitek, R.G., 2006. Giant sand waves at the mouth of San Francisco Bay. *Eos*, 87: 285–289.
- Beaudreau, A. and Essington, T., 2006. Food habits, trophic ontogeny, and size-based constraints on diets of lingcod (*Ophiodon elongatus*) in the San Juan Archipelago, WA. 14th Western Groundfish Conference presentation, Oregon.
- Bergh, S.G. 2002. Linked thrust and strike-slip faulting during Late Cretaceous terrane accretion in the San Juan thrust system, Northwest Cascades orogen, Washington. *GSA Bulletin*, 114: 8, 934-949.
- Bird, E., 2000. Coastal Geomorphology (CG), John Wiley & Sons, Ltd., New York: 322p.
- Blaine, J., 2006. Pacific sand lance (*Ammodytes hexapterus*) present in the sandwave field of central San Juan Channel, WA: Abundance, density, maturity, and sediment association. FISH 492 course, Unpublished Report, Friday Harbor Laboratories, 22p.
- Blondel, P. and Murton, B.J. 1997. Handbook of Seafloor Sonar Imagery, John Wiley & Sons, New York: 303p.
- Brockport, 2005, <http://www.weather.brockport.edu>
- Brown, J.; Bearman, G. (Ed.); Colling, A.; Park, D.; Phillips, J.; Rothery, D.; Wright, J., 2000 (2nd Edition). Waves, tides, and shallow-water processes. Butterworth-Heinemann in association with the Open University, Milton Keynes, 227p.

- Buckley, R.M., 1997. Substrate associated recruitment of juvenile *Sebastes* in artificial reef and natural habitats in Puget Sound and the San Juan Archipelago, Washington. Washington Department of Fish and Wildlife Technical Report, No. RAD97-06, 320p.
- Cannon, G.A.; Ebbesmeyer, C.C.; and Nairn, B.J., 2001. Circulation variations in the northern main basin of Puget Sound. Puget Sound Research, 6p.
- Cattaneo, A.; Correggiari, A.; Marsset, T.; Thomas, Y.; Marsset, B.; and Trincardi, F., 2004. Seafloor undulation pattern on the Adriatic Shelf and comparison to deep-water sediment waves. *Marine Geology*, 213: 121-148.
- Clayman S.D., 2001. Light intensity as an environmental cue for the burial and emergence behavior of the Pacific sand lance, *Ammodytes hexapterus*. Fish Ecology Class Papers, University of Washington, 29p.
- Coleman, J.M., 1969. Brahmapura River: Channel Processes and sedimentation. *Sedimentary Geology*, 3: 129-239.
- Coleman, N.; Gason, A.S.H.; and Poore, G.C.B., 1997. High species richness in the shallow marine waters of south east Australia. *Marine Ecological Progress Series*, 154: 17-26.
- Dalrymple, R.W. and Rhodes, R.N., 1995. Estuarine dunes and bars. In G.M.E. Perillo (Ed.), *Geomorphology and Sedimentology of Estuaries, Developments in Sedimentology*, 53: 359-422.
- Etter, R.J. and Grassle, F., 1992. Patterns of species diversity in the deep sea as a function of sediment particle size diversity. *Nature*, 360: 576-578.
- Feehan, J.G. and Brandon, M.T., 1999. Contribution of ductile flow to exhumation of low- temperature, high-pressure metamorphic rocks: San Juan-Cascade nappes, NW Washington State. *Journal of Geophysical Research*, 104: B5, 10,883-10,902.

- Field, L.J. 1988. Pacific sand lance, *Ammodytes hexapterus*, notes on related *Ammodytes* species, *In* Species synopses life histories of selected fish and shellfish of the northeast Pacific and Bering Sea. (Eds.) Willmovsky, N.J.; Incze, L.S.; and Westheim, S.J.). University of Washington, Seattle: Washington Sea Grant Program and Fisheries Research Institute, 15-33.
- Flemming, B.W., 2000. The role of grain size, water depth and flow velocity as scaling factors controlling the size of subaqueous dunes. *In* Trentesaux, A. and Garlan, T. (Eds.), Marine Sandwave Dynamics, 23-24 March 2000, University of Lille 1 (France), Proceedings, 55-60.
- Folk, R.L., 1974. The petrology of sedimentary rocks, Hemphill Publishing Company, Austin: 182 p.
- Garrison, K.J. and Miller, B.S., 1982. Review of the early life history of Puget Sound Fishes. Contract No. 80-ABA-3860 NMFS (NOAA) Seattle, Washington. University of Washington School of Fisheries Institution, 331-340.
- Geiger, A.C., 1987. Trophic interactions and diurnal activity patterns of the Pacific sand lance, *Ammodytes hexapterus*, at San Juan Island, Washington. Marine Fish Biology course, University of Washington, 1-15.
- Gerstner, C.L., 1998. Use of substratum ripples for flow refuging by Atlantic cod *Gadus morhua*. *Environmental Biology of Fishes*, 51: 455-460.
- Gerstner, C.L. and Webb, P.W., 1998. The station-holding performance of plaice, *Pleuronectes plates*, on artificial substratum ripples. *Canadian Journal of Zoology*, 76: 200-208.
- Gilmour, B.; Lockhart, D.; Millar, D., 2001. Advances in Multibeam Backscatter Data Processing and the Delivery of Data Products in a GIS Environment via the Internet. Internal Fugro Pelagos, Inc. document, 8p.

- Goff, J.A.; Mayer, L.A.; Traykovski, P.; Buynevich, I.; Wilkens, R.; Raymond, R.; Glang, G.; Evans, R.L.; Olsen, H.; and Jenkis, C., 2005. Detailed investigation of sorted bedforms, or “rippled scour depressions,” within the Martha’s Vineyard Coastal Observatory, Massachusetts. *Continental Shelf Research*, 25: 461-484.
- Gray, J.S.; Poore, G.C.B.; Ugland, K.I.; Wilson, R.S.; Olsgard, F.; and Johannessen, O., 1997. Coastal and deep-sea benthic diversities compared. *Marine Ecological Progress Series*, 159: 97-103.
- Greene, H.G.; Yoklavich, M.M.; Starr, R.M.; O’Connell, V.M.; Wakefield, W.W.; Sullivan, D.E.; McRea Jr., J.E; and Cailliet, G.M., 1999. A classification scheme for deep seafloor habitats. *Oceanologica Acta*, 22: 6, 663-678.
- Greene, H.G.; Bizzarro, J.J.; Tilden, J.E.; Lopez, H.L.; and Erdey, M.D., 2005. The benefits and pitfalls of geographic information systems in marine benthic habitat mapping, *In* Wright, D.J. and Scholz, A.J., (Eds.), *Place matters geospatial tools for marine science, conservation, and marine management in the Pacific Northwest* Oregon State University Press, Corvallis, OR, 34-46.
- Greene, H. G.; Bizzarro, J.J.; O’Connell, T.; and Brylinsky, T., 2007. Mapping potential marine benthic habitats using geographic information systems: A classification scheme and attributing code, *In* Todd, B.J. and Greene, H.G., (Eds.) *Mapping of the seafloor for habitat characterization: Geological Association of Canada, Special Paper 47*, 141-155.
- Gutierrez, B.T.; Voulgaris, G.; and Thielers, E.R., 2005. Exploring the persistence of sorted bedforms on the inner-shelf of Wrightsville Beach, North Carolina. *Continental Shelf Research* 25: 65-90.
- Habgood, E.L.; Kenyon, N.H.; Masson, D.G.; Akhmetzhanov, A.; Weaver, P.P.E.; Gardner, J.; and Mulder, T., 2003. Deep-water sediment wave fields, bottom current sand channels and gravity flow channel-lobe systems: Gulf of Cadiz, NE Atlantic. *Sedimentology*, 50: 483-510.
- Hewitt, A.T. and Mosher, D.C., 2001. Late Quaternary and seafloor geology of eastern Juan de Fuca Strait, British Columbia and Washington. *Marine Geology*, 177: 295-316.

- Hjulström, F. 1935. Studies in the morphological activity of rivers as illustrated by the River Fyris. Geological Institution of the University of Uppsala Bulletin, 25: 221-528.
- Hjulström, F. 1939. Transportation of detritus by moving water. In Trask, P.D., (Ed.), Recent Marine Sediments. American Association of Petrology and Geology, 5-31.
- Hoekstra, P.; Bell, P.; van Santen, P.; Roode, N.; Levoy, F.; and Whitehouse, R., 2004. Bedform migration and bedload transport on an intertidal shoal. Continental Shelf Research, 24: 1249-1269.
- Hobson, E.S., 1986. Predation on the Pacific sand lance, *Ammodytes hexapterus*, (Pisces: Ammodytidae), during the transition between day and night in southeastern Alaska. Copeia, 1: 223-226.
- Hughes Clarke, J.E.; Mayer, L.A.; and Wells, D.E., 1996. Shallow-water imaging multibeam sonars: A new tool for investigating seafloor processes in the coastal zone and on the continental shelf. Marine Geophysical Research, 18: 607-629.
- Ireland, K., 2004. Chromatic action spectrum and threshold feeding in adult Pacific sand lance, *Ammodytes hexapterus*, exposed to white light. Marine Fish Ecology, Friday Harbor Laboratories, University of Washington, 1-15.
- Kongsberg Maritime web site, 2004. <http://www.km.kongsberg.com/>
- Kostylev, V. and Erlandsson, J., 2001. A fractal approach for detecting spatial hierarchy and structure on mussel beds. Marine Biology 139:497-506.
- Krebs, C.J., 1999. Ecological Methodology, 2nd Edition, Addison-Wesley Educational Publishers, Inc., Menlo Park: 620p.
- Langton, R.W.; Steneck, R.S.; Gotceitas, V.; Juanes, F.; and Lawton, P., 1996. The interface between fisheries research and habitat management. North American Journal of Fisheries Management, 16: 1-7.

- Lane, E.W., 1938. Notes on the formation of sand. American Geophysical Union Transactions, 19: 505-508.
- Lindholm, J.; Auster, P.; and Valentine, P., 2004. Role of large marine protected area for conserving landscape attributes of sand habitats on Georges Bank (NW Atlantic). Marine Ecology Progress Series, 269: 61-68.
- Lockhart, D.; Saade, E.; Wilson, J., 2001. New Developments in multi-beam backscatter data collection and processing. Marine Technology Society Journal, 35, 4: 46-50.
- Mackas, D.L. and Harrison, P.J., 1997. Nitrogenous nutrient sources and sinks in the Juan de Fuca Strait, Strait of Georgia, Puget Sound estuarine system: Assessing the potential for eutrophication. Estuarine, Coastal and Shelf Science, 44: 1-21.
- Masson, D.G., 2003. Summary of geophysical techniques. In European Margin Sediment Dynamics: Sidescan Sonar and Seismic Images, Springer, Berlin: 256p.
- Matthews, K.R., 1990a. A comparative study of habitat use by young-of-the-year, sub adult, and adult rockfishes on four habitat types in central Puget Sound. Fishery Bulletin 88: 223-239.
- Matthews, K.R., 1990b. An experimental study of the habitat preferences and movement patterns of copper, quillback, and brown rockfishes (*Sebastes* spp.). Environmental Biology of Fishes, 29: 161-178.
- Middleton, G.V. and Southard, J. B., 1978. Mechanics of sediment movement. Society of economic paleontologists and mineralogists Short Course 3, 246p.
- Mitchell, N.C. and Hughes Clarke, J.E., 1994. Classification of seafloor geology using multibeam sonar data from the Scotian Shelf. Marine Geology, 121: 143-160.

- Mosher, D.C. and Thomson, R.E., 2000. Massive submarine sand dunes in the eastern Juan de Fuca Strait, British Columbia. Marine Sand Wave Dynamics. *In* Proceedings of an International Workshop, Lille, France, 23-24 March, 131-142.
- Mosher, D.C. and Thomson, R.E., 2002. The Foreslope Hills: large-scale, fine-grained sediment waves in the Strait of Georgia, British Columbia. *Marine Geology*, 192: 275-295.
- Murie, D.J.; Parykyn, D.C.; Clapp, B.G.; and Krause, G.G., 1994. Observations on the distribution and activities of rockfish, *Sebastes* spp. *In* Saanich Inlet, from the *Pisces IV* submersible. *Fishery Bulletin*, 92: 313-323.
- Norcross, B.L.; Blanchard, A.; and Holladay, B.A., 1999. Comparison of models for defining nearshore flatfish nursery areas in Alaskan waters. *Fisheries Oceanography*, 8: 50-67.
- Normark, W.R.; Piper, D.J.W.; Posamentier, H.; Pirmez, C.; and Migeon, S., 2002. Variability in form and growth of sediment waves on turbidite channel levees. *Marine Geology*, 192: 23-58.
- O'Connell, V.M. and Carlisle, D.W., 1994. Comparison of a remotely operated vehicle and a submersible for estimating abundance of demersal shelf rockfishes in the eastern Gulf of Alaska. *North American Journal of Fisheries Management*, 14: 1, 196-201.
- Ostrand, W.D.; Gotthardt, T.A.; Howlin S.; and Robards, M.D., 2005. Habitat selection models for Pacific sand lance (*Ammodytes hexapterus*) in Prince William Sound, Alaska. *Northwestern Naturalist*, 86:131-143.
- Pacunski, R.E. and Palsson, W.A., 2001. Macro- and micro-habitat relationships of adult and sub-adult rockfish, lingcod, and kelp greenling in Puget Sound. *Proceedings of the Puget Sound Research Conference: Bellevue, WA*, 11p.
- Palsson, W.A. and Tsou, T., 2005. Characterization of benthic marine fish communities in Puget Sound. *Proceedings of the 2005 Puget Sound Georgia Basin Research Conference*, 3p.

- Pettijohn, F.J., 1957. Sedimentary rocks, Harper & Row, New York: 718p.
- Pinto, J.M., 1984. Laboratory spawning of *Ammodytes hexapterus* from the Pacific Coast of North America with a description of its eggs and early larvae. *Copeia*, 1: 242-244.
- Pinto, J.M.; Pearson, W.H.; and Anderson, J.W., 1984. Sediment preferences and oil contamination in the Pacific sand lance *Ammodytes hexapterus*. *Marine Biology*, 83: 193-204.
- Porter, S.M., 1997. The effect of light on Pacific sandlance, *Ammodytes hexapterus*, feeding success and its implications for sandlance schools inhabiting Griffin Bay, San Juan Island, Washington. In Fish 565, Friday Harbor Laboratories, Summer 1997, University of Washington, Seattle, 137-158.
- Quinn, T., 1999. Revisiting the stock concept in Pacific salmon: insights from Alaska and New Zealand. *Northwest Science*, 73: 213-324.
- Reay, P.J., 1970. Synopsis of biological data on North Atlantic sandeels of the genus *Ammodytes*. FAO Fisheries Synopsis No. 82. Rome, Italy: Food and Agriculture Organization of the United Nations, 48p.
- Reineck, H.-E. and Singh, I.B., 1980. Depositional Sedimentary Environments, 2nd Revised and Updated Edition, Springer-Verlag, Berlin: 549p.
- Richards, L.J., 1986. Depth and habitat distributions of three species of rockfish (*Sebastes*) in British Columbia: observations from the submersible PISCES IV. *Environmental Biology of Fishes*, 17: 13-21.
- Richards, L.J., 1987. Copper rockfish (*Sebastes caurinus*) and quillback rockfish (*Sebastes maliger*) habitat in the Strait of Georgia, British Columbia. *Canadian Journal of Zoology*, 65: 3,188-3,191.

- Robards, M.D.; Piatt, J.F.; and Rose, G.A., 1999a. Maturation, fecundity, and intertidal spawning of Pacific sand lance in the northern Gulf of Alaska. *Journal of Fish Biology*, 54:1,050-1,068.
- Robards, M.D.; Willson, M.F.; Armstrong, R.H.; and Piatt, J.F. 1999b. Sand lance: a review of biology and predator relations and annotated bibliography. *Exxon Valdez Oil Spill Restoration Project Final Report* (Restoration Project 99346), 327p.
- Robards M.D. and Piatt J.F., 2000. Ecology and demographics of Pacific sand lance, *Ammodytes hexapterus* Pallas, in Lower Cook Inlet, Alaska. *Exxon Valdez Oil Spill Restoration Project Final Report* (Restoration Project 99306), U.S. Geological Survey, Alaska Science Center, Anchorage, Alaska, 1-8.
- Roberts, M.C. and Murty, T.S., 1989. Influence of delta growth on paleo-tidal flow: Fraser River delta, British Columbia, part 1. Geological framework and evolution of the delta. *Marine Geodesy*, 13: 221-228.
- Schlining, K.L., 1999. The spot prawn (*Pandalus platyceros* Brandt 1851) resource in Carmel submarine canyon, California: aspects of fisheries and habitat associations. Master's thesis at Moss Landing Marine Laboratories, 55p.
- Seibold, E. and Berger, W.H., 1996. The sea floor: An introduction to marine geology. 3rd Edition, Springer, Berlin, 288p.
- Sengupta, S., 1966. Studies on orientation and imbrication of pebbles with respect to cross- stratification. *Journal of Sedimentology and Petrology*, 36: 362-369.
- Shaw, J.; Courtney, R.C.; and Currie, J.R., 1997. Marine geology of St. George's Bay, Newfoundland, as interpreted from multibeam bathymetry and backscatter data. *Geo- Marine Letters*, 17: 188-194.
- Simrad, 2007a. EM 1002 specifications,
http://www.tdi-bi.com/downloads/EM1002_Product_specification.pdf

Simrad, 2007b. EM 3000 specifications,
<http://www.km.kongsberg.com/ks/web/NOKBG0397.nsf/>

Snelgrove, P.V.R., 1999. Getting to the bottom of marine biodiversity: sedimentary habitats – ocean bottoms are the most widespread habitat on Earth and support high biodiversity and key ecosystem services. *BioScience*, 49: 129-138.

Snover, M.L. and Commito, J.A., 1998. The fractal geometry of *Mytilus edulis* L. spatial distribution in a soft-bottom system. *Journal of Experimental Marine Biology and Ecology*, 223: 53-64.

Southard, J.B., 1975. Bed configuration. *Society of economic paleontologists and mineralogists Short Course 2*, 5-44.

Southard, J.B. and L.A., Boguchwal, 1990. Bed configurations in steady uni-directional water flows, Part 2. Synthesis of flume data. *Journal of Sedimentary Petrology*, 60: 658-679.

Stoner, A.W.; Manderson J.P.; and Pessutti J.P., 2001. Spatially explicit analysis of estuarine habitat for juvenile winter flounder: combining generalized additive models and geographic information systems. *Marine Ecological Progress Series*, 213: 253–271.

Stoner, A.W., 2003. What constitutes essential nursery habitat for a marine species? A case study of habitat form and function of queen conch. *Marine Ecology Progress Series*, 257: 275-289.

Stoner, A.W. and Titgen, R.H., 2003. Biological structures and bottom type influence habitat choices made by Alaska flatfishes. *Journal of Experimental Marine Biology and Ecology*, 292: 43-59.

Stoner, A.W.; M.L. Spencer; and C.H. Ryer, 2007. Flatfish-habitat associations in Alaska nursery grounds: Use of continuous video records for multi-scale spatial analysis. *Journal of Sea Research*, 57: 137-150.

- Sundborg, Å., 1956. The river Klarälven; A study of fluvial processes. *Geografiska Annaler*, 38: 125-316.
- Sundborg, Å., 1967. Some aspects on fluvial sediments and fluvial morphology. General views and graphic methods. *Geografiska Annaler*, 49: 333-343.
- Tilden, J., 2004. Marine Geology and Potential Adult Rockfish Habitat of the Southwestern San Juan Islands, WA. Master's thesis, Moss Landing Marine Laboratories, 121p.
- Todd, B.J., 2005. Morphology and composition of submarine barchan dunes on the Scotian Shelf, Canadian Atlantic margin. *Geomorphology*, 67: 487-500.
- Thrush, S.F.; Hewitt, J.E.; Funnell, G.A.; Cummings, V.J.; Ellis, J.; Schultz, D.; and Norkko, A., 2001. Fishing disturbance and marine biodiversity: role of habitat structure in simple soft-sediment systems. *Marine Ecology Progress Series*, 221: 255-264.
- Van de Koppel, J.; Rietkerk, M.; Dankers, N.; and Herman, P.M.J., 2005. Scale-dependent feedback and regular spatial patterns in young mussel beds. *The American Naturalist*, 165: 3, E66-E77.
- Verhagen, H.J., 1989. Sand waves along the Dutch coast. *Coastal Engineering*, 13: 129-147.
- Weiss, A. D. 2001. Topographic positions and landforms analysis, Proceedings of the 21st Annual ESRI User Conference (Map Gallery Poster), San Diego, CA, 1p.
- Wentworth, C.K., 1922. A scale of grade and class for clastic sediments. *Journal of Geology*, 30: 377-392.
- West, J.E.; Buckley, R.M.; Doty, D.C.; and Bookheim, B.E., 1995. Ecology and habitat use of juvenile rockfishes (*Sebastes* spp.) associated with artificial nursery habitats in Puget Sound, Washington. Puget Sound Research, Olympia, WA: Puget Sound Water Quality Authority, 191-202.

- Williams, H.; Hutchinson, I., 2000. Stratigraphic and microfossil evidence for late Holocene tsunamis at Swanton Marsh, Whidbey Island, Washington. *Quaternary Research*, 54: 218-227.
- Wright P.J.; Jensen H.; and Tuck I., 2000. The influence of sediment type on the distribution the lesser sandeel, *Ammodytes marinus*. *Journal of Sea Research*, 44:243-256.
- Wynn, R.B.; Weaver, P.P.E.; Ercilla, G.; Stow, D.A.V.; and Masson, D.G., 2000. Sedimentary processes in the Selvage sediment-wave field, NE Atlantic: new insights into the formation of sediment waves by turbidity currents. *Sedimentology*, 47:1,181-1,197.
- Wynn, R.B.; Masson, D.G.; and Bett, B.J., 2002a. Hydrodynamic significance of variable ripple morphology across deep-water barchan dunes in the Faroe-Shetland Channel. *Marine Geology*, S0025-3227(02)00561-3, 309-319.
- Wynn, R.B.; Piper, D.J.W.; and Gee, M.J.R., 2002b. Generation and migration of coarse-grained sediment waves in turbidity current channels and channel-lobe transition zones. *Marine Geology*, 192: 59-78.
- Wynn, R.B. and Stow, D.A.V., 2002. Classification and characterization of deep-water sediment waves. *Marine Geology*, 192: 7-22.
- Yalin, M.S., 1964. Geometrical properties of sand waves. *American Society of Civil Engineers. Proceedings, Hydraulics Division Journal*, 90: 105-119.
- Yalin, M.S., 1977. *Mechanics of Sediment Transport*, 2nd Edition. Pergamon Press, Toronto: 298p.
- Yalin, M.S., 1987. On the formation mechanisms of dunes and ripples. *Euromech Colloquium*, 261.

Appendix A: MULTIBEAM BACKSCATTER PROCESSING

Multibeam backscatter data was extracted from multibeam bathymetry data using a variety of GIS programs. At the Center for Habitat Studies at MLML, I processed backscatter data from the 2002 multibeam bathymetry dataset collected in southern San Juan Channel, Haro Strait and the Strait of Juan de Fuca. Several steps were completed when processing backscatter data from multibeam bathymetry data. Before processing begins, the georeferenced raw files were converted to data packets containing sonar, navigation, telemetry and bathymetry information. This was performed with a conversion program provided by Triton Elrics International. These files were read by the GIS program, ISIS®, which allowed for the initial processing of the backscatter data.

All of the lines were processed with the same threshold value of 4 (darkness/lightness intensity). Light and dark tones vary depending on the nature of the seafloor. For instance, high backscatter values (-10 to -30 dB for gravel) display dark tones while low backscatter values (-30 to -60 dB for fine-grained sand) show light tones (Mitchell and Hughes Clarke, 1994; Shaw et al., 1997).

Multibeam backscatter measures the intensity of the acoustic return and is obtained by sampling an individual time series for each beam in the system (Lockhart et al., 2001; Gilmour et al., 2001). The acoustic beams transmitted by the sonar head interact with the seafloor. The distance traveled from the acoustic transducer to the target of the seafloor is called the slant range (Masson, 2003) (Figure A-1). As with most sidescan sonar data, the backscatter data are scrolled on the computer screen, a water column can be seen (Figure A-2a) and slant range correction is necessary. However, while processing Simrad® multibeam backscatter data, the water column could not be

seen (Figure A-2b) as these data are not true sidescan data, but backscatter, or amplitude data, termed *pseudo sidescan sonar* data derived from the individual echosounder beams (Lockhart et al., 2001; Gilmour et al., 2001). Therefore, the slant range correction step was not necessary during post-processing. The layback, or the distance from the GPS antenna to the sonar head on the vessel, was set to zero. This is because there was not a sidescan fish being towed, but a hull-mounted multibeam system. The XYZ offsets between the GPS antenna and sonar head were already corrected for using Caris HIPS® software (Peter Milner, personal communication, 2003). Although multibeam bathymetric positioning is better than sidescan, the appearance of backscatter is similar to sidescan. Shadows are shorter due to the sonar system being higher in the water column, (Lockhart et al., 2001).

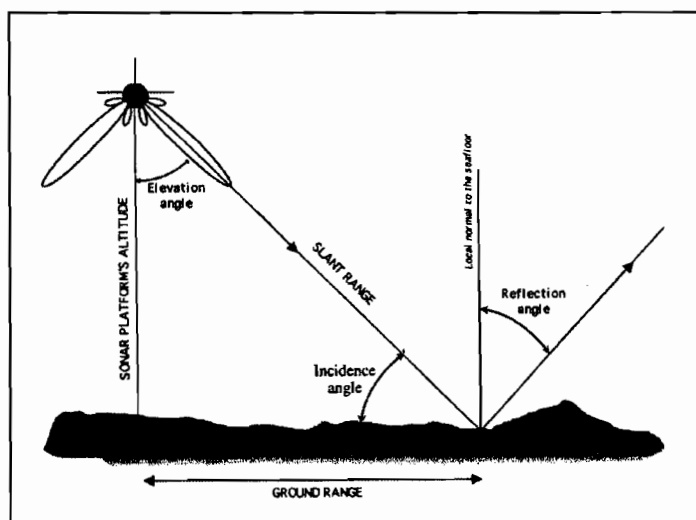


Figure A-1. Image depicting acoustic beams transmitted by the sonar which interact with the seafloor. Slant range is the distance traveled from the acoustic transducer to the target of the seafloor. The Angle of Incidence refers to the angle between the incoming wave and the seafloor (after Blondel and Murton, 1997).

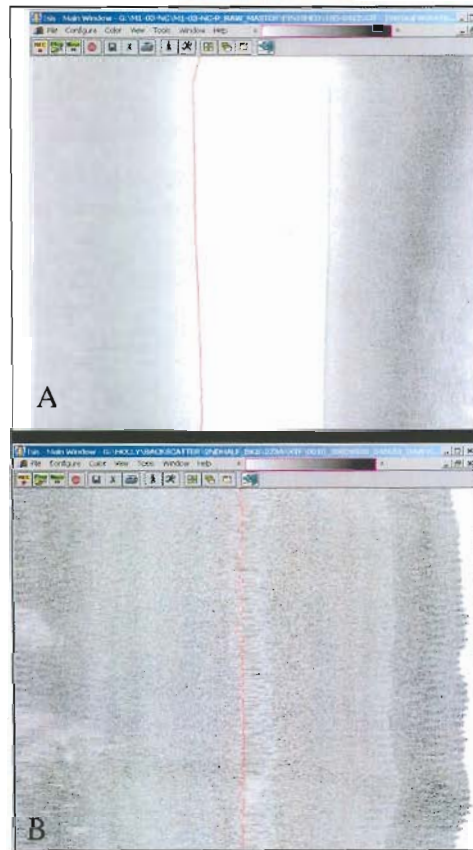


Figure A-2 Processing backscatter data without slant range where upper image is showing no slant range correction while processing backscatter data. Lower image is showing slant range correction while processing backscatter data.

Once the files were processed in ISIS® at 0.2 m resolution and projected in DelphMap®. In DelphMap®, the files were converted into GEOTIFFS which was read in both ArcView® and TnT Mips®. DelphMap® was also used to check lines before they were exported. Once the files were converted to GEOTIFFS, they were imported into TnT Mips® as *.rvc (raster) files. One raster was created from many as a mosaic. When mosaicking lines together, there were processing guidelines which needed to be followed, including maximizing good data coverage, covering all nadirs, and having all the shadows falling in the same direction by orienting lines in a constant direction. After

the lines were mosaicked, the data were examined and any poor or bad quality data which would not contribute to the interpretation of the dataset were extracted, ensuring that the best data were displayed. The final mosaics that were exported as GEOTIFFS in TnT Mips® were used in creating a map displaying processed backscatter data.

Appendix B: CREATION OF MARINE BENTHIC HABITAT MAPS

One of the products derived from analyzing multibeam bathymetry and backscatter datasets are marine benthic habitat maps. These maps identify varying geologic features and areas where fishes may be located. ROV video imagery and sediment samples, for instance, provide additional groundtruthing information that contributes to the creation of marine benthic habitat maps. These maps were useful for my thesis as they distinguished areas where bedforms are located, and possibly, where fishes/invertebrates occur.

The multibeam bathymetry and backscatter data collected in 2002 were interpreted and marine benthic habitat maps were created identifying bedforms within the Puget Sound/Georgia Basin region. There are several required steps for interpreting marine benthic habitat maps. To start, the multibeam bathymetry and backscatter data were acquired in Digital Elevation Model (DEM) (*.asc) and geotiff (*.tiff and *.tfw) format from the GSC and the CHS and viewed in a GIS (ArcMap®). Various images from raw and gridded data consisting of backscatter, slope-shaded, hill-shaded images from different angles (NW, SE) and contours were created and processed.

There are many steps necessary to perform when designing layouts used for interpretation and characterization of marine benthic habitat maps. To start, when designing the layouts, I decided on the number of layouts sheets needed. This number depended on the scale at which I wanted to interpret and depended on the area of the data (small or large data coverage in km²). Also, the number of layouts was based on various images available (slope shade, hill-shade, and backscatter). For instance, there may be three layouts at 1:10,000 with the same fixed extent displaying northwest hill-shaded

bathymetry with contours, slope-shaded bathymetry and backscatter. This may take five sheets due to the scale of interpretation.

While designing layouts, there are several components which need to be included such as deciding page setup (dimensions of layout, i.e. 33 x 44), adding a graticule which divides map by meridians and parallels, a north arrow, a scale bar, including tick marks and labels to depict coordinates and inserting text explaining the data, scale and coordinate system. The layouts were plotted on a large-scale plotter (HP DesignJet 3000CP®) onto (36") heavyweight coated paper. Individually, each layout was placed onto a light table. Mylar® was applied over each layout and using masking tape, four sides of layout were taped onto the Mylar®. Using a pencil, I traced five tick marks and four corners of the map from the layout onto the Mylar®. An outline of the data was traced creating polygons around areas of similar geologic structure. Once all the data had been traced and polygons were constructed, the Mylar® was detached from the layout and scanned the Mylar® using a Contex® FSC 5010 DSP full-scale color scanner and saved the scanned Mylar® image as a *.tif file. The *.tif was plotted on the large-scale plotter. This layout depicted all traced polygons from original layout. Scale was not considered for this layout because it was used solely for reference.

The next stage of marine benthic habitat map interpretation consists of applying colors to the assortment of distinguishable categories of the polygons, based on the data's spatial scale. These categories include Megahabitat (scale of 10s of kilometers to kilometers), Seafloor Induration (substrate hardness), Meso/Macrohabitat (1 kilometer to 1 meter), Modifier (seafloor texture/lithology), Seafloor Slope (slope), Seafloor

Complexity (calculated from slope data) and Geologic Unit (used when possible) (Greene et al., 1999). Using colored pencils, I assigned different colors to polygons which referred to geological and habitat characterization based on methods of Greene et al. (1999). Lighter colors such as yellow and tan represent younger, softer geologic material (for example, sandy, Holocene), while darker colors such as red and blue characterize older material (bedrock, Tertiary or older). This step was necessary because any changes which needed to be made, including closing polygons which may not have been closed during the interpretive process or adding or deleting lines, were identified and rectified in the upcoming processing steps. If there were several polygons which needed to be modified, it was helpful to re-scan the Mylar® and re-color the polygons, as the scanned *.tif was edited in future steps. Once all polygons were assigned colors and characterized, the *.tif was georeferenced in a GIS, using the program TnT Mips®, by applying geospatial information to the *.tif so it could be viewed in a GIS. I imported the *.tif as a *.rvc file so it could be readable in TnT Mips.

Interpreted polygons may be edited further in a GIS. The final editing steps involved raster editing which permitted editing the lines created while interpreting the data. Lines were added, erased and cleaned in TnT Mips®. The final cleaned raster lines were transformed into vector lines in a *raster to vector* conversion process. The multibeam bathymetry (*.tif) was exported as a *.rvc file and underlayed the vector file which allowed for more editing to the vector file. During this editing process, additional lines were added and erased. Once the final edits were made to the vector file, a shapefile (*.shp) was exported, which is readable in ArcGIS®. The shapefile was viewed

in ArcView® and created a table and fields which correspond to the classification scheme of Greene et al. (1999). For example, *Mega*, which stands for *Megahabitat*, was assigned the code *I* for *Inland Sea*. The shapefile has several associated files which compile one shapefile readable in ArcView®. One of these files is the database file (*.dbf) which was used in Microsoft Excel® to input information concerning the characterization of the data. In ArcView®, colors were assigned to the polygons. The final product was a shapefile of the entire area interpreted from multibeam and backscatter data.

Appendix C: HABTAT CLASSIFICATION DESCRIPTION AND SCHEME

Deep-Water Marine Benthic Habitat Classification Scheme
Explanation for Habitat Classification Code
 (Modified after Greene et al., 1999)

Habitat Classification Code

A habitat classification code, based on the deep-water habitat characterization scheme developed by Greene et al. (1999), was created to easily distinguish marine benthic habitats and to facilitate ease of use and queries within GIS (e.g., ArcView®, TNT Mips®, and ArcGIS®) and database (e.g., Microsoft Access® or Excel®) programs. The code is derived from several categories and can be subdivided based on the spatial scale of the data. The following categories apply directly to habitat interpretations determined from remote sensing imagery collected at the scale of 10s of kilometers to 1 meter: Megahabitat, Seafloor Induration, Meso/Macrohabitat, Modifier, Seafloor Slope, Seafloor Complexity, and Geologic Unit. Additional categories of Macro/Microhabitat, Seafloor Slope, and Seafloor Complexity apply to areas at the scale of 10 meters to centimeters and are determined from video, still photos, or direct observations. These two components can be used in conjunction to define a habitat across spatial scales or separately for comparisons between large and small-scale habitat types. Categories are explained in detail below. Not all categories were required or possible given the study objectives, data availability, or data quality and in these cases categories were omitted.

Explanation of Attribute Categories and their Use

Determined from Remote Sensing Imagery (for creation of large-scale habitat maps)

- 1) Megahabitat – This category is based on depth and general physiographic boundaries and is used to distinguish regions and features on a scale of 10s of kilometers to kilometers. Depth ranges listed for category attributes in the key are given as generalized examples. This category is listed first in the code and denoted with a capital letter.
- 2) Seafloor Induration – Seafloor induration refers to substrate hardness and is depicted by the second letter (a lower-case letter) in the code. Designations of hard, mixed and soft substrate can be further subdivided into distinct sediment types, and are then listed immediately afterwards in parentheses either in alphabetical order or in order of relative abundance.
- 3) Meso/Macrohabitat – This distinction is related to the scale of the habitat and consists of seafloor features ranging from 1 kilometer to 1 meter. Meso/Macrohabitats are noted as the third letter (a lower-case letter) in the code. If necessary, several Meso/Macrohabitats can be included either alphabetically or in order of relative abundance and separated by a backslash.

4) Modifier – The fourth letter in the code, a modifier, is noted with a lower-case subscript letter or separated by an underline in some GIS programs (e.g., ArcView®). Modifiers describe the texture or lithology of the seafloor. If necessary, several modifiers can be included alphabetically or in order of relative abundance and separated by a backslash.

5) Seafloor Slope – The fifth category, listed by a number following the modifier subscript, denotes slope. Slope is calculated for a survey area from x-y-z multibeam data and category values can be modified based on characteristics of the study region.

6) Seafloor Complexity – Complexity is denoted by the sixth letter and listed in caps. Complexity is calculated from slope data using neighborhood statistics and reported in standard deviation units. As with slope, category values can be modified based on characteristics of the study region.

7) Geologic Unit – When possible, the geologic unit is determined and listed subsequent to the habitat classification code, in parentheses.

Determined from video, still photos, or direct observation (for designation of small-scale habitat types)

8) Macro/Microhabitat – Macro/Microhabitats are noted by the eighth letter in the code (or first letter, if used separately) and preceded by an asterisk. This category is subdivided between geologic (surrounded by parentheses) and biologic (surrounded by brackets) attributes. Dynamic segmentation can be used to plot macroscale habitat patches on Mega/Mesoscale habitat interpretations (Nasby 2000).

9) Seafloor Slope – The ninth category (or second category, if used separately), listed by a number denotes slope. Unlike the previous slope designation (#5), the clarity of this estimate can be made at smaller scales and groundtruthed or compared with category #5. Category values can be modified based on characteristics of the study region.

10) Seafloor Complexity – The designations in this category, unlike those in category #6, are based on seafloor rugosity values calculated as the ratio of surface area to linear area along a measured transect or patch. Category letters are listed in caps and category values can be modified based on characteristics of the study region.

Literature Cited:

Greene, H.G., M.M. Yoklavich, R.M. Starr, V.M. O'Connell, W.W. Wakefield, D.E. Sullivan, J.E. McRea Jr., and G.M. Cailliet. A classification scheme for deep seafloor habitats. *Oceanologica Acta*. Vol. 22: 6. pp. 663-678.

Nasby, N.M. 2000. Integration of submersible transect data and high-resolution sonar imagery for a habitat-based groundfish assessment of Heceta Bank, Oregon. M.S. Thesis, College of Oceanic and Atmospheric Science, Oregon State University. pp. 49.

Deep-Water Marine Benthic Habitat Classification Scheme
Key to Habitat Classification Code for Mapping and use with GIS programs
 (Modified after Greene et al., 1999)

Interpreted from remote sensing imagery for mapping purposes

Megahabitat – Use capital letters (based on depth and general physiographic boundaries; depth ranges approximate and specific to study area).

- A = Aprons, continental rise, deep fans and bajadas (3000-5000 m)
- B = Basin floors, Borderland types (floors at 1000-2500 m)
- F = Flanks, continental slope, basin/island-atoll flanks (200-3000 m)
- I = Inland seas, fiords (0-200 m)
- P = Plains, abyssal (>5000 m)
- R = Ridges, banks and seamounts (crests at 200-2500 m)
- S = Shelf, continental and island shelves (0-200 m)

Seafloor Induration - Use lower-case letters (based on substrate hardness).

- h = hard substrate, rock outcrop, relic beach rock or sediment pavement
- m = mixed (hard & soft substrate)
- s = soft substrate, sediment covered

Sediment types (for above indurations) - Use parentheses.

- (b) = boulder
- (c) = cobble
- (g) = gravel
- (h) = halimeda sediment, carbonate
- (m) = mud, silt, clay
- (p) = pebble
- (s) = sand

Meso/Macrohabitat - Use lower-case letters (based on scale).

- a = atoll
- b = beach, relic
- c = canyon
- d = deformed, tilted and folded bedrock
- e = exposure, bedrock
- f = flats, floors
- g = gully, channel
- i = ice-formed feature or deposit, moraine, drop-stone depression
- k = karst, solution pit, sink
- l = landslide
- m = mound, depression; includes short, linear ridges
- n = enclosed waters, lagoon
- o = overbank deposit (levee)

p = pinnacle, cone (Note: Pinnacles are often difficult to distinguish from boulders. Therefore, these features may be used in conjunction [as (b)/p] to designate a meso/macrobiohabitat.

r = rill

s = scarp, cliff, fault or slump

t = terrace

w = sediment waves

y = delta, fan

z_# = zooxanthellae hosting structure, carbonate reef

1 = barrier reef

2 = fringing reef

3 = head, bommie

4 = patch reef

Modifier - Use lower-case subscript letters or underscore for GIS programs (textural and lithologic relationship).

a = anthropogenic (artificial reef/breakwall/shipwreck)

b = bimodal (conglomeratic, mixed [includes gravel, cobbles and pebbles])

c = consolidated sediment (includes claystone, mudstone, siltstone, sandstone, breccia, or conglomerate)

d = differentially eroded

f = fracture, joints-faulted

g = granite

h = hummocky, irregular relief

i = interface, lithologic contact

k = kelp

l = limestone or carbonate

m = massive sedimentary bedrock

o = outwash

p = pavement

r = ripples

s = scour (current or ice, direction noted)

u = unconsolidated sediment

v = volcanic rock

Seafloor Slope - Use category numbers. Typically calculated for survey area from x-y-z multibeam data.

1 Flat (0-1°)

2 Sloping (1-30°)

3 Steeply Sloping (30-60°)

4 Vertical (60-90°)

Overhang (> 90°)

Seafloor Complexity - Use category letters (in caps). Typically calculated for survey area from x-y-z multibeam slope data using neighborhood statistics and reported in standard deviation units.

- A Very Low Complexity (-1 to 0)
- B Low Complexity (0 to 1)
- C Moderate Complexity (1 to 2)
- D High Complexity (2 to 3)
- E Very High Complexity (3+)

Geologic Unit – When possible, the associated geologic unit is identified for each habitat type and follows the habitat designation in parentheses.

Examples: Shp_d1D(Q/R) - Continental shelf megahabitat; flat, highly complex hard seafloor with pinnacles differentially eroded. Geologic unit = Quaternary/Recent.

Fhd_d2C (Tmm) - Continental slope megahabitat; sloping hard seafloor of deformed (tilted, faulted, folded), differentially eroded bedrock exposure forming overhangs and caves. Geologic unit = Tertiary Miocene Monterey Formation.

Determined from video, still photos, or direct observation.

Macro/Microhabitat – Preceded by an asterisk. Use parentheses for geologic attributes, brackets for biologic attributes. Based on observed small-scale seafloor features.

Geologic attributes (note percent grain sizes when possible)

- (a) = area, patches, and fields
- (b) = boulder
- (c) = cobble
- (d) = deformed, faulted, or folded
- (e) = exposure, bedrock (sedimentary, igneous, or metamorphic)
 - (e-r) = rough or rugged bedrock exposure
 - (e-s) = smooth bedrock exposure
- (f) = fans
- (g) = gravel
- (h) = halimeda sediment, carbonate slates or mounds
- (i) = interface
- (j) = joints, cracks, crevices, and overhangs (differentially eroded)
- (k) = knob or ridge
- (l) = limestone or carbonate
- (m) = mud, silt, or clay
 - (m-c) = consolidated
 - (m-u) = unconsolidated
 - (mx) = mixed sediment
- (p) = pebble
- (q) = coquina (shell hash)

- (r) = rubble
- (s) = sand
- (t) = flat terrace-like seafloor including sedimentary pavements
- (w) = wall, scarp, or cliff

Biologic attributes

- [a] = algae
 - [a-rb] = red, bladed
 - [a-rf] = red, filamentous
- [b] = bryozoans
- [c] = corals
- [d] = detritus, drift algae
- [e] = eelgrass
- [g] = gorgonians
- [k] = kelp
 - [k-bb] = brown, bladed
 - [k-bf] = brown, filamentous
- [n] = anemones
- [o] = other sessile organisms
 - [o-c] = crinoids
- [s] = sponges
- [t] = tracks, trails, or trace fossils, holes and burrows (bioturbation)
- [u] = unusual organisms, or chemosynthetic communities
- [w] = worm tubes

Seafloor Slope - Use category numbers. Estimated from video, still photos, or direct observation.

- 1 Flat (0-1°)
- 2 Sloping (1-30°)
- 3 Steeply Sloping (30-60°)
- Vertical (60 - 90°)
- Overhang (90°+)

Seafloor Complexity - Use category numbers. Estimated from video, still photos, or direct observation. Numbers represent seafloor rugosity values calculated as the ratio of surface area to linear area along a measured transect or patch.

- A Very Low Complexity (1 to 1.25)
- B Low Complexity (1.25 to 1.50)
- C Moderate Complexity (1.50 to 1.75)
- D High Complexity (1.75 to 2.00)
- E Very High Complexity (2+)

Examples: *(m)[w]1C - Flat or nearly flat mud (100%) bottom with worm tubes; moderate complexity.

*(s/c)1A - Sand bottom (>50%) with cobbles. Flat or nearly flat with very low complexity.

*(h)[c]1E - Coral reef on flat bottom with halimeda sediment. Very high complexity.

Shp_d1D(Q/R)*(m)[w]1C - *Large-scale habitat type:* Continental shelf megahabitat; flat, highly complex hard seafloor with pinnacles differentially eroded. Geologic unit = Quaternary/Recent. *Small-scale habitat type:* Flat or nearly flat mud (100%) bottom with worm tubes; moderate complexity.